BEST AVAILABLE IMAGES

Defective images within this document are accurate representations of the original documents submitted by the applicant.

Defects in the images may include (but are not limited to):

- BLACK BORDERS
- TEXT CUT OFF AT TOP, BOTTOM OR SIDES
- FADED TEXT
- ILLEGIBLE TEXT
- SKEWED/SLANTED IMAGES
- COLORED PHOTOS
- BLACK OR VERY BLACK AND WHITE DARK PHOTOS
- GRAY SCALE DOCUMENTS

IMAGES ARE BEST AVAILABLE COPY.

As rescanning documents *will not* correct images, please do not report the images to the Image Problem Mailbox.

REMARKS

Claims 1-6, 8-15, 17-24, 26 and 27 are pending in the instant application. Claim 3 has been amended to correct a typographical error resulting in an improper antecedent basis in dependent claim 4. This amendment adds no new matter. Support for this amendment can be found in original claim 4 as well as throughout the application. Claims 6, 9, 15, 18, 24 and 27 have been amended to correct a formality in Markush group claim language. Support for these amendments is inherent to the application as filed, and, accordingly these amendments add no new matter.

Applicants note that the Examiner has acknowledged Applicants' amendment to Figure 6, as well as the new Oath/Declaration and insertion of priority claim language in the instant application. Applicants gratefully acknowledge the Examiner's withdrawal of rejections under 35 USC §112, second paragraph (claims 19-27), and under 35 USC §112, first paragraph (written description) (claims 1-6, 8-15, 17-24, 26 and 27). Applicants further acknowledge the Examiner's withdrawal of the rejection of claims 10, 14, 15, 17 and 18 under 35 U.S.C. §102(b), as being anticipated by Chen *et al.* (U.S. Patent No. 6,013,786), in view of Applicants last response.

I. *The claims are valid under 35 U.S.C. §112, first paragraph (enablement).*

Claims 1-6, 8-15, 17-24, 26 and 27 have been rejected under 35 U.S.C. §112, first paragraph, "because the specification.....does not reasonably provide enablement for a method for potentiating the activity of a prodrug (by) coadministering a polyanion (oligonucleotide) with the prodrug." In particular, the Office Action states that "[t]he issue is would any/all oligonucleotides have the biological activity to function to statistically significantly potentiate the activity of a prodrug?" Applicants respectfully traverse this rejection for the reasons which follow.

In their last response, Applicants pointed out that the method of the invention utilizes oligonucleotides as a general class, and not oligonucleotides of any particular sequence. Further

explicit disclosure of methods of making innumerable oligonucleotides not having the sequence corresponding to SEQ ID NO: 1 for use in the claimed invention, beyond the teachings of the instant application, are not needed to support enablement, because such oligonucleotides not having the sequence corresponding to SEQ ID NO: 1 are well known in the art and would, accordingly, not require undue experimentation to make and use.

Applicants here respectfully note that the instant application teaches how to make and use the method of the invention, in which oligonucleotides are utilized in a sequence-nonspecific manner to potentiate the activity of a prodrug. Indeed, there is exemplary support for the sequence-independence claimed in the application as filed.

For example, Example 1 demonstrates that both an mbm-2-specific antisense oligonucleotide (Oligo 1) and an anti-HIV oligonucleotide (Oligo 2) produce a statistically significant and dose-dependent potentiation of Camptosar efficacy (page 14, lines 10-13). Since the anti-HIV antisense oligonucleotide has no target in this uninfected mouse model, the potentiation from Oligo 2 occurs in a target sequence-independent manner.

Further support for the sequence-independent effect is shown in Example 2 (pages 14-15). In this example, a mouse model for pancreatic cancer (Panc 1 tumor) was used. Both the mdm-2 antisense oligonculeotide and a third oligonucleotide of arbitrary sequence (referred to again as Oligo 2, but have the sequence corresponding to SEQ ID NO: 3) showed statistically significant potentiation of prodrug efficacy. Because the Panc1 tumor has a nonfunctional (mutant) p53 gene, and, further, since the mdm-1 antisense oligonucleotide acts primarily by upregulating p53 expression, both oligonucleotides in this example appear to act in a target sequence-independent manner to potentiate the produg. Indeed, in these studies prodrug treatment alone was ineffective (*i.e.*, without either of these two oligonucleotides, no statistically-significant effect of the prodrug over the vehicle control was observed (page 15, lines 9-17)).

Still further, in addition to the exemplary support for a sequence-independent effect provided in the specification, Applicants note numerous post-filing reports confirming their

observation. For example, Wang *et al.* ((2001) Clin. Cancer Res. 7: 3613-24) show that a "mismatch control" antisense oligonculeotide, designed to prevent antisense-mediated repression of a target gene, shows a synergistic effect on tumor growth inhibition when used in combination with the prodrug irinotecan (see Exhibit A, at page 3622). Still further, *Agrawal et al.* ((2001) Intl. J. Onc. 18: 1061-9) show that numerous oligonucleotides, designed as negative controls against any antisense-specific mode of action, each effectively potentiated prodrug action (see Exhibit B). Notably, Agrawal *et al.* further observe that two antisense oligonucleotides, designed to target the human protein kinase RI α subunit, also have a prodrug potentiating effect. Therefore, numerous post-filing references have corroborated and confirmed the sequence independent, prodrug-potentiating activity of oligonucleotides for use in the method of the instant invention.

Applicants further note that the Agrawal *et al.* reference discussed above has been cited in the Final Office Action as supporting the enablement rejection. Specifically, the Office Action states that this reference "indicates that specific oligonucleotides will act to potentiate prodrug efficacy while others will not." However the cited portion of Agrawal *et al.* does not support this assertion. Rather, Agrawal *et al.* actually recites that "the potentiation of antitumor activity of irinotecan is dependent on the dose of irinotecan and chemically modified oligonucleotide, suggesting requirement of the presence of a certain level of irinotecan and oligonucleotide in the system" (emphases added). This recitation of Agrawal *et al.* does not support the lack of enablement of the method of the invention. Indeed, the teachings of Agrawal *et al.*, in their totality, actually support the significance of the sequence-independent potentiation effect observed and the method of the invention as a whole. As stated above, Agrawal *et al.* show that numerous oligonucleotides, including those designed as negative controls not capable of antisense repression, act in a sequence-independent manner to potentiate prodrug activity. This reference provides still further support for enablement of the claimed invention.

In particular, the cited portion of Agrawal *et al.* discusses the fact that "potentiation of antitumor activity...is dependent on the dose...(of prodrug)...and chemically modified oligonucleotide." But the dose-dependence of a drug effect is an art-recognized indicium of its

biological significance. Indeed, dose-dependence of a therapeutic effect distinguishes real biological effects from statistical coincidences and/or placebo effects. Therefore, the dose-dependence observed by Agrawal *et al.* supports enablement of the instant invention.

Further, Agrawal *et al.* goes on to state that "a certain level of oligonucleotide in the system (is needed for prodrug potentiation)." This observation follows logically from the dose-dependence effect observed. Indeed, the clear requirement that some dose of oligonucleotide be present "in the system" is inherent to the instant invention and is acknowledged and supported by numerous teachings in the specification which emphasize that more physiologically-stable (nuclease resistant) modified oligonucleotides are generally preferred for use in the invention because their level in a biological system is more easily maintained (see, *e.g.*, the application at page 3, lines 13 and 14, "especially oligonucleotide phosphorothioates or phosphorodithionates"). The doses to be delivered in the method of the invention are directly supported in the examples in the specification. Indeed, the section of Agrawal *et al.* quoted in the Office Action is immediately followed by the statement "a dose of 20 mg/kg of chemically modified oligonucleotide.....was found to be optimal." This is precisely the dose taught in Example 2 of the application (see page 15, lines 3-6). Furthermore, alternative oligonucleotide doses for use in the method of the invention are known in the art or readily discerned by the person of ordinary skill at the time of the invention without recourse to undue experimentation.

Finally, the Office Action still further states that "such a broad definition (of oligonucleotide) might also read on previously characterized oligonucleotides, or alternatively, might include oligonucleotides with additional functions or activities neither envisioned nor enabled by applicants in the current invention." In response, Applicants respectfully note that the method of the invention is novel and nonobvious because it uses both old and new oligonucleotides in a new way, namely, in a method for statistically significantly potentiating the activity of a prodrug by co-administering the oligonucleotide and the prodrug. It is well settled law that a new use for an old composition of matter, such as the broad class of oligonucleotides utilized in the instant invention, is patentable.

Therefore, in view of the numerous examples of sequence-independent prodrug potentiation by oligonucleotides in the application as filed, as well as the numerous post-filing publications which confirm the sequence-independent potentiation of prodrugs by oligonucleotides (*e.g.*, Agrawal, *et al.*), and further in view of the well established patentability of new uses for old compositions, Applicants respectfully request reconsideration and withdrawal of the enablement rejection.

II. *The claims are valid under 35 U.S.C. §103.*

Claims 1-6, 8-15, 17-24, 26 and 27 have been rejected under 35 U.S.C. § 103(a) as being obvious in view of Totora *et al.* ((1997) Proc. Natl. Acad. Sci. (USA) 94: 12586-91), Wang *et al.* ((1999) Int. J. Oncol. 15: 653-60), and Bracchini *et al.* (U.S. Patent No. 5,801,154). In particular, the Office Action states that "one of ordinary skill in the art would have been motivated to potentiate the activity of a cytotoxic prodrug, such as CPT-11, with phosphorothioate oligonucleotides since Tortora *et al.* teach synergistic inhibition of human cancer cell growth by cytotoxic drugs, including prodrugs, and phosphorothioate antisense oligonucleotides" (emphasis added). The Office Action further states "the prodrug taught by Tortora et al. is docetaxel." Applicants respectfully traverse this rejection for the reasons that follow.

First, Applicants respectfully note that, contrary to the assertions made in the rejection, docetaxel is not a prodrug. A prodrug is defined in the specification as "a compound comprising an active compound covalently linked to another moiety by a cleavable linkage, wherein the pharmacological activity of the active compound is greater than the pharmacological activity of the prodrug, and wherein the active compound is produced in the body by cleavage of the cleavable linkage" (at page 5, lines 19-22). This definition is consistent with the use of the term in the art. For example, the Oxford Dictionary of Biochemistry and Molecular Biology ((2000), Oxford University Press, New York) defines a prodrug as "a drug molecule that is itself inert but has pharmacological effect after bioactivation."

Docetaxal is a proprietary name for a semisynthetic analog of taxol (which itself is also known by the proprietary name Paclitaxel). Docetaxal is largely similar in structure to taxol, except, notably, for the presence of an alcohol group where an ester group is present in taxol (see structural formulas for docetaxal and taxol from the Merck Index (Exhibit C)). Applicants respectfully assert that neither naturally-occurring taxol, nor synthetic docetaxal act as prodrugs. Rather, they act chemotherapeutically in a direct fashion, without requiring activation, by binding to, and thereby stabilizing, microtubules. Microtubule depolymerization is essential for the G to M transition in the cell cycle. Since this process is blocked by taxol/docetaxal, cancer cell division is blocked.

As added proof that Docetaxal is not a prodrug, Applicants refer to Herbst and Khuri ((2003) Can. Treat. Rev. 29: 407-15) entitled "Mode of Action of Docetaxel – A Basis for Combination with Novel Anticancer Agents" (Exhibit D). This publication represents a recent extensive review of "docetaxel's mechanism of action and explains the rationale for its combination with a variety of novel anticancer agents" (quoting reference at top of page 408). Applicants respectfully note that Herbst and Khuri do not describe, characterize or otherwise reveal that docetaxel is a prodrug, despite the fact that the primary purpose of the publication is to review docetaxel's "mode of action." Applicants still further make reference to Gilbert *et al.* ((2003) J. Exp. Ther. Oncol. 3: 27-35) (Exhibit E). Gilbert *et al.* states that "several approved drugs in current use have side chains that can be used to form prodrugs...(including) taxanes (Paclitaxel and Docetaxal)" (emphasis added), thereby implicitly stating that unmodified Docetaxel is, itself, not a prodrug. Indeed, the Gilbert *et al.* reference describes the creation of a new prodrug form of taxol through modification of a chemical side chain group with a bifunctional linker ("A-Z-CINN™"). Accordingly, Applicants respectfully note that they could find no support in the literature for Decetaxel being a prodrug, but did find much that would contradict the assertion that it is.

Applicants respectfully conclude that, having relied upon Tortora *et al.* to show "synergistic inhibition of human cancer cell growth by cytotoxic drugs, including prodrugs, and phosphorothioate antisense oligonucleotides," the Office Action has not established a *prima facie*

case for obviousness because the cited combination of references does not teach or suggest all the limitations of the claims. *See In re Zurko*, 111 F.3d 887, 888-889 (Fed. Cir. 1997); *In re Wilson*, 424 F.2d 1382,1385 (C.C.P.A. 1970) ("All words in a claim must be considered in judging the patentability of that claim against the prior art.").

Accordingly, reconsideration and withdrawal of this §103 rejection is respectfully requested.

CONCLUSION

In view of the foregoing remarks, Applicants respectfully submit that the pending claims are in condition for allowance. If a telephone interview would advance prosecution of the application, the Examiner is invited to call the undersigned at the number listed below.

A Petition for a one (1) Month Extension of Time and authorization of payment of the corresponding fee accompanies this Response. Please charge any additional fees or refund any overpayment to Deposit Account No. 08-0219.

Respectfully submitted,

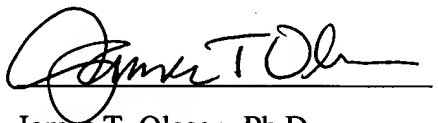

James T. Olesen, Ph.D.
Attorney for Applicant
Reg. No.: 46,967

Date: March 3, 2004

HALE AND DORR LLP
60 State Street
Boston, MA 02109
Tel: (617) 526-6000
Fax: (617) 526-5000

EXHIBIT A

Antisense Anti-MDM2 Oligonucleotides As a Novel Therapeutic Approach to Human Breast Cancer: *In Vitro* and *in Vivo* Activities and Mechanisms[1]

Hui Wang, Li Nan, Dong Yu, Sudhir Agrawal, and Ruiwen Zhang[2]

Department of Pharmacology and Toxicology [H. W., L. N., R. Z.], Division of Clinical Pharmacology [H. W., L. N., R. Z.], Comprehensive Cancer Center [R. Z.], and Gene Therapy Center [R. Z.], University of Alabama at Birmingham, Birmingham, Alabama 35294, and Hybridon, Inc., Cambridge, Massachusetts 01757 [D. Y., S. A.]

ABSTRACT

The mouse double minute 2 (MDM2) oncogene has been suggested as a target for cancer therapy. It is amplified or overexpressed in many human cancers, including breast cancer, and MDM2 levels are associated with poor prognosis of several human cancers, including breast cancer, ovarian cancer, osteosarcoma, and lymphoma. In the present study, we investigated the functions of MDM2 oncogene in the growth of breast cancer and the potential value of MDM2 as a drug target for cancer therapy by inhibiting MDM2 expression with a specific antisense antihuman-MDM2 oligonucleotide (oligo). The selected antisense mixed-backbone oligo was evaluated for its *in vitro* and *in vivo* antitumor activity in human breast cancer models: MCF-7 cell line containing wild-type p53 and MDA-MB-468 cell line containing mutant p53. In MCF-7 cells, p53 and p21 levels were elevated, resulting from specific inhibition of MDM2 expression by the antisense oligo (AS). In MDA-MB-468 cells, after inhibition of MDM2 expression, p21 levels were elevated, although p53 levels remained unchanged. After i.p. administration of the antisense anti-MDM2 oligo, *in vivo* antitumor activity occurred in a dose-dependent manner in nude mice bearing MCF-7 or MDA-MB-468 xenografts. In both models, *in vivo* synergistically or additive therapeutic effects of MDM2 inhibition and the clinically used cancer chemotherapeutic agents irinotecan, 5-fluorouracil, and paclitaxel (Taxol) were observed. These results suggest that MDM2 have a role in tumor growth through both p53-dependent and p53-independent mechanisms. We speculate that MDM2 inhibitors, such as ASs, have a broad spectrum of antitumor activities in human breast cancers, regardless of p53 status. This study should provide a basis for future development of anti-MDM2 ASs as cancer therapeutic agents used alone or in combination with conventional chemotherapeutics.

INTRODUCTION

The tumor suppressor gene TP53/P53 product p53 (1) regulates the normal cell cycle by activating the transcription of genes that control progression through the cycle and of other genes that help maintain the genomic integrity of the cells as it coordinates the cellular response to DNA damage by inducing cell cycle arrest or apoptosis (1–6). Alterations of the *p53* gene are the most frequent genetic abnormalities in human malignancies (3, 4, 7–17). Mutations in p53 arise with an average frequency of 50%, but the incidence varies from zero in carcinoid lung tumor (13) through 30–86% in breast cancers (14–16) to 97% in primary melanomas (17). Mutations in p53 correlate strongly with a poor prognosis in breast cancer (18), and the level of p53 protein expression may be a predictor of distant metastasis of human breast cancers (19).

p53 also plays an important role in cancer therapy. DNA damaging treatments, such as chemotherapy and radiation therapy, increase p53 levels, leading to cell growth arrest or apoptosis (20–23). p53 induces the expression of many genes, including *MDM2*[3] (24), *GADD45* (25), and *CIP1/WAF1* (26). It has been suggested that modulating p53-mediated cell arrest and/or apoptosis may lead to the sensitization of tumor cells to DNA damaging chemotherapeutic agents and radiation therapy. Human cancer cell lines with mutant p53 tend to exhibit less growth inhibition than wild-type p53 lines after treatment with the majority of clinically used anticancer agents, such as bleomycin, 5-FU, and cisplatin (27). In contrast, cell lines containing wild-type p53 better respond to γ-irradiation and chemotherapy, showing an increase in G1 arrest and in expression of p53 reporter genes *MDM2*, *CIP1/WAF1*, and *GADD45* (27). These studies suggest that p53 be a target for improving therapeutic effects of cancer chemotherapy and radiation therapy. *P53* gene therapy has also been suggested as a new approach to human cancer treatment (28–32). The transfection of human cancer cell lines (including breast carcinoma) that have mutant p53 with a wild-type *P53* gene significantly inhibits tumor cell growth (28,

Received 1/31/01; revised 8/24/01; accepted 8/27/01.
The costs of publication of this article were defrayed in part by the payment of page charges. This article must therefore be hereby marked *advertisement* in accordance with 18 U.S.C. Section 1734 solely to indicate this fact.
[1] Supported by NIH Grant R01 CA 80698 (to R. Z.).
[2] To whom requests for reprints should be addressed, at Department of Pharmacology and Toxicology, University of Alabama at Birmingham, VH 113, Box 600, 1670 University Boulevard, Birmingham, AL 35294-0019. Phone: (205) 934-8558; Fax: (205) 975-9330; E-mail: ruiwen.zhang@ccc.uab.edu.

[3] The abbreviations used are: MDM2, mouse double minute 2; Oligo, oligonucleotides; AS, antisense oligonucleotide; ASM, mismatch control oligonucleotide; HCPT, 10-hydroxycamptothecin; 5-FU, 5-fluorouracil; SN-38, 10-hydroxy, 7-ethyl camptothecin; FBS, fetal bovine serum.

29). The tumorigenicity of breast cancer cell lines with mutations in both *P53* and *RB1* (retinoblastoma gene) is reduced by the expression of wild-type forms of either *P53* or *RB1* (30). Extensive preclinical studies of *p53* gene therapy have now been carried out (32). However, studies have suggested that the effectiveness of p53-mediated therapy may be hindered because of the impact of MDM2, a negative regulator of p53.

The MDM2 oncogene was first cloned as an amplified gene on a murine double-minute chromosome in the 3T3DM cell line, a spontaneously transformed derivative of BALB/c 3T3 cells (33). Overexpression of the *MDM2* gene in NIH 3T3 cells confers the tumorigenicity (33). Additional evidence supporting MDM2 as an oncogene comes from a study of mice with targeted overexpression of MDM2 in the mammary epithelium during lactation (34). In the mammary glands with the high levels of MDM2, normal mammary development and terminal differentiation were inhibited, with many cells becoming multinucleated and polyploid that are typical phenotypes of cells with inactive p53 and high incidence of mammary gland tumor being observed (34), indicating that overexpression of MDM2 is directly associated with the mammary tumorigenesis. The connection between MDM2 and cancer is also shown in human cancers (reviewed in Ref. 35). The *MDM2* gene is amplified in a number of human tumors, including breast cancer (36–41). Studies analyzing both MDM2 amplification and p53 mutations demonstrate that mutations in *MDM2* and *P53* genes do not generally occur within the same tumor and that 29 of 33 MDM2 amplification-positive tumors had wild-type p53, indicating overexpression of MDM2 is a means of inactivation of p53. Using immunohistochemical techniques, overexpression of MDM2 protein (with or without gene amplification) has now been reported in various human cancers, including breast cancer (36, 37, 41–45).

The expression of MDM2 is induced by p53 (24, 46), and mdm2 oncoprotein binds to p53 with high affinity, inhibiting its ability to act as a transcription factor (47), indicating that MDM2 functions as a negative regulator of p53. Studies have shown that MDM2 knockout mouse embryos die shortly after implantation; however, mice carrying both inactivated *MDM2* and *P53* genes are viable (48, 49), additionally demonstrating the important function of MDM2 that negatively regulates p53. In cell culture studies, MDM2 overexpression abrogates the ability of p53 to induce cell cycle arrest and apoptosis (50–52). In addition, MDM2 has also been shown to enhance the degradation of p53 (53, 54), suggesting that it can regulate p53 functions through multiple mechanisms. In addition, MDM2 has been shown to bind to the pRB (55), E2F-1 (56), ribosomal protein L5 (57), and RNA (58), suggesting that MDM2 has p53-independent activities that may be associated with transforming properties of MDM2.

Many studies suggest that overexpression of MDM2 be associated with inactivation of wild-type p53 (reviewed in Ref. 35). It has also been demonstrated that many cancer therapeutic agents exert their cytotoxic effects through activation of wild-type p53. However, the activation of p53 by DNA damaging treatments, such as cancer chemotherapy and radiation, may be limited in cancers with MDM2 expression, especially those with MDM2 overexpression. Therefore, inactivation of the MDM2-p53 negative feedback loop may increase the magnitude of p53 activation after DNA damaging treatments, thus enhancing their therapeutic effectiveness. It is also possible to overcome some drug resistance in tumors with dysfunctional p53 and overexpression of MDM2.

In our laboratory, we have been interested in developing novel genetically based cancer therapy, with an emphasis on antisense approach. Antisense oligos have been shown to be unique research tools in the study of the regulation of gene expression and gene functions. They are also potential therapeutic agents based on rational gene-based drug design. Antisense oligos may achieve their effects by targeting mRNA with which they can hybridize and specifically block protein expression (59, 60). Recently, we *et al.* (61–63) have developed anti-MDM2 oligos that showed antitumor activities both *in vitro* and *in vivo*. In the present study, we used an anti-MDM2 oligo designed with an advanced chemistry (mixed-backbone oligos) as a research tool to investigate the role of MDM2 in the development and treatment of human breast cancer and, by using *in vivo* approaches, to systematically evaluate the antisense oligo as a therapeutic agent used alone or in combination with cancer chemotherapeutics. These studies will not only provide the proof of principle for anti-MDM2 oligo itself but also contribute to the evaluation of the usefulness of antisense therapy in general.

MATERIALS AND METHODS

Test Oligos. The anti-MDM2 AS, Oligo AS, a 20-mer mixed-backbone oligo (5′-UGACACCTGTTCTCACUCAC-3′) and its mismatch control (Oligo ASM, 5′-UG*T*CAC-C*CTTTTT*CA*T*UCAC-3′) were synthesized, purified, and analyzed as described previously (62, 64). Two nucleosides at the 5′-end and four nucleosides at the 3′-end are 2′-*O*-methylribonucleosides (represented by boldface letters); the remaining are deoxynucleosides. The italicized nucleosides of Oligo ASM are the sites of the mismatch controls compared with Oligo AS. For both mixed-backbone oligos, all internucleotide linkages are phosphorothioate. The purity of the oligos was shown to be >90% by capillary gel electrophoresis and PAGE, with the remainder being n-1 and n-2 products (62). The integrity of the internucleotide linkages was confirmed by ^{31}P NMR.

Chemicals and Reagents. Cell culture media, PBS, 5-FU, and antihuman β-actin (SC-15) monoclonal antibody were obtained from Sigma Chemical Co. (St. Louis, MO). FBS, Lipofectin, trypsin, penicillin-streptomycin, and trypan blue stain were purchased from Life Technologies, Inc. (Grand Island, NY). The antihuman MDM2 (SMP-14) monoclonal antibody was purchased from Santa Cruz Biotechnology, Inc. The monoclonal antibodies against p53 (Ab-6) and p21 (Ab-1) were purchased from Oncogene Research Products (Boston, MA). Irinotecan was obtained from Pharmacia (Kalamazoo, MI). Paclitaxel (Taxol) was obtained from Mead Johnson Oncology Products (Princeton, NJ).

Cell Culture. The tumor cell lines MCF-7 and MDA-MB-468 were obtained from the American Type Culture Collection (Rockville, MD) and cultured following their instruction. MCF-7 cells were grown in MEM media containing 10% FBS, 1 mM nonessential amino acids and Earle's balanced salt solution, 1 mM sodium pyruvate, and 10 mg/liter bovine insulin.

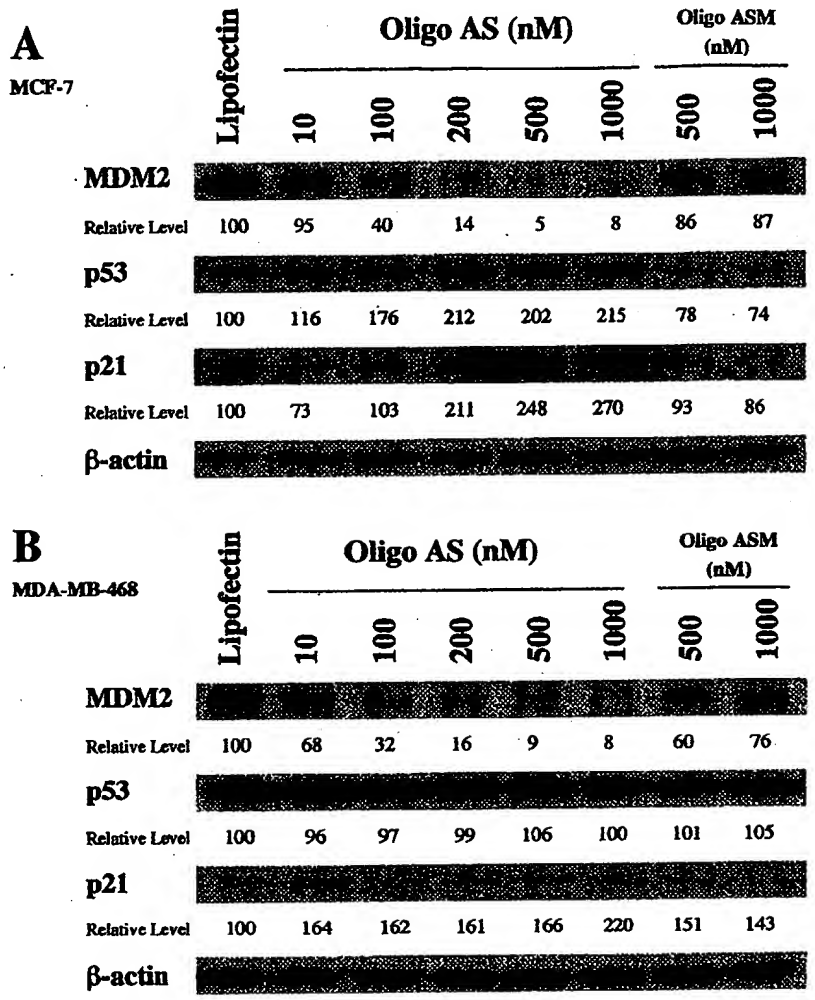

Fig. 1 Effects of anti-MDM2 AS on MDM2, p53, and p21 protein levels in MCF-7 (*A*) and MDA-MB-468 cells in culture (*B*). Cells were incubated with Oligos AS or ASM at various concentrations for 24 h, in the presence of Lipofectin (7 μg/ml). Identical total protein (20 μg) was analyzed by SDS-PAGE, followed by Western blotting. Inhibitory effects of Oligo AS on MDM2 expression are shown in a dose-dependent manner. The protein levels of p53 and/or p21 were increased in a dose-dependent manner. Oligo ASM had no effect on the levels of these proteins. Relative levels of each protein were expressed as a percentage of control, normalized by corresponding β-actin level.

MDA-MB-468 cells were grown in DMEM/Ham's F-12 medium (DMEM/F-12 1:1 mixture) containing 10% FBS. In *in vitro* studies, cells were incubated with Oligos AS or ASM at various concentrations for 24 h in the presence of Lipofectin (7 μg/ml). *In vitro* cell growth inhibition by oligos was determined by the microculture tetrazolium assay, using the conditions described earlier (62, 65–67) after an incubation with various concentrations of Oligo AS or ASM (10–500 nM) for 72 h.

Animal Tumor Model. Human cancer xenograft models were established using the methods reported previously (62, 65–67). The protocol for animal use and care was approved by the Institutional Animal Care and Use Committee in the University of Alabama at Birmingham. Female athymic nude mice or C.B-17-scid/scid mice (4–6 weeks old) were purchased from Frederick Cancer Research and Development Center (Frederick, MD) and accommodated for 5 days for environmental adjustment before study. To establish MCF-7 human breast xenografts, each of the nude mice was implanted a 60-day s.c. slow release estrogen pellet (SE-121, 1.7 mg of 17β-estradiol/pellet; Innovative Research of America, Sarasota, FL). Cultured MCF-7 cells were harvested from the monolayer cultures, washed twice with MEM medium, resuspended in MEM, and injected s.c. (10×10^6 cells, total volume 0.2 ml) into the left inguinal area of the mice. To establish MDA-MB-468 human breast xenografts, cultured MDA-MB-468 cells were harvested from the monolayer cultures, washed twice with 10% DMEM Ham's F-12 medium, resuspended in serum-free DMEM Ham's F-12 medium:Matrigel basement membrane matrix (2:1), and injected s.c. (10×10^6 cells, total volume 0.2 ml) into the left inguinal area of the C.B-17-scid/scid mice.

The animals were monitored by general clinical observation, body weight, and tumor growth. Tumor growth was monitored by the measurement, with calipers, of two perpendicular diameters of the implant. Tumor size (weight in grams) was calculated by the formula, $1/2a \times b^2$, where "a" is the long diameter (cm) and "b" is the short diameter (cm). The animals were used in the chemotherapy study when the tumor size reached 50–150 mg.

***In Vivo* Chemotherapy.** The animals bearing human cancer xenografts were randomly divided into various treatment groups and a control group (six mice per group). The control (nonoligo treated) group received physiological saline only. The oligos dissolved in physiological saline (0.9% NaCl) were administered by i.p. injection at a dose of 25 mg/kg/day, 5 days/

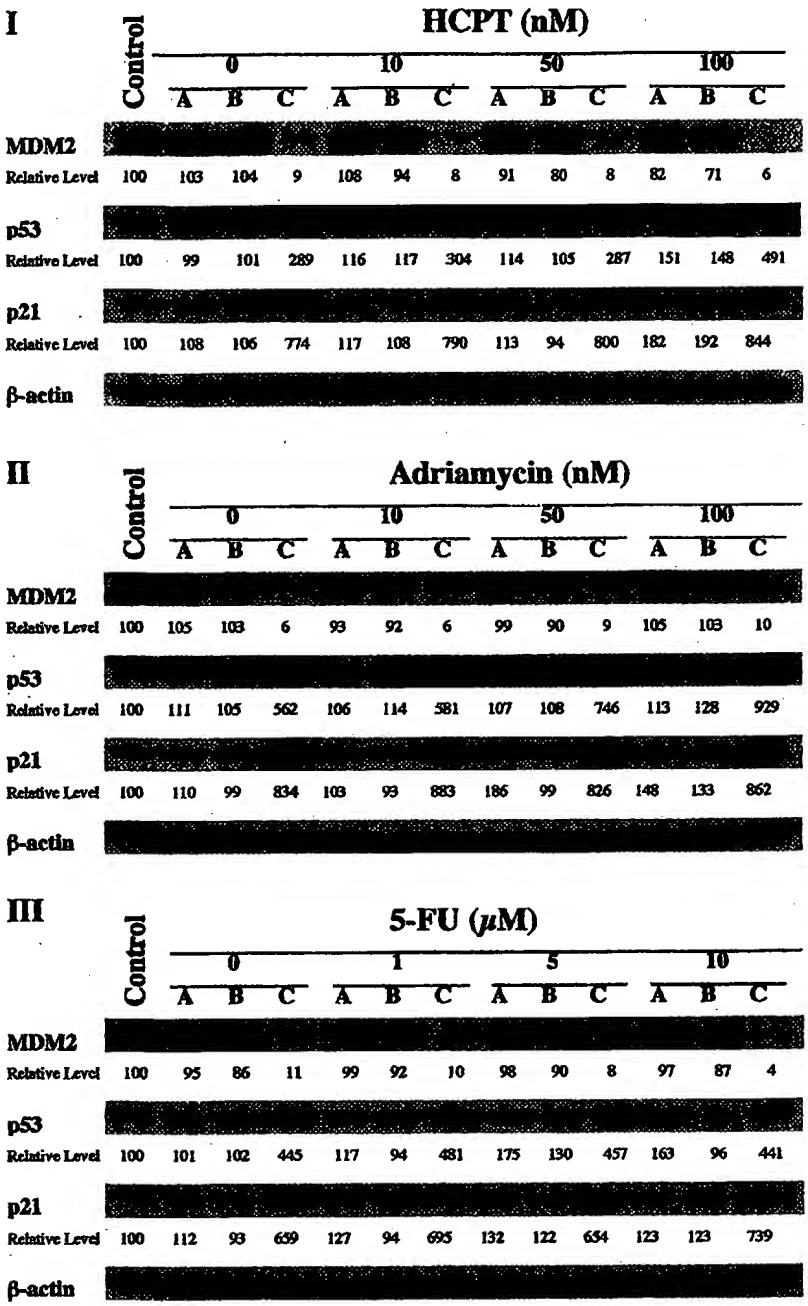

Fig. 2 Synergistic effects of combination treatment of anti-MDM2 oligo AS and the cancer chemotherapeutic agents on MDM2, p53, and p21 protein levels in MCF-7 cells in culture. Cells were incubated with 200 nM Oligo AS or ASM in the presence of Lipofectin for 24 h, followed by an addition of various concentrations of HCPT (*I*), adriamycin (*II*), or 5-FU (*III*) and incubation for an additional 24 h. At various concentrations, the effects on MDM2, p53, and p21 levels were evaluated after treatment with cytotoxic agents alone (*Lanes A*), pretreatment with Oligo ASM (*Lanes B*), or pretreatment with Oligo AS (*Lanes C*). Relative levels of each protein were expressed as a percentage of control, normalized by corresponding β-actin level.

week for 3 weeks in MCF-7 model and 5 weeks in MDA-MB-468 model. 5-FU was given i.p. at 10 mg/kg/day, 5 days/week for 3 weeks in MCF-7 model and 5 weeks in MDA-MB-468 model. Irinotecan (50 mg/kg/day) was given i.p. on days 0, 7, and 14 in MCF-7 model or on days 0, 14, and 28 in MDA-MB-468 model. Paclitaxel (10 mg/kg/day) was given i.p. on days 1, 4, 8, 11, and 15 in MCF-7 model and on days 1, 4, 14, 18, 29, and 32 in MDA-MB-468 model.

Western Blot Analysis. The MDM2, p53, and p21 levels in cultured cells or tumor xenografts were analyzed by using the methods described previously (61–63, 67). In brief, cell lysates or tumor tissue homogenates containing identical amounts of total protein were fractionated by SDS-PAGE and transferred to Bio-Rad *Trans*-Blot nitrocellulose membranes (Bio-Rad Laboratories, Hercules, CA). The nitrocellulose membrane was then incubated with blocking buffer (PBS containing 0.1% Tween 20 and 5% nonfat milk) for 1 h at room temperature and washed twice with the washing buffer (PBS containing 0.1% Tween 20) for 5 min. The membrane was incubated with primary (anti-MDM2, anti-p53, anti-p21, or anti-β-actin) antibody overnight at 4°C or for 1 h at room temperature with gentle shaking. The membrane was washed with the washing buffer for 15 min, twice for 5 min, and then incubated with 1:3000 diluted goat antimouse IgG-horse radish peroxidase conjugated antibody

(Bio-Rad Laboratories) for 1 h at room temperature. After washing as described above, the protein of interest was detected by enhanced chemiluminescence reagents from Amersham (Arlington Heights, IL). The density of each protein band was analyzed by a densitometry measurement (Bio-Rad Model GS-670 Imaging Densitometer; Bio-Rad Laboratories).

RESULTS

***In Vitro* Inhibition of MDM2 Expression and Activation of p53 and p21 in Human Breast Cancer MCF-7 Cells That Contain Wild-Type p53 by Anti-MDM2 Oligo Administered Alone or in Combination with Cancer Chemotherapeutics.** *In vitro* inhibition of MDM2 expression by Oligo AS was shown in a sequence-specific, dose-dependent manner, and p53 and p21 levels were elevated accordingly (Fig. 1*A*). Oligo ASM had little or no effect on MDM2, p53, or p21 protein levels at 500 and 1000 nM, the highest concentrations tested in the study. Oligo AS inhibited the growth of tumor cell lines *in vitro* in a dose-dependent manner, with a mean IC_{50} being 67 nM for a 72-h treatment. Oligo ASM had minimal effect on tumor cell growth.

After *in vitro* exposure to combinations of Oligos and the chemotherapeutic agents HCPT, adriamycin, and 5-FU, the protein levels of MDM2, p53, and p21 were determined in MCF-7 cells. Cells were incubated with 200 nM Oligo AS or ASM in the presence of Lipofectin for 24 h, followed by an addition of various concentrations of chemotherapeutic agents and an incubation for an additional 24 h. As illustrated in Fig. 2, *panel I, Lanes A*, HCPT induced p53 and p21 in a dose-dependent manner, as we reported in an early study with MCF-7 cells (67). After the treatment with Oligo AS, MDM2 expression was inhibited, resulting in a significant elevation in p53 and p21 levels by 3–8-fold (*panel I, Lanes C*). The mismatch control Oligo ASM showed minimal effect on the protein levels of MDM2, p53, or p21 (*panel I, Lanes B*). Adriamycin slightly induced p53 and p21 in MCF-7 cells (*panel II, Lanes A*). After the combination treatment with Oligo AS, MDM2 expression was inhibited, resulting in a significant elevation in p53 and p21 levels by 5–9-fold (*panel II, Lanes C*). The mismatch control Oligo ASM showed minimal effect on the protein levels of MDM2, p53, or p21 (*panel II, Lanes B*). The effects of Oligo AS on 5-FU-induced p53 and p21 levels were also evaluated (Fig. 2, *panel III*). 5-FU slightly induced p53 and p21 levels (*panel III, Lanes A*). After the treatment with Oligo AS, MDM2 expression was inhibited, resulting in a significant increase in p53 and p21 levels by 4–7-fold (*panel III, Lanes C*). The mismatch control Oligo ASM showed minimal effect on the protein levels of MDM2, p53, or p21 (*panel III, Lanes B*).

***In Vivo* Antitumor Activity of Anti-MDM2 Oligo in Human Breast Cancer MCF-7 Xenograft Model That Contains Wild-Type p53.** On the basis of previous studies with cell lines that contain wild-type p53 (62), the effect of Oligo AS on *in vivo* tumor growth was evaluated in the MCF-7 xenograft model at a daily i.p. dose of 25 mg/kg. Oligo AS showed significant inhibitory effects on tumor growth (Fig. 3*A*; Table 1). After 5-FU treatment (10 mg/kg/day), tumor growth was inhibited by ~50% on day 18 (Fig. 3*A*). After the combination treatment of Oligo AS and 5-FU, significant additive effects were observed (Fig. 3*A*; Table 1). Similar significant additive effects were observed after the combination treatment of Oligo AS and paclitaxel (Fig. 3*B*; Table 1). The mismatch control Oligo ASM showed no effect on tumor growth when administered alone and no effect on 5-FU- or paclitaxel-associ-

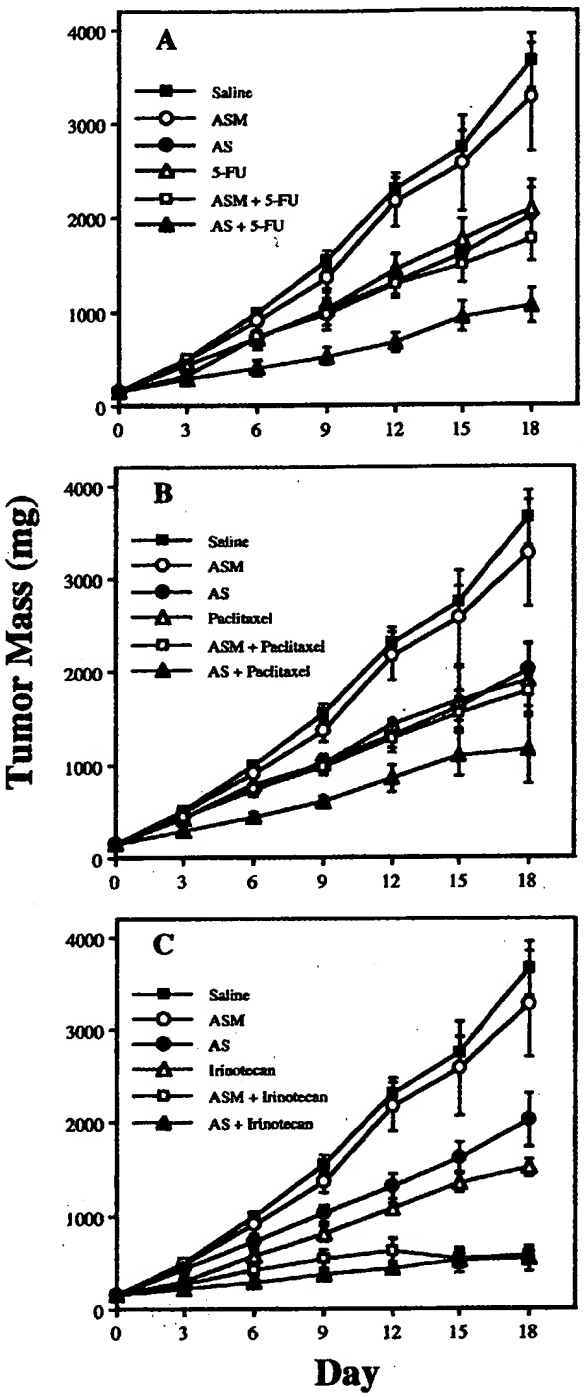

Fig. 3 In vivo synergistic effects between Oligo AS and chemotherapeutic agents 5-FU (*A*), paclitaxel (*B*), and irinotecan (*C*) in mice bearing human breast cancer MCF-7 xenografts. Additive or synergistic effects on tumor growth were noted in combination therapy.

Table 1 Therapeutic effectiveness of Anti-MDM2 oligonucleotide administered alone or in combination with chemotherapeutic agents (mean growth ratio: % T:C)[a]

The relative ratio ([2]/[1] or [3]/[1]) can be used to illustrate the potential additive or synergistic effects when the oligos were given in combination with cytotoxic agents. When the ratio for combination therapy (AS or ASM + chemotherapeutic agent) is <100% (compared with cytotoxic agents alone), an effect of Oligo is indicated. If the ratio for combination therapy is the same as that of oligo treatment alone, an additive effect is indicated. If the ratio for combination therapy is significantly smaller than that of oligo treatment alone, a synergistic effect is indicated, *e.g.*, at the end of the experiment (day 18) with MCF-7 model, the ratio for 5-FU + AS/5-FU is 51% (29:57%) and <100%, indicating an effect of oligo AS, and, in addition, this ratio is similar to that for oligo AS alone (55%; AS/saline), indicating an additive effect between 5-FU and Oligo AS. However, the ratio for irinotecan + AS/irinotecan is 36% (15:41%) and <100%, indicating an effect of oligo AS, and this ratio is significantly less than the ratio for oligo ASM alone (72%), indicating no synergistic effect but an additive effect, than that Oligo AS alone (55%), indicating a synergistic effect between irinotecan and Oligo AS. In conclusion, additive or synergistic effects between Oligo AS 5-FU, paclitaxel, or irinotecan were found throughout the treatment period. Synergistic effects between Oligo ASM and irinotecan were also found.

	No Oligo	+ Oligo ASM		+ Oligo AS	
Treatment	[1] (%)	[2] (%)	Ratio (%) ([2]/[1])	[3] (%)	Ratio (%) ([3]/[1])
MCF-7 xenograft model					
Oligo alone	100	89	89	55[b]	55
5-FU	57[b]	49[b]	85	29[b]	51[c]
Paclitaxel	52[b]	49[b]	94	32[b]	62[c]
Irinotecan	41[b]	16[b]	37[c]	15[b]	36[c]
MDA-MB-468 xenograft model					
Oligo alone	100	96	96	60[b]	60
5-FU	78[b]	72[b]	92	31[b]	40[c]
Paclitaxel	70[b]	52[b]	74[c]	29[b]	41[c]
Irinotecan	46[b]	18[b]	39[c]	4[b]	9[c]

[a] % T:C, percentage of mean tumor mass of treated group compared with the control group treated with saline.
[b] $P < 0.01$ when compared with saline control.
[c] $P < 0.01$ when compared with corresponding chemotherapeutics.

ated tumor growth inhibition in combination treatment (Fig. 3, *A* and *B*; Table 1). Western blot analyses of pooled MCF-7 xenograft tissues indicated that Oligo AS specifically inhibited MDM2 expression and activated p53 *in vivo* (Fig. 4*A*). The control Oligo ASM had no effect on the protein levels, additionally demonstrating the specificity of Oligo AS.

As shown in Fig. 3*C*, Oligo AS had significant synergistic effects on tumor growth with combination therapy with irinotecan (Fig. 3*C*; Table 1). Interestingly, the mismatch control Oligo ASM also showed the similar effects (Fig. 3*C*; Table 1). Although the underlying mechanism is not yet understood, Oligo AS and ASM may affect the pharmacokinetics and metabolism of irinotecan, a prodrug as a topoisomerase I inhibitor. Our preliminary data indicated that oligos increased the uptake of irinotecan in tumor tissues and the activation of irinotecan into its active form SN-38.[4]

***In Vitro* Activity of Antisense Anti-MDM2 Oligo AS in Human Breast Cancer MDA-MB-468 Model That Contains Mutant p53.** *In vitro* inhibition of MDM2 expression by Oligo AS occurred in a sequence-specific, dose-dependent manner (Fig. 1*B*). No significant changes in the protein levels of the mutant p53 were observed after Oligo AS treatment (Fig. 1*B*). The p21 levels were elevated, which is independent of p53 (Fig. 1*B*). The control Oligo ASM had significantly less effect on MDM2, p53, or p21 protein levels at 500 and 1000 nM concentrations. Oligo AS inhibited the growth of MDA-MB-468 cells *in vitro* in a dose-dependent manner, with a mean IC_{50} being 150 nM for a 72-h treatment. Oligo ASM had minimal effect on tumor cell growth.

The protein levels of MDM2, p53, and p21 were determined in MDA-MB-468 cells after *in vitro* combination treatment with Oligos and the chemotherapeutic agents HCPT, adriamycin, and 5-FU (Fig. 5). Cells were incubated with 200 nM Oligo in the presence of Lipofectin for 24 h, followed by an addition of various concentrations of chemotherapeutic agents and incubation for an additional 24 h. As shown in Fig. 5, after the treatment with Oligo AS, MDM2 expression was inhibited (*panels I–III, Lanes C*). The mismatch control Oligo ASM showed minimal effects on MDM2 levels (*panels I–III, Lanes B*). As shown in Fig. 5 (*panels II and III, Lanes C*), after the combination treatment with Oligo AS and adriamycin or 5-FU, p21 levels were elevated. The mismatch control Oligo ASM showed minimal effects on the p21 levels (*Lanes B*). No significant changes in p21 levels were observed with HCPT treatment (*panel I*). No changes in p53 levels in cells untreated or treated with HCPT, adriamycin, or 5-FU were observed, additionally indicating that the changes in MDM2 and p21 levels were independent of p53.

***In Vivo* Antitumor Activity of Anti-MDM2 Oligo in Human Breast Cancer MDA-MB-468 Model That Contains Mutant p53 after the Treatment of Oligo Alone or in Combination with Cancer Chemotherapeutics.** The effect of Oligo AS on *in vivo* tumor growth was demonstrated in the MDA-MB-468 xenograft model (Fig. 6*A*; Table 1). After the treatment of 5-FU alone (10 mg/kg/day, 5 days/week), limited tumor growth inhibition was observed (Fig. 6*A*; Table 1). After the treatment of combination with Oligo AS and 5-FU, however, significant synergistic effects on tumor growth were observed

[4] Wang, H. *et al.*, unpublished data.

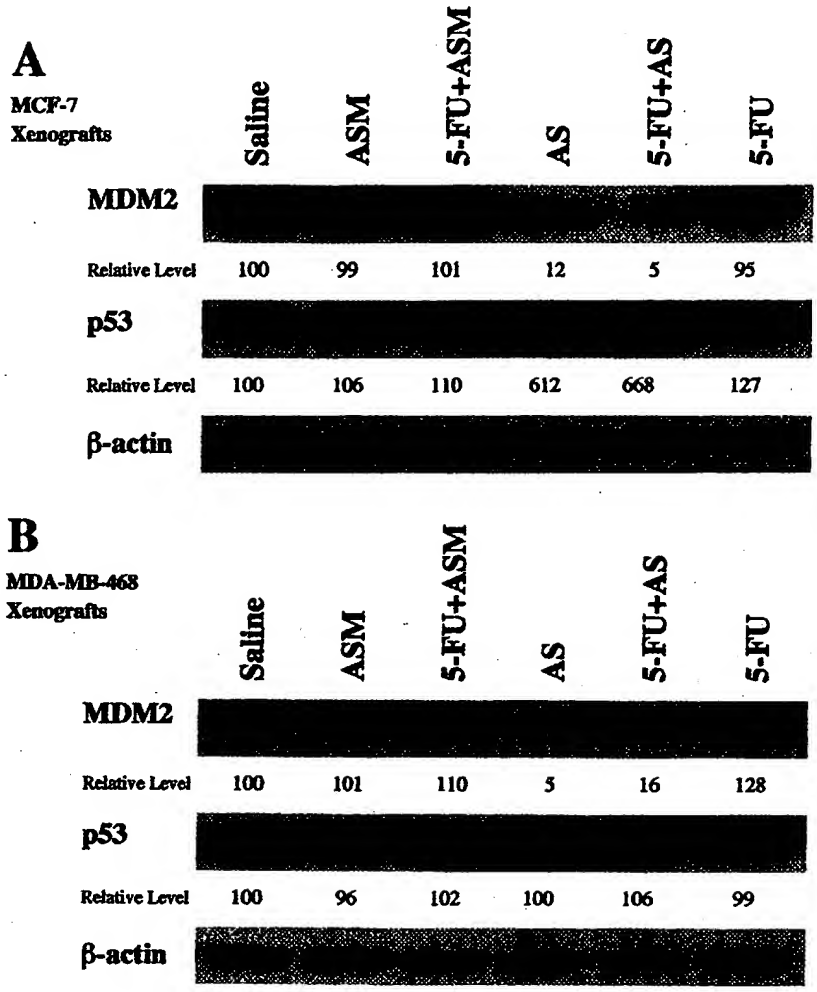

Fig. 4 *In vivo* inhibition of MDM2 expression by Oligos. Oligo AS inhibited the MDM2 expression in MCF-7 xenograft (*A*) and MDA-MB-468 xenograft (*B*). Identical amounts of total protein from the tumor homogenates (100 μg) were analyzed by Western blot using a monoclonal anti-MDM2 or anti-p53 antibody. The mismatch oligo, Oligo ASM, showed no effect. The p53 levels were elevated in MCF-7 model, and no change in p53 levels was observed in MDA-MB-468 model. Relative levels of each protein were expressed as a percentage of control (*Saline*), normalized by corresponding β-actin level.

(Fig. 6*A*; Table 1). Similar significant synergistic effects were observed after the combination treatment of Oligo AS and paclitaxel (Fig. 6*B*; Table 1). The mismatch control Oligo ASM showed no effect on 5-FU or Paclitaxel-induced tumor growth inhibition (Fig. 6, *A* and *B*; Table 1), additionally confirming the specificity of Oligo AS as an antisense agent. Western blot analyses of pooled MDA-MB-468 xenograft tissues indicated that Oligo AS specifically inhibited MDM2 expression *in vivo*, with p53 levels remaining unchanged (Fig. 4*B*). Oligo ASM had no effect on the protein levels, additionally demonstrating the specificity of Oligo AS. The combination treatment of Oligo AS and irinotecan induced tumor regression in the MDA-MB-468 xenograft model, additionally demonstrating the effect of Oligo AS as a sensitizer of chemotherapy (Fig. 6*C*; Table 1). The control oligo ASM showed less impact on irinotecan effectiveness.

DISCUSSION

MDM2 oncogene has been suggested as a novel target for cancer therapy, especially the p53-MDM2 interaction pathway. In the past few years, several strategies have been used to test the hypothesis that, by disrupting p53-MDM2 interaction, the negative regulation of p53 by MDM2 is diminished, and the cellular functional p53 level is increased, particularly after DNA damaging treatment, resulting in tumor growth arrest and/or apoptosis that leads to better therapeutic responses. These approaches include the use of polypeptides (68), antibodies (69–71), and antisense oligos (61–63). The purpose of the present study was to investigate additionally the role of MDM2 in human breast cancer by using *in vitro* and *in vivo* models that contain wild-type p53 (MCF-7) or mutant p53 (MDA-MB-468) but with MDM2 expression. In the present study, we have demonstrated at least five significant results: (*a*) the novel anti-MDM2 mixed-backbone oligo, Oligo AS, specifically inhibited MDM2 expression in both MCF-7 and MDA-MB-468 cells in a dose-dependent manner, regardless of p53 status; (*b*) in a dose-dependent manner, the *in vivo* antitumor effects of Oligo AS were observed in both tumor xenograft models; (*c*) after combination therapy with Oligo AS and conventional cancer chemotherapeutic agents 5-FU, paclitaxel, and irinotecan, *in vivo* synergistic or additive therapeutic effects were found in both models, regardless of p53 status; (*d*) in MCF-7 cells, combination treatment with Oligo AS and cancer chemotherapeutic agents HCPT, adriamycin, and 5-FU significantly

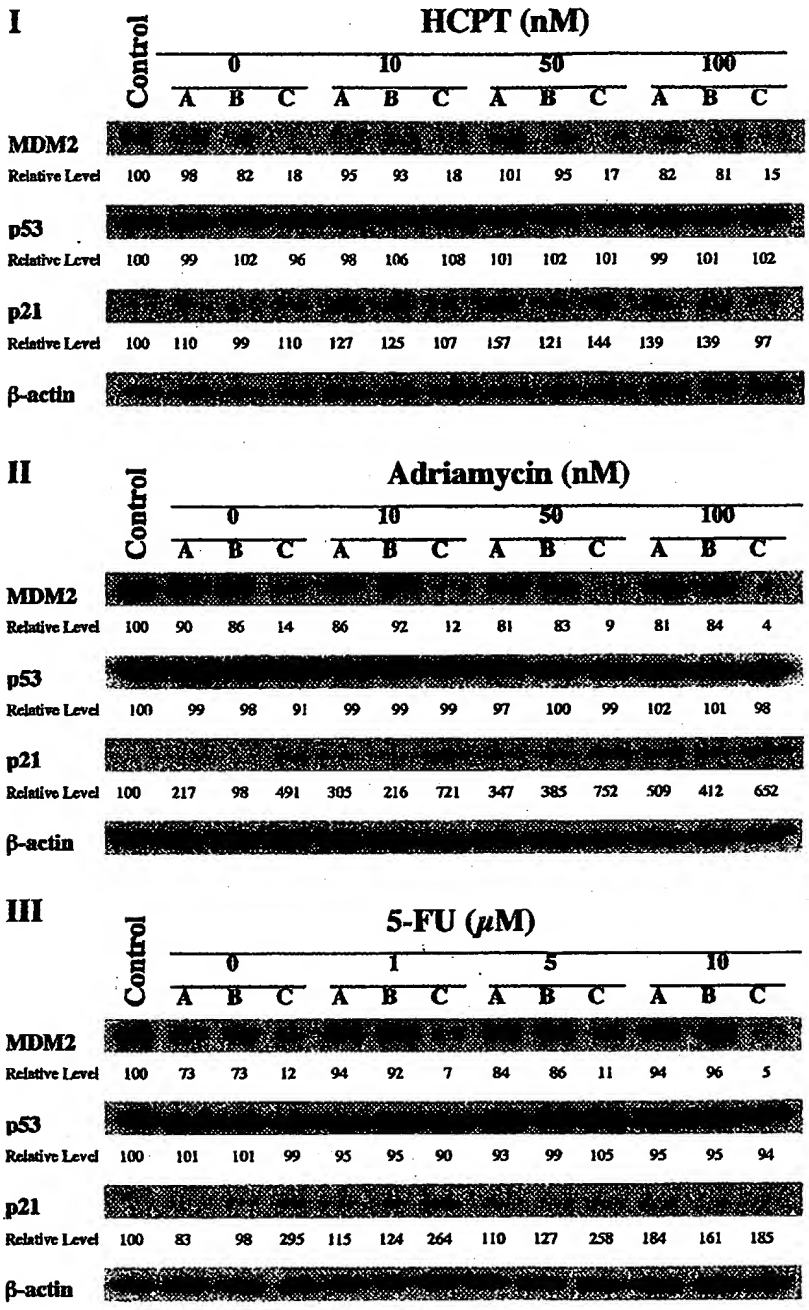

Fig. 5 Synergistic effects of combination treatment of Oligo AS and the cancer chemotherapeutic agents on MDM2, p53, and p21 protein levels in MDA-MB-468 cells in culture. Cells were incubated with 200 nM Oligo AS or ASM in the presence of Lipofectin for 24 h, followed by an addition of various concentrations of HCPT (*I*), adriamycin (*II*), or 5-FU (*III*) and incubation for an additional 24 h. At various concentrations, the effects on MDM2, p53, and p21 levels were evaluated after treatment with cytotoxic agents alone (*Lanes A*) or pretreatment with Oligo ASM (*Lanes B*) or Oligo AS (*Lanes C*). Relative levels of each protein were expressed as a percentage of control, normalized by corresponding β-actin level.

elevated chemotherapeutic agent-induced p53 and p21 levels, resulting from MDM2 expression, indicating that the *in vivo* synergistic effects between Oligo AS and conventional chemotherapeutic agents be associated with a p53-dependent pathway in cancers containing wild-type p53 expression; and (*e*) in MDA-MB-468 cells, combination treatment with Oligo AS and the cancer chemotherapeutic agents HCPT, adriamycin, and 5-FU had no effect on the mutant p53 levels. Oligo AS specifically inhibited MDM2 expression and increased p21 levels, indicating that the *in vivo* synergistic or additive effects between Oligo AS and conventional chemotherapeutic agents are independent of p53 but associated with MDM2 and possibly with p21.

The role of MDM2 in human cancer has been extensively studied. Overexpression of MDM2 is associated with poor prognosis in human malignancies, including breast cancer. Studies suggest that overexpression of MDM2 be associated with inactivation of wild-type p53, and inhibiting MDM2 expression in these tumors may lead to reactivation of p53 and induction of cell growth arrest or apoptosis. The majority of clinically used cancer therapeutic agents exert their cytotoxic effects through activation of wild-type p53, and the restoration of wild-type p53

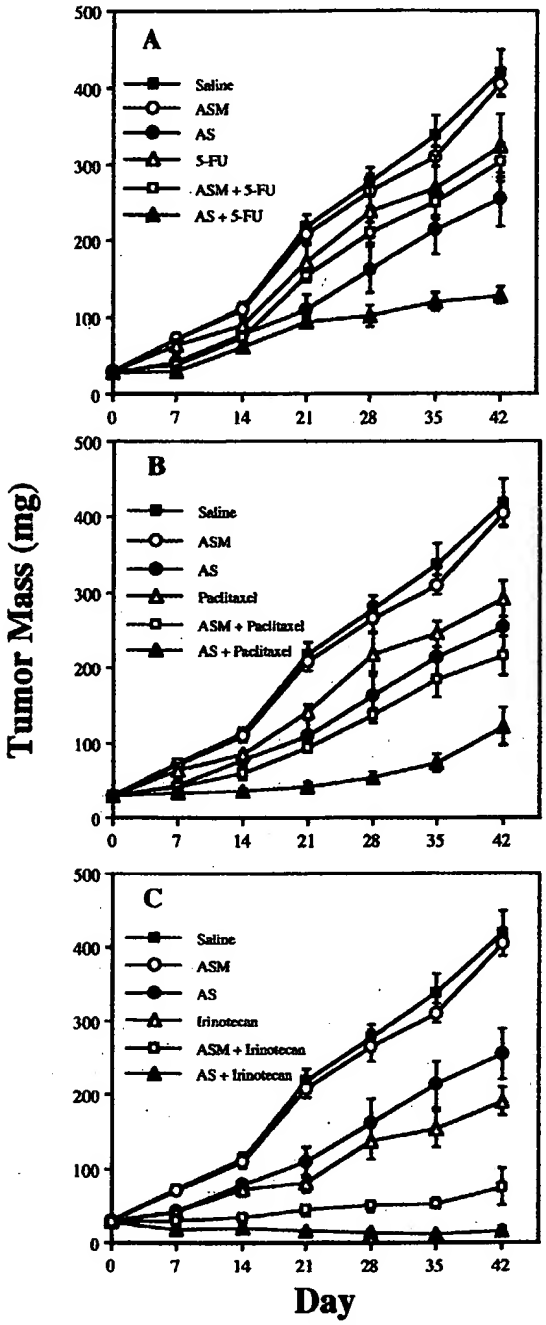

Fig. 6 *In vivo* synergistic effects between Oligo AS and chemotherapeutic agents 5-FU (*A*), paclitaxel (*B*), and irinotecan (*C*) in mice bearing human breast cancer MDA-MB-468 xenografts. Synergistic or additive effects on tumor growth were noted in combination therapy.

can increase the sensitivity of tumors to DNA-damaging agents. Restoration of wild-type p53 may also overcome the drug resistance of human cancers associated with dysfunction of p53. Activation of p53 by DNA damage, such as cancer chemotherapy and radiation treatment, may, however, be limited in cancers with MDM2 expression. Therefore, inactivation of the MDM2 negative feedback loop may increase the magnitude of p53 activation after DNA damage, thus enhancing the therapeutic effectiveness of DNA damaging drugs. In the present study, we provided experimental evidence supporting this hypothesis. In MCF-7 cells that contain wild-type p53, the cancer chemotherapeutic agents HCPT, adriamycin, and 5-FU induced p53 levels, which, however, was limited because of MDM2 expression. After treatment with Oligo AS, MDM2 expression was specifically inhibited, resulting in significant increases in cytotoxic agent-induced p53 and p21 levels. These findings are consistent with the *in vivo* synergistic effects after combination treatment of Oligo AS and cytotoxic agents 5-FU, paclitaxel, and irinotecan. These results additionally confirm our earlier findings with cell lines that contain amplified *MDM2* gene and overexpressed MDM2 protein (61–63). Therefore, we conclude that the MDM2-p53 interaction can serve as a novel drug target, even if MDM2 and/or p53 are expressed at basal levels.

p53-independent activity of MDM2 has also been suggested (72–75). *MDM2* gene products include at least five forms of polypeptide, representing alternatively spliced MDM2 variants (76). Various alternatively spliced MDM2 polypeptides are present in several human tumors (77–79). Of the five forms of MDM2 analogues, only one retains p53 binding capacity. However, cDNAs coding for all five forms of alternatively spliced MDM2 independently transform NIH 3T3 cells, indicating that these MDM2 transcripts have the p53-independent transforming ability (78, 79). The effects of MDM2 overexpression on mammary tumorigenicity are seen in p53-null mice (34), indicating that MDM2 can cause transformation and tumor formation via a p53-independent mechanism. Furthermore, overexpression of MDM2 is associated with resistance to the antiproliferative effects of transforming growth factor β, which is p53 independent (80).

In the present study, we have provided direct evidence supporting the possibility of p53-independent activity of MDM2. In MDA-MB-468 cells that contain mutant p53, Oligo AS and the cancer chemotherapeutic agents HCPT, adriamycin, and 5-FU had no effect on the mutant p53 levels. After treatment with Oligo AS, MDM2 expression was specifically inhibited, resulting in a significant increase in cytotoxic agent-induced p21 levels. More important, *in vivo* antitumor activity of Oligo AS was observed in the MDA-MB-468 model after administration alone or in combination with cytotoxic agents 5-FU, paclitaxel, and irinotecan, which is independent of p53 status. Although the mechanisms responsible for increasing p21 levels after MDM2 inhibition were not determined in the present study, the interaction between MDM2 and p21 is indicated. Our earlier studies indicated that in human tumor cells treated with HCPT, up-regulation of p21 is both p53 dependent and p53 independent (67). Additional study should elucidate the potential interaction between MDM2 and p21 and its role in tumor transformation and growth.

One of the advantages of using antisense oligos or MDM2-specific antibodies is that these agents may exert their effects in all MDM2-expressing tumors regardless of p53 status. This is important because the p53-independent activity of MDM2 may play a role in MDM2 tumorigenicity, and ~50% of human cancers have mutant p53 expression. Inhibition of MDM2 expression will ultimately prevent the interaction of MDM2 and other cellular proteins, *e.g.*, the antisense anti-MDM2 oligo we

developed (61–63) increases E2F-1 levels after microinjection, as demonstrated by others (81).

To our surprise, both Oligo AS and ASM showed synergistic effects on tumor growth inhibition when used in combination with irinotecan. Although the exact mechanisms are not determined in the present study, both pharmacokinetic and pharmacodynamic mechanisms may be involved, including uptake and retention of the parent drug (irinotecan) and its active form (SN-38), plasma protein binding of the drug, conversion of irinotecan to SN-38, or interaction of oligo with the drug target (topoisomerase I) and DNA. Nevertheless, the finding that oligos significantly increase the therapeutic effectiveness of irinotecan, a clinically used cancer therapeutic agent, will provide a new means to best use this agent and its analogues. More recently, Oligo AS, but not ASM, has been shown to specifically increase therapeutic effects of two analogues of irinotecan, HCPT (62) and topotecan (82), indicating a unique interaction between oligos and irinotecan.

In conclusion, we have demonstrated that the selected specific antihuman-MDM2 mixed-backbone oligo had significant antitumor activity in both *in vitro* and *in vivo* breast cancer models, regardless of p53 status, suggesting that MDM2 has a role in tumor growth through both p53-dependent and p53-independent mechanisms. We speculate that MDM2 inhibitors, such as antisense anti-MDM2 oligos, have a broad spectrum of antitumor activities in human cancers regardless of p53 status. Therefore, this study should provide a basis for future development of anti-MDM2 antisense oligos as cancer therapeutic agents used alone or in combination with conventional chemotherapeutics.

ACKNOWLEDGMENTS

We thank Zhuo Zhang and Gautam Prasad for excellent technical assistance.

REFERENCES

1. Zakut-Houri, R., Bienz-Tadmor, B., Givol, D., and Oren, M. Human P53 cellular tumor antigen: cDNA sequence and expression in COS cells. EMBO J., *4:* 1251–1255, 1983.

2. Prives, C., and Hall, P. A. The p53 pathway. J. Pathol., *187:* 112–126, 1999.

3. Donehower, L. A., and Bradley, A. The tumor suppressor p53. Biochim. Biophys. Acta, *1155:* 181–205, 1993.

4. Vogelstein, B., and Kinzler, K. W. p53 function and dysfunction. Cell, *70:* 523–526, 1992.

5. Livingstone, L. R., White, A., Sprouse, J., Livanos, E., Jacks, T., and Tlsty, T. D. Altered cell cycle arrest and gene amplification potential accompany loss of wild-type p53. Cell, *70:* 923–935, 1992.

6. Kastan, M. B., Zhan, Q., El-Deiry, W. S., Carrier, F., Jacks, T., Walsh, W. V., Plunkett, B. S., Vogelstein, B., and Fornace, A. J. A mammalian cell cycle checkpoint pathway utilizing p53 and GADD45 is defective in ataxia-telangiectasia. Cell, *71:* 587–597, 1992.

7. Hollstein, M. D., Sidransky, D., Vogelstein, B., and Harris, C. C. p53 mutations in human cancers. Science (Wash. DC), *253:* 49–53, 1991.

8. Hainaut, P., Soussi, T., Shomer, B., Hollstein, M., Greenblatt, M., Hovig, E., Harris, C. C., and Montesano, R. Database of *p53* gene somatic mutations in human tumors and cell lines: updated compilation and future prospects. Nucleic Acids Res., *25:* 151–157, 1997.

9. Slingerland, J. M., Minden, M. D., and Benchimol, S. Mutation of the *p53* gene in human acute myelogenous leukemia. Blood, *77:* 1500–1507, 1991.

10. Gaidano, G., Ballerimi, P., Gong, J. Z., Inghirami, G., Neri, A., Newcomb, E. W., Magrath, I. T., Knowles, D. M., and Dalla-Favera, R. p53 mutations in human lymphoid malignancies: association with Burkitt lymphoma and chronic lymphocytic leukemia. Proc. Natl. Acad. Sci. USA, *88:* 5413–5417, 1991.

11. Bartek, J., Iggo, R., Gannon, J., and Lane, D. P. Genetic and immunochemical analysis of mutant p53 in human breast cancer cell lines. Oncogene, *5:* 893–899, 1990.

12. Nigro, J. M., Baker, S. J., Preisinger, A. C., Jessup, J. M., Hostetter, R., Cleary, K., Bigner, S. H., Davidson, N., Baylin, S., Devilee, P., Glover, T., Collins, F. S., Weston, A., Modali, R., Harris, C. C., and Vogelstein, B. Mutations in the *p53* gene occur in diverse human tumor types. Nature (Lond.), *342:* 705–707, 1989.

13. Iggo, R., Gatter, K., Bartek, J., Lane, D., and Harris, A. L. Increased expression of mutant forms of p53 oncogene in primary lung cancer. Lancet, *335:* 675–679, 1990.

14. Horak, E., Smith, K., Bromley, L., Lejeune, S., Greenall, M., Lane, D., and Harris, A. L. Mutant p53, EGF receptor and c-erbB-2 expression in human breast cancer. Oncogene, *6:* 2277–2284, 1991.

15. Varley, J. M., Brammar, W. J., Lane, D., Swallow, J. E., Dolan, C., and Walker, R. A. Loss of chromosome 17p13 sequences and mutation of p53 in human breast carcinomas. Oncogene, *6:* 413–421, 1991.

16. Saitoh, S., Cunningham, J., De Vries, E. M. G., McGovern, R. M., Schroeder, J. J., Harmann, A., Blaszyk, H., Wold, L. E., Schaid, D., Sommer, S. S., and Kovach, J. S. P53 gene mutations in breast cancers in midwestern US women: null as well as missense-type mutations are associated with poor prognosis. Oncogene, *9:* 2869–2875, 1994.

17. Akslen, L. A., and Morkve, O. Expression of p53 protein in cutaneous melanoma. Int. J. Cancer, *52:* 13–16, 1992.

18. Kovach, J. S., Hartmann, A., Blaszyk, H., Cunnigham, J., Schaid, D., and Sommer, S. S. Mutation detection by highly sensitive methods indicates that p53 gene mutations in breast cancer can have important prognostic value. Proc. Natl. Acad. Sci. USA, *93:* 1093–1096, 1996.

19. Silvestrini, R., Daidone, M. G., Benini, E., Faranda, A., Tomasic, G., Boracchi, P., Salvadori, B., and Veronesi, U. Validation of p53 accumulation as a predictor of distant metastasis at 10 years of follow-up in 1400 node-negative breast cancers. Clin. Cancer Res., *2:* 2007–2013, 1996.

20. Kastan, M. B., Onyekwere, O., Sidransky, D., Vogelstein, B., and Craig, R. W. Participation of p53 protein in the cellular response to DNA damage. Cancer Res., *51:* 6304–6311, 1991.

21. Clarke, A. R., Purdie, C. A., Harrison, D. J., Morris, R. G., Bird, C. C., Hooper, M. L., and Wyllie, A. H. Thymocyte apoptosis induced by p53-dependent and independent pathways. Nature (Lond.), *362:* 849–852, 1993.

22. Di Leonardo, A., Linke, S. P., Clarkin, K., and Wahl, G. M. DNA damage triggers a prolonged p53-dependent G1 arrest and long-term induction of Cip1 in normal human fibroblasts. Genes Dev., *8:* 2540–2551, 1994.

23. Kuerbits, S. J., Plundett, B. S., Walsh, W. V., and Kastan, M. B. Wild-type p53 is a cell cycle checkpoint determinant following irradiation. Proc. Natl. Acad. Sci. USA, *89:* 7491–7495, 1992.

24. Wu, X., Bayle, J. H., Olson, D., and Levine, A. J. The p53-mdm2 autoregulatory feedback loop. Genes Dev., *7:* 1126–1132, 1993.

25. Fornace, A. J., Jr., Nebert, D. W., Hollander, M. C., Luethy, J. D., Papathanasiou, M. A., Fargnoli, J., and Holbrook, N. J. Mammalian genes coordinately regulated by growth arrest signals and DNA-damaging agents. Mol. Cell. Biol., *9:* 4196–4203, 1989.

26. El-Deiry, W. S., Harper, J. W., O'Connor, P. M., Velculescu, V. E., Canman, C. E., Jackman, J., Pietenpol, J. A., Burrell, M., Hill, D. E., Wang, Y., Wiman, K. G., Mercer, W. E., Kastan, M. B., Kohn, K. W., Elledge, S. J., Kinzler, K. W., and Volgelstein, B. WAF1/CIP1 is induced in p53-mediated G1 arrest and apoptosis. Cancer Res., *54:* 1169–1174, 1994.

27. O'Connor, P. M., Jackman, J., Bae, I., Myers, T. G., Fan, S., Mutoh, M., Scudiero, D. A., Monks, A., Sausville, E. A., Weinstein, J. N., Friend, S., Fornace, A. J., and Kohn, K. W. Characterization of the p53 tumor suppressor pathway in cell lines of the National Cancer Institute

anticancer drug screen and correlations with the growth-inhibitory potency of 123 anticancer agents. Cancer Res., *57:* 4285–4300, 1997.

28. Baker, S. J., Markowitz, S., Fearon, E. R., Willson, J. K. V., and Vogelstein, B. Suppression of human colorectal carcinoma cell growth by wild-type p53. Science (Wash. DC), *249:* 912–915, 1990.

29. Diller, L., Kassel, J., Nelson, C. E., Gryka, M. A., Litwak, G., Gebhardt, M., Bressac, B., Ozturk, M., Baker, S. J., Vogelstein, B., and Friend, S. H. p53 functions as a cell cycle control protein in osteosarcomas. Mol. Cell. Biol., *10:* 5772–5781, 1990.

30. Wang, N. P., To, H., Lee W-H., and Lee, EY-HP. Tumor suppressor activity of *RB* and *p53* genes in human breast carcinoma cells. Oncogene, *8:* 279–288, 1993.

31. Dorigo, O., Turla, S. T., Lebedeva, S., and Gjerset, R. A. Sensitization of rat glioblastoma multiforme to cisplatin *in vivo* following restoration of wild-type p53 function. J. Neurosurg., *88:* 535–540, 1998.

32. Nielsen, L. L., and Maneval, D. C. P53 tumor suppressor gene therapy for cancer. Cancer Gene Ther., *5:* 52–63, 1998.

33. Fakharzadeh, S. S., Trusko, S. P., and George, D. L. Tumorigenic potential associated with enhanced expression of a gene that is amplified in a mouse tumor cell line. EMBO J., *10:* 1565–1569, 1991.

34. Lundgren, K., Montes de Oca Luna, R., Mcneill, Y. B., Emerick, E. P., Spencer, B., Barfield, C. R., Lozano, G., Rosenberg, M. P., and Finlay, C. A. Targeted expression of MDM2 uncouples S phase from mitosis and inhibits mammary gland development independent of p53. Genes Dev., *11:* 714–725, 1997.

35. Zhang, R., and Wang, H. MDM2 oncogene as a novel target for human cancer therapy. Curr. Pharm. Des., *6:* 393–416, 2000.

36. McCann, A. H., Kirley, A., Carney, D. N., Corbally, N., Magee, H. M., Keating, G., and Dervan, P. A. Amplification of the *MDM2* gene in human breast cancer and its association with MDM2 and p53 protein status. Br. J. Cancer, *71:* 981–985, 1995.

37. Marchetti, A., Buttitta, F., Girlando, S., Dalla Palma, P., Pellegrini, S., Fina, P., Doglioni, C., Bevilacqua, G., and Barbareschi, M. *mdm2* gene alterations and mdm2 protein expression in breast carcinomas. J. Pathol., *175:* 31–38, 1995.

38. Quesnel, B., Preudhomme, C., Fournier, J., Fenaux, P., and Peyrat, J. P. *MDM2* gene amplification in human breast cancer. Eur. J. Cancer, *30A:* 982–984, 1994.

39. Courjal, F., Cuny, M., Rodriguez, C., Louason, G., Speiser, P., Katsaros, D., Tanner, M. M., Zeillinger, R., and Theillet, C. DNA amplifications at 20q13 and MDM2 define distinct subsets of evolved breast and ovarian tumours. Br. J. Cancer, *74:* 1984–1989, 1996.

40. Fontana, X., Ferrari, P., Abbes, M., Monticelli, J., Namer, M., and Bussiere, F. Study of *mdm2* gene amplification in primary breast tumors. Bull. Cancer (Paris), *81:* 587–592, 1994.

41. Cuny, M., Kramar, A., Courjal, F., Johannsdottir, V., Iacopetta, B., Fontaine, H., Grenier, J., Culine, S., and Theillet, C. Relating genotype and phenotype in breast cancer: an analysis of the prognostic significance of amplification at eight different genes or loci and of p53 mutations. Cancer Res., *60:* 1077–1083, 2000.

42. Sheikh, M. S., Shao, Z-M., Hussain, A., and Fontana, J. A. The p53-binding protein *MDM2* gene is differentially expressed in human breast carcinoma. Cancer Res., *53:* 3226–3228, 1993.

43. Jiang, M., Shao Z-M., Wu, J., Lu, J-S., Yu, L-M., Yuan, J-D., Han, Q-X., Shen, Z-Z., and Fontana, J. A. P21/waf1/cip1 and mdm-2 expression in breast carcinoma patients as related to prognosis. Int. J. Cancer, *74:* 529–534, 1997.

44. Giannikaki, E., Kouvidou, C. H., Tzardi, M., Stefanaki, K., Koutsoubi, K., Gregoriou, M., Zois, E., Kakolyris, S., Mavroudi, C., Delides, G., Georgoulias, V., and Kanavaros, P. P53 protein expression in breast carcinoma. Comparative study with the wild type p53 induced proteins mdm2 and p21/waf1. Anticancer Res., *17:* 2123–2128, 1997.

45. O'neill, M., Campbell, S. J., Save, V., Thompson, A. M., and Hall, P. A. An immunochemical analysis of mdm2 expression in human breast cancer and the identification of a growth-regulated cross-reacting species p170. J. Pathol., *186:* 254–261, 1998.

46. Barak, Y., Juven, T., Haffner, R., and Oren, M. Mdm2 expression is induced by wild type p53 activity. EMBO J., *12:* 461–468, 1993.

47. Momand, J., Zambetti, G. P., Olson, D. C., George, D., and Levine, A. J. The mdm-2 oncogene product forms a complex with the p53 protein and inhibits p53-mediated transactivation. Cell, *69:* 1237–1245, 1992.

48. Oca-Luan, R. M., Wagner, D. S., and Lozano, G. Rescue of early embryonic lethality in mdm-2-deficient mice by deletion of p53. Nature (Lond.), *378:* 203–206, 1995.

49. Jones, S. N., Roe, A. E., Donehower, L. A., and Bradley, A. Rescue of embryonic lethality in Mdm2-deficient mice by absence of p53. Nature (Lond.), *378:* 206–208, 1995.

50. Chen, C. Y., Oliner, J. D., Zhan, Q., Fornace, A. J., Jr., Vogelstein, B., and Kastan, M. B. Interactions between p53 and MDM2 in a mammalian cell cycle checkpoint pathway. Proc. Natl. Acad. Sci. USA, *91:* 2684–2688, 1994.

51. Chen, J., Wu, X., Lin, J., and Levine, A. J. Mdm-2 inhibits the G1 arrest and apoptosis functions of the p53 tumor suppressor protein. Mol. Cell. Biol., *16:* 2445–2452, 1996.

52. Chen, J., Lin, J., and Levine, A. J. Regulation of transcription functions of the p53 tumor suppressor by the mdm2 oncogene. Mol. Med., *1:* 142–152, 1995.

53. Haupt, Y., Maya, R., Kazaz, A., and Oren, M. Mdm2 promotes the rapid degradation of p53. Nature (Lond.), *387:* 296–299, 1997.

54. Kubbutat, M. H. G., Jones, S. N., and Vousden, K. H. Regulation of p53 stability by mdm2. Nature (Lond.), *387:* 299–303, 1997.

55. Xiao, Z., Chen, J., Levine, A. J., Modjtahedi, N., Xing, J., Sellers, W. R., and Livington, D. M. Interaction between the retinoblastoma protein and the oncoprotein MDM2. Nature (Lond.), *375:* 694–698, 1995.

56. Martin, K., Trouche, D., Hagemeier, C., Sorensen, T. S., La Thangue, N. B., and Kouzarides, T. Stimulation of E2F1/DP1 transcriptional activity by MDM2 oncoprotein. Nature (Lond.), *375:* 691–694, 1995.

57. Marechal, V., Elenbaas, B., Piette, J., Nicholas, J., and Levine, A. J. The ribosomal L5 protein is associated with mdm-2 and mdm-2-p53 complexes. Mol. Cell. Biol., *14:* 7414–7420, 1994.

58. Elenbaas, B., Matthias, D., Roth, J., Shenk, T., and Levine, A. J. The MDM2 oncoprotein binds specifically to RNA through its RING finger domain. Mol. Med., *2:* 439–451, 1996.

59. Zamecnik, P. C. History of antisense oligonucleotides. *In:* S. Agrawal (ed.), Antisense Therapeutics, pp.1–12. Totowa: Humana Press, 1996.

60. Diasio, R. B., and Zhang, R. Pharmacology of Therapeutic Oligonucleotides. Antisense Nucleic Acid Drug Dev., *7:* 239–243, 1999.

61. Chen, L., Agrawal, S., Zhou, W., Zhang, R., and Chen, J. Synergistic activation of p53 by inhibition of MDM2 expression and DNA damage. Proc. Natl. Acad. Sci. USA, *95:* 195–200, 1998.

62. Wang, H., Oliver, P., Zeng, X., Chen, J., Chen, L., Zhou, W., Agrawal, S., and Zhang, R. MDM2 oncogene as a target for cancer therapy: an antisense approach. Int. J. Oncol., *15:* 653–660, 1999.

63. Chen, L., Lu, W., Agrawal, S., Zhou, W., Zhang, R., and Chen, J. Ubiquitous induction of p53 in tumor cells by antisense inhibition of MDM2 expression. Mol. Med., *5:* 21–34, 1999.

64. Agrawal, S., Jiang, Z., Zhao, Q., Shaw, D., Cai, Q., Roskey, A., Channavajjala, L., Saxinger, C., and Zhang, R. Mixed-backbone oligonucleotides as second generation antisense oligonucleotides: *in vitro* and *in vivo* studies. Proc. Natl. Acad. Sci. USA, *94:* 2620–2625, 1997.

65. Cai, Q., Lindsey, J. R., and Zhang, R. Regression of human colon cancer xenografts in SCID mice following oral administration of water-insoluble camptothecins, natural product topoisomerase I inhibitors. Int. J. Oncol., *10:* 953–960, 1997.

66. Wang, H., Cai, Q., Zeng, X., Yu, D., Agrawal, S., and Zhang, R. Anti-tumor activity and pharmacokinetics of a mixed-backbone antisense oligonucleotide targeted to RIα subunit of protein kinase A after oral administration. Proc. Natl. Acad. Sci. USA, *96:* 13989–13994, 1999.

67. Liu, W., and Zhang, R. Upregulation of p21/$^{WAF1/CIP1}$ in human breast cancer cell lines MCF-7 and MDA-MB-468 undergoing apoptosis induced by natural product anticancer agents 10-hydroxycamptothecin and camptothecin through p53-dependent and independent pathways. Int. J. Oncol., *12:* 793–804, 1998.

68. Bottger, A., Bottger, V., Sparks, A., Liu, W. L., Howard, S. F., and Lane, D. P. Design of a synthetic Mdm2-binding mini protein that activates the p53 response *in vivo*. Curr. Biol., *7:* 860–869, 1997.

69. Midgley, C. A., and Lane, D. P. P53 protein stability in tumor cells is not determined by mutation but is dependent on Mdm2 binding. Oncogene, *15:* 1179–1189, 1997.

70. Bottger, A., Bottger, A., Garcia, E. C., Garcia-Echeverria, C., Chene, P., Hochkeppel, H-K., Smapson, W., Ang, K., Howard, S. F., Picksley, S. M., and Lane, D. P. Molecular characterization of the hdm2–p53 interaction. J. Mol. Biol., *269:* 744–756, 1997.

71. Blattner, C., Sparks, A., and Lane, D. Transcription factor E2F-1 is upregulated in response to DNA damage in a manner analogous to that of p53. Mol. Cell. Biol., *19:* 3704–3713, 1999.

72. Juven-Gershon, T., and Oren, M. Mdm2: the ups and downs. Mol. Med., *5:* 71–83, 1999.

73. Freedman, D. A., Wu, L., and Levine, A. J. Functions of the MDM2 oncoprotein. Cell Mol. Life Sci., *55:* 96–107, 1999.

74. Freedman, D. A., and Levine, A. J. Regulation of p53 protein by MDM2 oncoprotein: thirty eighth G. H. A. Clowes memorial award lecture. Cancer Res., *59:* 1–7, 1999.

75. Momand, J., Jung, D., Wilczynski, S., and Niland, J. The MDM2 gene amplification database. Nucleic Acids Res., *26:* 3453–3459, 1998.

76. Olson, D. C., Marechal, V., Momand, J., Chen, J., Romocki, C., and Levine, A. Identification and characterization of multiple mdm-2 proteins and mdm-2-p53 protein complexes. Oncogene, *8:* 2353–2360, 1993.

77. Sigalas, I., Calvert, A. H., Anderson, J. J., Neal, D. E., and Lunec, J. Alternatively spliced mdm2 transcripts with loss of p53 binding domain sequences: transforming ability and frequent detection in human cancer. Nat. Med., *2:* 912–917, 1996.

78. Matsumoto, R., Tada, M., Nozaki, M., Zhang, C-L., Sawamura, Y., and Abe, H. Short alternative splice transcripts of the mdm2 oncogene correlate to malignancy in human astrocytic neoplasms. Cancer Res., *58:* 609–613, 1998.

79. Pinkas, J., Naber, S. P., Butel, J. S., Medina, D., and Jerry, D. J. Expression of MDM2 during mammary tumorigenesis. Int. J. Cancer, *81:* 292–298, 1999.

80. Sun, P., Dong, P., Dai, K., Hannon, G. J., and Beach, D. p53-independent role of MDM2 in TGFβ1 resistance. Science (Wash. DC), *282:* 2270–2272, 1998.

81. Blattner, C., Sparks, A., and Lane, D. Transcription factor E2F-1 is upregulated in response to DNA damage in a manner analogous to that of p53. Mol. Cell. Biol.,19: 3704–3713, 1999.

82. Tortora, G., Caputo, R., Damiano, V., Bianco, R., Chen, J., Agrawal, S., Bianco, A. R., and Ciardiello, F. A novel MDM2 anti-sense oligonulveotide has anti-tumor activity and potentiates cytotoxic drugs acting by different mechanisms in human colon cancer. Int. J. Cancer, *88:* 804–809, 2000.

EXHIBIT B

Potentiation of antitumor activity of irinotecan by chemically modified oligonucleotides

SUDHIR AGRAWAL[1], EKAMBAR R. KANDIMALLA[1], DONG YU[1], BETH A. HOLLISTER[2], SHIH-FONG CHEN[2], DANIEL L. DEXTER[2], TERRI L. ALFORD[2], BRENDA HILL[2], KAREN S. BAILEY[3], CHRISTINE P. BONO[3], DEBORAH L. KNOERZER[3] and PHILLIP A. MORTON[3]

[1]Hybridon, Inc., 345 Vassar Street, Cambridge, MA 02139; [2]Piedmont Research Center, 3300 Gateway Center, Morrisville, NC 27560; [3]Discovery Oncology/Pharmacology, Pharmacia Corporation, 700 Chesterfield Village Parkway North, St. Louis, MO 63198, USA

Received February 2, 2001; Accepted March 5, 2001

Abstract. Co-administration of synthetic chemically modified oligonucleotides with irinotecan, a selective topoisomerase I inhibitor, provided a significant enhancement in the antitumor activity of irinotecan. The enhancement of antitumor activity of irinotecan with co-administration of chemically modified oligonucleotides was observed in several tumor models - pancreatic cancer (Panc-1), colon cancer (HCT-116) and melanoma (A375). Inhibition of tumor growth in all three models required the co-administration of irinotecan and chemically modified oligonucleotides, but was independent of the nucleotide sequence of the oligonucleotides. The potentiation of antitumor activity was dependent on the dose of irinotecan and chemically modified oligonucleotides administered. The enhancement of antitumor activity of irinotecan was also observed by co-administration of a phosphorothioate oligonucleotide, however, to a lesser extent than did chemically modified oligonucleotides, suggesting that metabolic stability of the oligonucleotide contributes to the enhancement of antitumor activity seen with irinotecan. The co-administration of dextran sulfate sodium with irinotecan showed insignificant potentiation of antitumor activity of irinotecan, suggesting that the enhancement of antitumor activity of irinotecan observed was not a result of polyanionic characteristic of oligonucleotides. Co-administration of irinotecan and chemically modified oligonucleotides did not result in increased toxicity in the tumor models studied. Potentiation of antitumor activity of irinotecan observed with co-administration of oligonucleotides suggests that the oligonucleotides affect the pharmacokinetics and/or metabolism of irinotecan. The use of chemically modified oligonucleotides together with irinotecan may increase the therapeutic index of irinotecan in cancer patients and continued development of such agents should be considered.

Correspondence to: Dr Sudhir Agrawal, Hybridon, Inc., 345 Vassar Street, Cambridge, MA 02139, USA
E-mail: sagrawal@hybridon.com

Abbreviations: AO, antisense oligonucleotide; CR, complete tumor regression; DSS, dextran sulfate sodium; mdm2, mouse double minute2; PKA, protein kinase A; PR, partial tumor regression; MDS, mean day survival; TGI, tumor growth inhibition

Key words: anticancer, combination therapy, oligonucleotides, prodrug, tumor xenografts

Introduction

Irinotecan [7-ethyl-10-(4-piperidinol)-1-piperidinocarbonyloxy-camptothecin, CPT-11, or Camptosar®] is a semi-synthetic camptothecin analog that acts by inhibiting the enzyme topoisomerase I (1). Irinotecan has shown antitumor activity against a number of malignancies in xenografts (2) and in human clinical trials (3). Irinotecan has been approved to treat patients with advanced colorectal cancer in combination with 5-flurouracil (5-FU) and leucovorin (4). Irinotecan is a prodrug that is extensively metabolized in the liver, undergoing hydrolysis *in vivo* to the more potent metabolite, SN-38, which is responsible for topoisomerase I activity. The SN-38 formed is further metabolized in the liver to an inactive SN-38-glucuronide and eliminated through the bile (5). The major dose-limiting side effect observed with irinotecan administration in human is diarrhea.

In the past few years, use of antisense oligonucleotides (AOs) to down-regulate various genes for cancer therapy, including genes for growth factors, signal transduction agents, and oncogenes, has been extensively studied (6,7). In recent years, AOs in combination with a variety of cytotoxic drugs such as etoposide (8), hydroxycamptothecin (9), paclitaxel (10), docetaxel (11), cisplatin (8,12), doxorubicin (8,9,13), mitoxantrone (14) and 5-FU (14,15) have been studied both *in vitro* and *in vivo*. Currently, several AOs are being tested as monotherapies and in combination with a number of cytotoxic drugs in human clinical trials (16).

We have recently examined AOs targeted to mdm2 mRNA that specifically down-regulate the expression of mdm2 protein and stabilize p53, thereby inducing p21 expression (17), as an anticancer therapy. The selected mdm2 AO showed synergistic activity in a sequence-specific manner when used in combination with adriamycin, 5-FU and hydroxycampto-

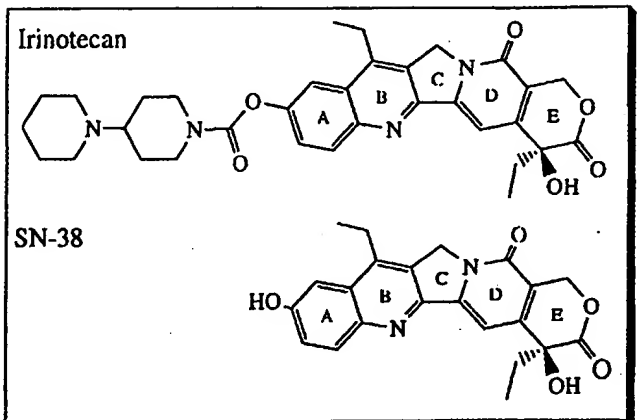

Oligo-1	5'-UGACACCTGTTCTCACUCAC-3'
Oligo-2	5'-UCCCACCTATTCTTACUCCC-3'
Oligo-3	5'-UGCTACTTCTTCTTCCUCAC-3'
Oligo-4	5'-UGTCACCCTTTTTCATUCAC-3'
Oligo-5	5'-GCGUGCCTCCTCACUGGC-3'
Oligo-6	5'-TGACACCTGTTCTCACTCAC-3'

Figure 1. Chemical structures of irinotecan and its active metabolite SN-38, and the sequences of chemically modified oligonucleotides used in the study. The nucleoside bases shown in plain and bold represent 2'-deoxy- and 2'-O-methyl-ribonucleosides, respectively. The nucleoside bases underlined in oligo sequences 2-4 represent mismatched bases. All oligonucleotides contain phosphorothioate internucleotide linkages. Oligo-1 is complementary to a portion of human mdm2 mRNA, and oligos-5 and -6 are complementary to a portion of human PKA-RIα subunit mRNA.

thecin, a topoisomerase I inhibitor, in both cell culture and tumor xenograft studies (9).

In the present study, we extended our studies using AOs to mdm2 mRNA and the cytotoxic drug irinotecan in expectation of obtaining synergistic antitumor activity of irinotecan as previously observed with hydroxycamptothecin and the same AO. We co-administered irinotecan and either a chemically modified (oligo-1) or phosphorothioate AO complementary to mdm2 mRNA (oligo-6), its control chemically modified oligonucleotides (oligos-2 to 4) with mismatched bases, or a chemically modified AO (oligo-5) complementary to the RIα regulatory subunit of protein kinase A (PKA) (12) (Fig. 1) to mice bearing human tumor xenografts HCT-116 (colon cancer), Panc-1 (pancreatic cancer), or A375 (melanoma). The co-administration of oligonucleotides with irinotecan resulted in a marked potentiation of antitumor activity of irinotecan in a dose-dependent manner in all three xenografts and, surprisingly, in a nucleotide sequence-independent manner, in contrast with earlier studies using other cytotoxic drugs.

Materials and methods

Oligonucleotides were synthesized using ß-cyanoethyl phosphoramidite chemistry on an automated gene synthesizer. [illegible] and other reagents required for synthesis were obtained from Perceptive Biosystems, Framingham, MA or Glen Research, Sterling, VA. After synthesis, oligonucleotides were purified by preparative reverse-phase HPLC. The purity and integrity of the oligonucleotides were characterized by analytical polyacrylamide gel electrophoresis, capillary gel electrophoresis, UV, ^{31}P-NMR, and mass spectrometry (MALDI-TOF). The oligonucleotides were filtered and lyophilized before use.

Female Nu/Nu or NCr-nude mice, 6-8 weeks of age, were fed *ad libitum* water (reverse osmosis, 1 ppm Cl) and an autoclaved standard rodent diet (Picolab Mouse Diet 20) consisting of 20% protein, 9% fat, 4% fiber, 6.5% ash, 13% moisture, and 2.5% minerals. Mice were housed in micro-isolators on a 12-h light cycle at 22°C and 40-60% humidity.

Mice were subcutaneously implanted with 1 mm^3 HCT-116 human colon carcinoma or A375 human melanoma or Panc-1 human pancreatic carcinoma fragments in the flank. Tumor growth was monitored initially twice weekly and then daily as neoplasms reached the desired size, approximately 100 mg in weight. When the carcinoma reached desired the size as calculated in tumor weight, the animals were sorted into various treatment groups so that the mean and the SEM of tumors in each group was approximately the same.

The estimated tumor weight was calculated using the formula:

$$\text{Tumor Weight (mg)} = \frac{w^2 \times l}{2}$$

where, w and l stand for width and length of carcinoma in mm.

Neutral phosphate-buffered saline (PBS) was used as the vehicle. Oligos-1 to 6 and dextran sulfate were dissolved in PBS to the required concentration and used. Dextran sulfate sodium (DSS) (mol. wt. 5000) was purchased from Sigma Chemicals. Irinotecan (Pharmacia & Upjohn) was obtained as the marketed drug.

Animals were sorted into different groups (nine or ten per group as specified in the text for each experiment) on day 1. The treatment schedules are described in the text and figure legends for each experiment. Typically, irinotecan was given intravenously (except in the Panc-1 model where it was given intraperitoneally) on qwk x 3 schedule, starting on day 1, unless specified in the text, at 25, 50, or 100 mg/kg. Oligonucleotides were administered intraperitoneally starting on day 1 on a (5 days on/2 days off) x 6/7-week schedule. Oligonucleotides were given at doses of 5, 10, or 20 mg/kg as specified in the text. The control group received PBS/vehicle intraperitoneally on a (5 day on/2 day off) x 6/7-week schedule as in the case of oligonucleotide administration.

The tumor growth delay (TGD) endpoint method was used. Treatment-effected mean increases in survival of various groups were compared to each other and to the mean survival time of control mice treated with vehicle. In the TGD method, each mouse was euthanized when its neoplasm reached a size of 1.5 g (HCT-116), 2.0 g (A375), or 1.2 g (Panc-1); this was considered a cancer death. Mean Day Survival (MDS) was calculated for each group based on the [illegible]

$$\text{Time to endpoint (calculated)} = \text{Time to exceed endpoint (observed)} - \frac{Wt_2 - \text{endpoint weight}}{\frac{Wt_2 - Wt_1}{D_2 - D_1}}$$

where, time to exceed endpoint (observed), number of days it took for each tumor to grow past the endpoint (cut-off) size. This was the day the animal was euthanized as a cancer death; D_2, day animal was euthanized; D_1, last day of caliper measurement before tumor reached the endpoint; Wt_2, tumor weight (mg) on D_2; Wt_1, tumor weight (mg) on D_1; Endpoint weight, predetermined 'cut-off' tumor size for the model being used.

Treatment may also cause complete tumor regression (CR) or partial tumor regression (PR) or cause a carcinoma to grow only to a small size, but not reach the cut-off weight (stable disease). The duration of CR, PR, or stable disease response in a host was recorded throughout the study. In addition, the antitumor activity of irinotecan in the absence and presence of oligos was also determined by tumor growth inhibition (TGI) method. The TGI was calculated using average tumor weights on a specific day as following:

$$TGI = 100\% - \{\frac{Wt_t}{Wt_c} \times 100\%\}$$

where, Wt_t and Wt_c stand for average of treated tumor weight and average of control tumor weight, respectively.

Animals were weighed twice weekly during the study. Mice were examined frequently for clinical signs of any drug-related, adverse side effects. Acceptable toxicity for cancer drugs in mice is defined by the National Cancer Institute (NCI) as no mean group weight loss of over 20% during the test, and not more than one toxic death among ten treated animals.

The unpaired t-test and Mann-Whitney U test (analyzing means and medians, respectively) were used to determine the statistical significance of any difference in survival times between the groups. All statistical analyses were conducted at a p-level of 0.05 (two-tailed). Statistical analyses were carried out using Prism (GraphPad) version 3.0 software.

Results

Antitumor activity of irinotecan and chemically modified oligonucleotide monotherapies in colon cancer xenograft HCT-116. Irinotecan alone showed modest antitumor activity at 25 and 50 mg/kg doses administered once a week for three weeks (qwk x 3) in mice with human colon cancer xenograft HCT-116. The mean day of survival (MDS) of 23.6±1.8 days (P=0.05) and 36.5±5.4 days (P=0.003) were observed at 25 and 50 mg/kg doses, respectively. The control group treated with vehicle (PBS) showed an MDS of 16.7±3.4 days. Treatment of mice with 25 or 50 mg/kg of irinotecan resulted in tumor growth inhibition (TGI) of 44% and 64%, respectively, on day 18. In these studies, neither mdm2 (oligo-1) nor PKA AOs (oligo-5 or -6) or the mismatched oligos-2 to 4 alone showed antitumor activity at the doses

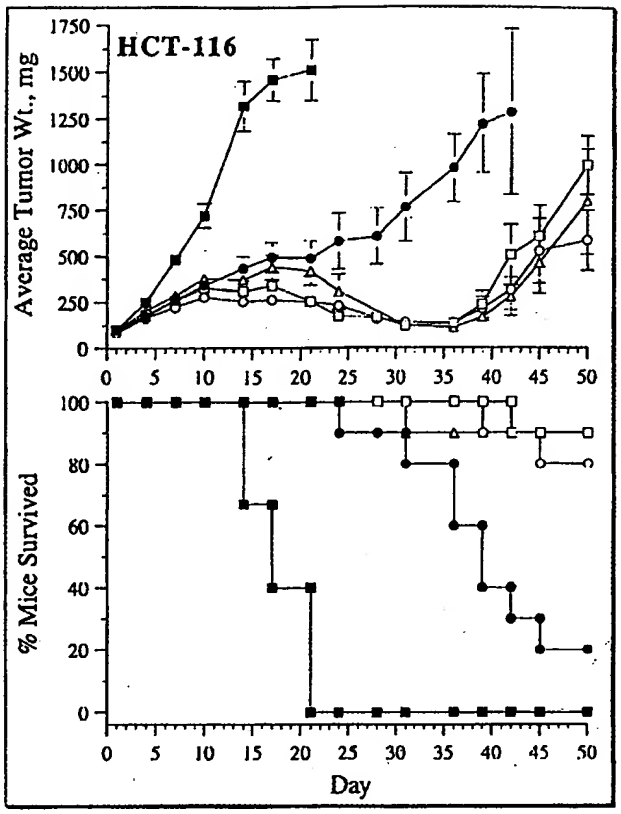

Figure 2. The co-administration of chemically modified oligonucleotides enhances the antitumor activity of irinotecan in a nucleotide sequence-independent manner in human colon cancer xenograft HCT-116. The top plot shows tumor growth inhibition and the bottom plot shows the % mice survived as a result of treatment. Filled squares represent control group that received PBS, filled circles represent irinotecan (50 mg/kg), and open symbols represent irinotecan at the same dose plus oligo-1 (20 mg/kg) (squares), oligo-2 (20 mg/kg) (circles), and oligo-3 (20 mg/kg) (triangles). Each group had 10 animals. The treatment schedule: irinotecan was administered qwk x 3 weeks starting on day 1 and the oligonucleotides were administered starting on day 1 on a (5 days on/2 days off) x 7-week schedule.

Sequence-independent potentiation of antitumor activity of irinotecan by chemically modified oligonucleotides. The co-administration of chemically modified oligonucleotides with irinotecan showed a significant increase in MDS and TGI, when compared with irinotecan monotherapy. We administered 20 mg/kg of oligos-1 to 4 separately in combination with 50 mg/kg of irinotecan to the mice bearing HCT-116 xenograft to study the enhancement of antitumor activity. The co-administration of oligo-1 and irinotecan resulted in a statistically significant MDS of 52±1.7 days (P=0.009) compared with the group that received 50 mg/kg of irinotecan alone (MDS 39.7±3.9 days). The co-administration of oligo-1 and irinotecan, and irinotecan-alone treatments showed TGI of 77% and 66%, respectively, on day 17 (Fig. 2). The co-administration of mismatched oligos-2 and -3 also showed significant enhancement of antitumor activity of irinotecan (Fig. 2). The co-administration of oligo-2 (20 mg/kg) with irinotecan (50 mg/kg) resulted in an MDS of 55.1±1.7 days (P=0.0086). This combination (oligo-2/irinotecan) treatment also showed a TGI of 82% on day 17. The co-administration of oligo-3 and irinotecan showed a TGI of

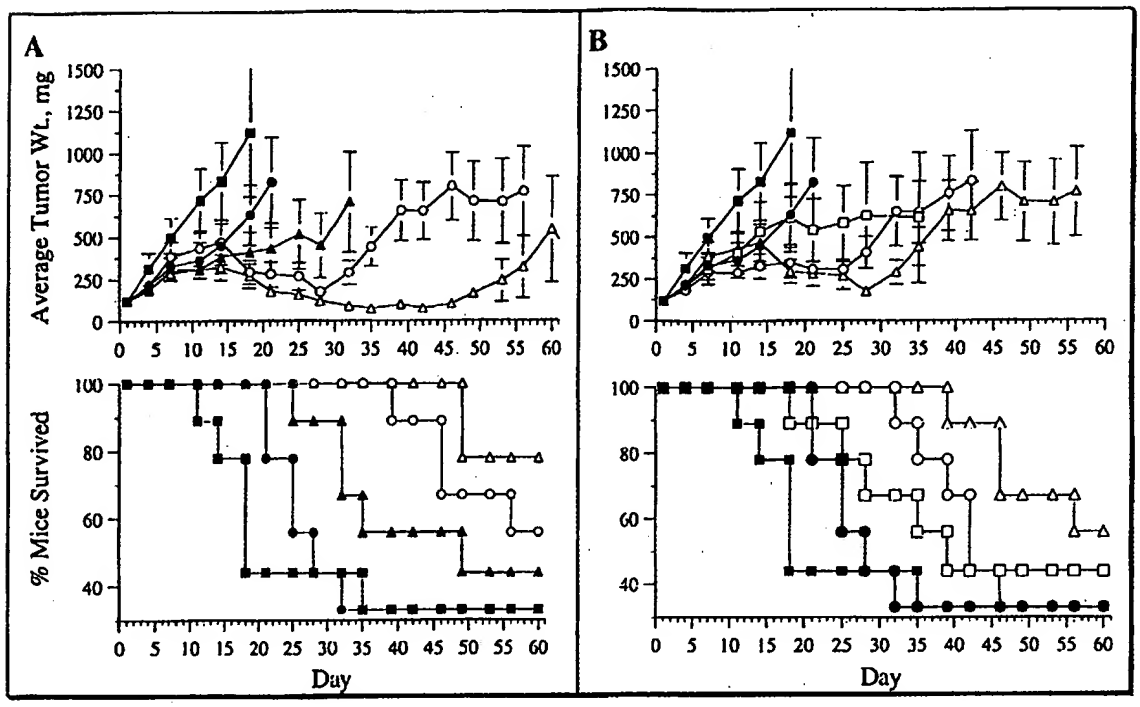

Figure 3. Enhancement of antitumor activity of irinotecan by co-administration of chemically modified oligo-1 in human colon cancer xenograft HCT-116 as a function of (A) irinotecan dose and (B) oligonucleotide dose. The top plots show change in average tumor weight with treatment in different groups of mice and the bottom plots show % mice survived in each group. A, Filled squares represent the group of animals that received PBS, filled circles and filled triangles represent the groups of mice that were treated with irinotecan 25 mg/kg or 50 mg/kg, respectively; and open circles and open triangles represent the groups of mice that were treated with irinotecan 25 mg/kg or 50 mg/kg plus oligo-1 (20 mg/kg), respectively. B, Filled squares represent the group of animals that received PBS, filled circles represent the group of animals that were treated with irinotecan (25 mg/kg), and the open symbols represent the groups of animals that were treated with irinotecan (25 mg/kg) plus oligo-1 5 mg/kg (squares), 10 mg/kg (circles) or 20 mg/kg (triangles), respectively. Treatment schedule was as described in Fig. 2. The number of mice in each group was 9.

combination, however, did not result in statistically significant increase in mice survival (46.7±4.5 days) (P=0.27) compared with irinotecan monotherapy.

Dependence of antitumor activity of irinotecan/chemically modified oligonucleotide combination on the dose of irinotecan. In order to confirm the potentiation of antitumor activity of irinotecan by co-administration of chemically modified oligonucleotides, we next examined the dependence of antitumor activity on the dose of irinotecan used together with oligonucleotides. Fig. 3A shows the antitumor activity of irinotecan when administered at a dose of 25 or 50 mg/kg on a schedule of qwk x 3 starting on day 1 with the co-administration of oligo-1 (20 mg/kg) daily five times a week starting on day 1 for seven consecutive weeks in mice with colon cancer xenograft HCT-116. The mice treated with oligo-1 (20 mg/kg) and irinotecan (25 mg/kg) showed a statistically significant MDS of 45.9±5.1 days (P=0.0012). This is an increase of about 95% survival extension compared with the group that received irinotecan (25 mg/kg) as monotherapy (23.6±1.8 days).

There were six 60-day survivors (one CR, one PR, and four cases of stable disease) (only one tumor reached the end point with an MDS of 56.7 days) in the group treated with oligo-1 (20 mg/kg) and irinotecan (50 mg/kg), compared with three 60-day survivors (one CR, one PR, and a case of stable disease) in the group treated with irinotecan (50 mg/kg) alone (lower plot Fig. 3A). The combination treatment of irinotecan (25 or 50 mg/kg) with oligo-1 (20 mg/kg) showed TGI of 74% or 76%, respectively, on day 18.

Dependence of antitumor activity of irinotecan/chemically modified oligonucleotide combination on the dose of oligonucleotide. To further understand if the enhancement of the antitumor activity of irinotecan is dependent on the dose of oligonucleotide, we co-administered varying doses of oligo-1 with a fixed dose of irinotecan. Fig. 3B shows that the enhancement of antitumor activity of irinotecan is dependent on the dose of oligo-1 co-administered. Oligo-1 was administered to mice at 5, 10, or 20 mg/kg with irinotecan (25 mg/kg) following the same treatment schedule as described above. The lowest dose of oligo-1 (5 mg/kg) co-administration with irinotecan (25 mg/kg) resulted in an MDS of 26.3±3.7 days (P=0.5) compared with MDS of 23.6±1.8 days for irinotecan (25 mg/kg) alone. The TGI of 45% observed at this combination dose on day 18 compared with irinotecan (25 mg/kg) alone (TGI 44%) was insignificant. The groups that received oligo-1 (10 mg/kg or 20 mg/kg) with irinotecan (25 mg/kg) showed statistically significant MDS of 38.1±2.1 days (P=0.0004) and 45.9±5.1 days (P=0.0012), respectively, compared with irinotecan (25 mg/kg) monotherapy. The same doses of oligo-1 (10 and 20 mg/kg) with irinotecan (25 mg/kg) showed TGI of 69% and 74%, respectively, on day 18. The percentage of mice surviving in each treatment group is shown

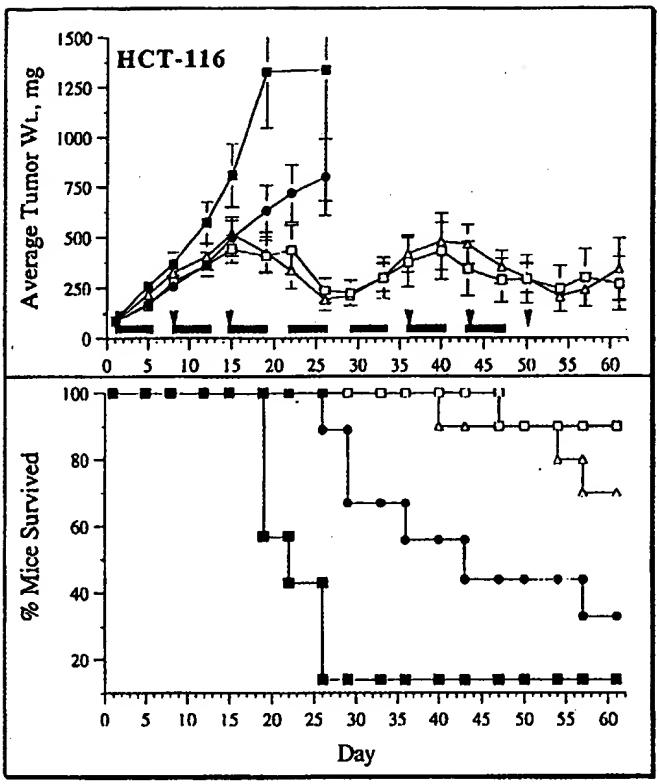

Figure 4. Effect of second cycle of irinotecan administration on tumor growth inhibition in HCT-116 colon cancer xenograft. The top plot shows tumor growth inhibition and the bottom plot shows the % mice survived as a result of treatment. Filled squares represent the control group that received PBS, filled circles represent irinotecan (25 mg/kg) alone, and open symbols represent irinotecan at the same dose as in monotherapy plus oligo-1 (10 mg/kg) (squares), or oligo-3 (10 mg/kg) (triangles). In all groups, where appropriate, irinotecan was given qwk x 3 weeks starting on day 1 (indicated by arrows), oligonucleotides were administered starting on day 1 on a (5 days on/2 days off) x 7-week schedule (indicated by bars), and the control group received vehicle/PBS starting on day 1 on a (5 days on/2 days off) x 7-week schedule. In addition the two groups that were on combination treatment received an additional dose of irinotecan (25 mg/kg) on days 36, 43 and 50. Bars and arrows represent oligo and irinotecan dosing schedule, respectively. Each group had 10 mice.

in the lower plot of Fig. 3B. Similar enhancement of antitumor activity was observed with the co-administration of oligo-1 (10 or 20 mg/kg) with irinotecan (50 mg/kg) as well (data not shown).

Dependence of antitumor activity with irinotecan/chemically modified oligonucleotide combination on the irinotecan administration schedule and duration of oligonucleotide treatment. In addition to irinotecan and oligonucleotide doses, enhancement of antitumor activity was also dependent on irinotecan administration schedule and duration of oligonucleotide treatment. In the studies described above, the initial dose of irinotecan was administered just before oligonucleotide administration on day 1. To determine if treatment schedule had any impact on the enhancement of antitumor activity, irinotecan was administered on days 1, 8, and 15 (schedule A) or on days 3, 10, and 17 (schedule B), to two groups of mice bearing HCT-116 tumor xenografts, while following the same schedule for oligo co-administration. Schedules A and B showed MDS of 38.1±2.1 days and 42.1±4.0 days ($P<0.002$), respectively, with oligo-1 (10 mg/kg) and irinotecan (25 mg/kg), compared with the group treated with irinotecan (25 mg/kg) alone (MDS 23.6±1.8 days) (data not shown). The TGI of 74% and 71% on day 18 for schedules A and B, respectively, is significant. However, the studies showed that when oligonucleotide was administered prior to irinotecan administration (schedule B), tumor growth was controlled more effectively than when the first dose of irinotecan was administered prior to oligonucleotide administration (schedule A) (data not shown). In addition, a reduction in antitumor activity of irinotecan was observed when oligonucleotide administration was restricted to the first four weeks compared with a more prolonged treatment schedule for six or seven weeks as in the case of above described experiments (data not shown).

Dependence of antitumor activity of irinotecan/chemically modified oligonucleotide combination on second cycle of irinotecan administration. To examine if a second cycle of irinotecan treatment would suppress tumor growth for an extended time period, we administered additional doses of irinotecan (25 mg/kg) on days 36, 43, and 50. Fig. 4 shows that a second cycle of irinotecan administration inhibited tumor growth efficiently. The effect of the initial course of treatment with irinotecan in the presence of chemically modified oligonucleotide was lost by approximately day 30, and the tumors then rapidly increased in size (Fig. 4). The administration of a second course of irinotecan on days 36, 43, and 50 inhibited tumor growth for at least another 4 weeks (day 61, experiment termination day). The first cycle of irinotecan administration showed TGI of 82% and 84% on day 26 with oligos-1 and -3 (10 mg/kg), respectively. Irinotecan alone showed only 40% TGI. In this study, co-administration of oligos-1 and -3 resulted in similar levels of enhancement of antitumor activity of irinotecan, supporting again the sequence-independent effect by oligonucleotides.

Enhancement of antitumor activity of irinotecan by chemically modified oligonucleotides in melanoma xenograft A375. Since irinotecan has a broad spectrum of antitumor activity, we expanded our irinotecan/chemically modified oligonucleotide studies to other tumor xenograft models. In mice bearing human melanoma xenografts (A375) an MDS of 44.3±1.7 days ($P<0.0001$) was observed for the group treated with oligo-1 (20 mg/kg) and irinotecan (50 mg/kg) compared with the group that received irinotecan (50 mg/kg) alone (MDS 25.3±0.9 days). The MDS determined for the control group that received PBS was 14.1±1.1 days. The TGI of 74% observed on day 11 with oligo-1 (20 mg/kg) and irinotecan (50 mg/kg) was significantly higher than the TGI of 41% observed on the same day for irinotecan (50 mg/kg) monotherapy (Fig. 5A). In addition, co-administration of oligo-3 or -5 with irinotecan also enhanced antitumor activity, further suggesting that enhancement of antitumor activity of irinotecan in p53 wt tumors is independent of the nucleotide sequence of the oligonucleotide co-administered.

Enhancement of antitumor activity of irinotecan by chemically modified oligonucleotides in pancreatic cancer xenograft Panc-1. Irinotecan is as effective against tumors that express

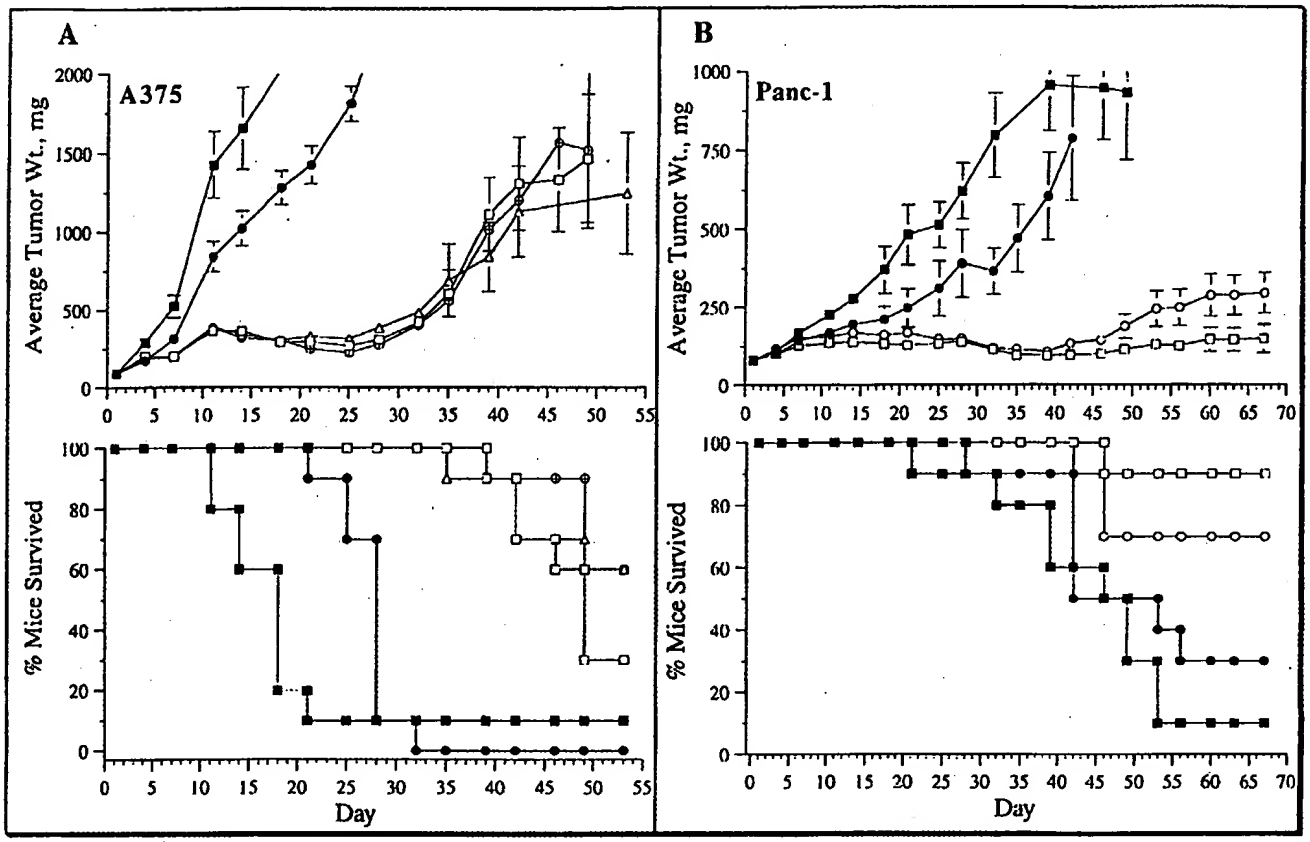

Figure 5. Enhancement of antitumor activity of irinotecan by chemically modified oligonucleotides in human melanoma xenograft, A375 (left panels) and pancreatic cancer xenograft, Panc-1 (right panels). The top plot shows tumor growth inhibition and the bottom plot shows the % mice survived as a result of treatment. A375 study (left panels), filled squares represent the control group that received PBS, filled circles represent irinotecan (50 mg/kg) alone, and open symbols represent irinotecan at the same dose as in monotherapy plus oligo-1 (20 mg/kg) (squares), oligo-3 (20 mg/kg) (triangles), or oligo-5 (20 mg/kg) (circles with a plus sign). Irinotecan was given qwk x 3 weeks starting on day 3, oligonucleotides were administered starting on day 1 on a (5 days on/2 days off) x 7-week schedule, and the control group received vehicle/PBS starting on day 1 on a (5 days on/2 days off) x 7 weeks schedule. Each group had 10 mice. Panc-1 study (right panels), filled squares represent the control group that received PBS, filled circles represent irinotecan (100 mg/kg) alone, and open symbols represent irinotecan at the same dose as in irinotecan monotherapy plus oligo-1 (20 mg/kg) (squares), or oligo-2 (20 mg/kg) (circles). Irinotecan was given qwk x 3 weeks starting on day 1, oligonucleotides were administered starting on day 1 on a (5 days on/2 days off) x 6-week schedule, and the control group received PBS/vehicle starting on day 1 on a (5 days on/2 days off) x 6-week schedule. Each group had 10 mice.

wild-type p53 as those that express mutant p53 (17). After observing increased antitumor activity of irinotecan in HCT-116 and A375 tumor xenografts that express wild-type p53, we extended our studies to a human pancreatic cancer (Panc-1) xenograft, which contains a mutant form of p53. In mice bearing Panc-1 xenografts, the oligo-1/irinotecan combination showed a significantly higher antitumor activity than did irinotecan treatment alone (Fig. 5B). The MDS of 42.3±3.3 days determined for irinotecan (100 mg/kg) treatment was approximately two days longer than the MDS of 40.5±3.6 days determined for the control group that was treated with PBS. The combination of oligo-1 (20 mg/kg) and irinotecan (100 mg/kg) resulted in one CR, one PR, and seven cases of stable disease compared with two PRs and one case of stable disease in the group that received irinotecan (100 mg/kg) alone ($P<0.05$). The nine 67-day (experiment termination day) survivors recorded in the group treated with oligo-1/irinotecan combination surpassed three 67-day survivors in the group that received irinotecan (100 mg/kg) alone. The TGI of 86% on day 32 oligo-1/irinotecan combination treatment was highly significant compared with a TGI of 54% for irinotecan oligo-2/irinotecan (20/100 mg/kg) also showed enhancement of antitumor activity similar to that of the oligo-1/irinotecan combination. Similar enhancement of antitumor activity of irinotecan was also observed in another colon cancer xenograft (HT-29) containing a mutated form of p53 gene when oligo-1, -2, or -5 (10 mg/kg) was co-administered with irinotecan (50 mg/kg) (data not shown).

Dependence of antitumor activity of irinotecan on the metabolic stability of oligonucleotide co-administered. The chemically modified oligonucleotides used in the study are metabolically more stable than phosphorothioate oligodeoxynucleotides (PS-oligonucleotides) that are currently in clinical trials. In order to examine whether, the metabolic stability of oligonucleotide co-administered would influence the potentiation of antitumor activity of irinotecan, we co-administered a chemically modified oligonucleotide, oligo-5, at 10 mg/kg or 20 mg/kg, or a PS-oligonucleotide, oligo-6, at 20 mg/kg, with irinotecan (50 mg/kg) to mice bearing A375 melanoma xenograft. The co-administration of oligo-5 or -6 at 20 mg/kg with irinotecan (50 mg/kg) resulted in an

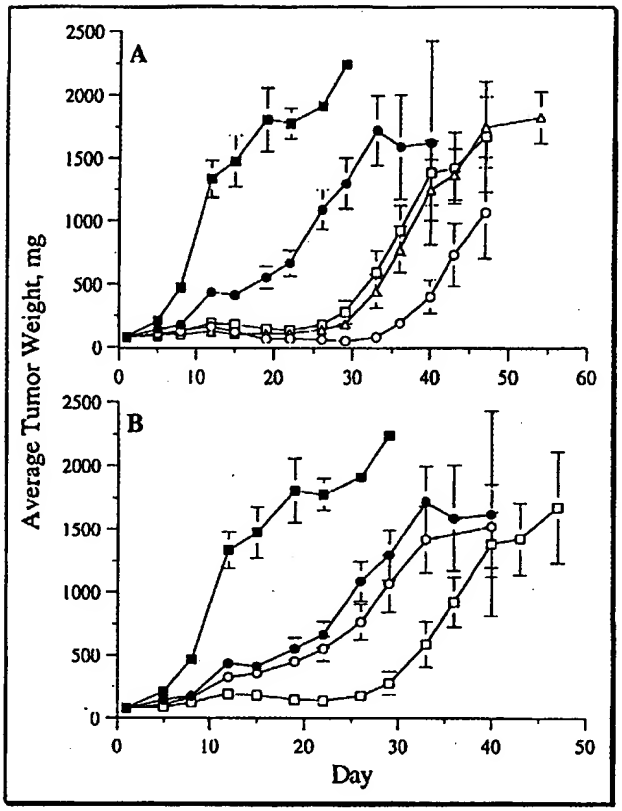

Figure 6. Enhancement of antitumor activity of irinotecan by chemically modified oligonucleotide, PS-oligonucleotide and DSS in human melanoma xenograft, A375. A, Filled squares represent the control group that received PBS, filled circles represent irinotecan (50 mg/kg) alone, and open symbols represent irinotecan at the same dose as in monotherapy plus oligo-5 (20 mg/kg) (circles), or (10 mg/kg) (squares) or oligo-6 (20 mg/kg) (triangles). B, Filled squares represent the control group that received PBS, filled circles represent irinotecan (50 mg/kg) alone, and open symbols represent irinotecan at the same dose as in monotherapy plus oligo-5 (20 mg/kg) (squares), or DSS (10 mg/kg) (circles) In both A and B irinotecan was given qwk x 3 weeks starting day 3, oligonucleotides were administered starting on day 1 on a (5 days on/2 days off) x 7 weeks schedule, and the control group received vehicle/PBS starting on day 1 on a (5 days on/2 days off) x 7 weeks schedule. Each group had 10 mice.

respectively, compared to an MDS of 33±1.1 days (P=0.0001) for irinotecan monotherapy. Although the MDS were the same for both oligos-5 and -6, there were five mice that survived for 61 days (experiment termination day) in the group that was treated with oligo-5 (20 mg/kg) and irinotecan (50 mg/kg) compared with none surviving in the group that was treated with oligo-6 and irinotecan at the same doses. The tumor inhibition plots in Fig. 6A show that oligo-6 (20 mg/kg) produced TGI similar to that of oligo-5 (10 mg/kg) with the same dose of irinotecan (50 mg/kg).

Potentiation of antitumor activity of irinotecan by oligonucleotides is not dependent on the polyanionic characteristic. To examine whether the enhancement of antitumor activity of irinotecan by co-administration of oligonucleotides is the result of the polyanionic nature of the oligonucleotides, we co-administered dextran sulfate sodium (DSS), a polyanionic agent, at 10 mg/kg with irinotecan (50 mg/kg) to mice bearing A375 melanoma xenograft. The MDS of 34.9±1.9 days (P=0.41) observed for the group treated with DSS and irinotecan was insignificant compared with the MDS of 33±1.1 days (P=0.0001) observed for the group of mice that was treated with irinotecan (50 mg/kg) alone.

Discussion

Irinotecan is a water-soluble semisynthetic prodrug that undergoes sequential metabolism *in vivo* to generate a more potent metabolite SN-38, along with other non-active metabolites (5,18). Irinotecan has shown broad spectrum anticancer activity in a number of experimental tumor models, including multidrug-resistant cells expressing P-glycoprotein (19), and cancers that express both wild-type and mutated p53 (20). The primary site for metabolism of irinotecan is the liver. Hepatic UDP-glucuronosyl transferase converts SN-38 to its inactive metabolite, SN-38-glucuronide (SN-38-G), which is then excreted in the bile (5). In the intestine, SN-38-G is converted to SN-38 by the action of ß-glucuronidase and the SN-38 formed is recirculated through the enterohepatic system (5).

We have recently shown that AOs targeted to the mdm2 oncogene synergistically enhance the antitumor efficacy of cytotoxic drugs such as adriamycin, 5-FU, and hydroxycamptothecin, a camptothecin analogue (9). In the present study, we expected to observe synergistic enhancement of antitumor activity of irinotecan as in the case of other cytotoxic drugs with the co-administration of AOs. To our surprise, we observed that oligonucleotides potentiated antitumor activity of irinotecan in a nucleotide sequence-independent fashion in contrast to what had been observed with other cytotoxic drugs such as adriamycin, 5-FU, and hydroxycamptothecin.

To our knowledge this is the first report of enhancement of antitumor activity of a cytotoxic drug by the co-administration of oligonucleotides in a sequence-independent fashion. AOs to mdm2, and PKA-RIα mRNAs (oligos-1, -5 and -6) as well as several control oligos (oligos-2 to 4), showed a similar enhancement of antitumor activity of irinotecan. Irinotecan/oligonucleotide combinations showed consistently higher efficacy than irinotecan or oligonucleotide treatment alone both in p53-dependent and -independent tumor models. Irinotecan alone showed a modest antitumor activity in colon cancer (HCT-116), pancreatic cancer (Panc-1), and melanoma (A375) xenografts when administered once a week for three weeks at doses of 25, 50 and 100 mg/kg.

In the present studies, neither AOs (oligos-1 and -5) nor mismatched oligonucleotides (oligos-2 to 4) alone showed antitumor activity. This was a surprising result, because we have previously demonstrated sequence-specific antitumor activity by the same AOs in tumor xenograft models (6). The difference between the present and earlier studies was that in the present study tumor growth was initiated in mice by implanting carcinoma fragments subcutaneously, whereas in the earlier studies the tumors were grown by injecting cancer cells subcutaneously (9). We have carried out similar studies in tumor models by injecting cells. In those studies, AOs alone showed antitumor activity (Zhang R. and Agrawal S., unpublished data).

The potentiation of antitumor activity of irinotecan is dependent on the dose of irinotecan and chemically modified

oligonucleotide, suggesting requirement of the presence of a certain level of irinotecan and oligonucleotide in the system. A dose of 20 mg/kg of chemically modified oligonucleotide and 50 mg/kg of irinotecan was found to be optimal. The enhancement of antitumor activity of irinotecan by chemically modified oligonucleotides was also dependent on the administration schedule of irinotecan. In general, the administration of oligonucleotide prior to irinotecan administration was found to control tumor growth more effectively than when the two agents were co-administered on day 1, although MDS were not significantly different.

A prolonged antitumor effect of irinotecan, resulting in about 3-5 days longer MDS, was observed for the group that was co-administered with chemically modified oligonucleotide for a longer duration of about 6 or 7 weeks instead of 4 weeks while following the same dose and schedule for irinotecan administration. An enhanced and persistent antitumor activity of irinotecan could be achieved by continued treatment with oligos, perhaps as a consequence of the increased half-life of irinotecan or its metabolites in the presence of chemically modified oligonucleotides.

The co-administration of a 20 mg/kg dose of a PS-oligonucleotide with 50 mg/kg irinotecan resulted in a tumor suppression that was almost equivalent to that observed with a 10 mg/kg dose of chemically-modified oligonucleotide of the same nucleotide sequence and 50 mg/kg of irinotecan. This could be as a consequence of faster degradation of PS-oligonucleotide *in vivo* compared with chemically modified oligonucleotide (21). In addition, oligonucleotides are negatively charged molecules and could potentiate polyanion-related effects as in the case of heparin and DSS. The failure of DSS (10 mg/kg) to potentiate the antitumor activity of irinotecan (50 mg/kg) is strong evidence that the potentiation of irinotecan activity observed by co-administration of oligonucleotides is not the result of their polyanionic charge.

Although it is difficult to postulate the mechanism of action for the enhancement of antitumor activity of irinotecan by co-administration of oligonucleotides from these *in vivo* antitumor studies, a few conclusions can be drawn. The observation that oligos enhance the antitumor activity of irinotecan in a sequence-independent fashion strongly suggests that this could be the result of interaction of the two drugs at the pharmacokinetic level, rather than additive efficacy of antisense and cytotoxic agents. The fact that AOs (oligo-1, antisense to mdm2 or oligo-5, antisense to PKA) showed no antitumor activity in these models further rules out additive effect of the two agents leading to synergistic activity.

The enhanced suppression of tumor growth when the oligonucleotides were administered prior to irinotecan administration, compared with when the two agents were administered simultaneously, suggests that the oligos alter the pharmacokinetics and/or metabolism of irinotecan, thereby enhancing its antitumor activity. In addition, the potentiation of antitumor activity of irinotecan observed with prolonged oligo treatment schedules clearly suggests drug interaction at a pharmacokinetic and/or metabolic level. A better potentiation of antitumor activity of irinotecan with metabolically more stable chemically modified oligonucleotides compared with less stable PS-oligodeoxynucleotides suggests that the of antitumor activity of irinotecan and the interaction of the two drugs (oligonucleotide and irinotecan) is at pharmacokinetic and/or metabolic level.

The co-administration of chemically modified oligonucleotides did not result in toxicity in the tumor models studied as indicated by the group mean body weight gains. The ongoing pharmacokinetic studies in mice and additional antitumor studies with other prodrugs will lead to better understanding of the mechanism of sequence-independent synergistic interaction between irinotecan and chemically modified oligonucleotide agents.

In conclusion, our results suggest that potentiation of antitumor activity of a prodrug cytotoxic agent, irinotecan, by oligonucleotides is unique for irinotecan or perhaps the class of prodrugs. The potentiation of antitumor activity of irinotecan by oligonucleotides was not dependent on the nucleotide sequence of oligonucleotides or their polyanionic nature. However, the potentiation of antitumor activity was dependent on the dose of both agents, the administration schedule of both oligonucleotide and irinotecan, and the metabolic stability of the oligonucleotide co-administered. These results indicate that the use of chemically modified oligonucleotides together with irinotecan may increase the therapeutic index of irinotecan in cancer patients. Therefore, it is important to continue testing and development of such agents.

References

1. Shimada Y, Rotenherg M, Hilsenbeck SG, Burris HA III, Degen D and von Hoff DD: Activity of CPT-11 (irinotecan hydrochloride), a topoisomerase I inhibitor, against human tumor colony-forming units. Anticancer Drugs 5: 202-206, 1991.
2. Kawato Y, Furuta T, Aonuma M, Yasuoka M, Yokokura T and Matsumoto K: Antitumor activity of a camptothecin derivative, CPT-11, against human tumor xenografts in nude mice. Cancer Chemother Pharmacol 28: 192-198, 1991.
3. Horowitz RW, Wadler S and Wiernik PH: A review of the clinical experience with irinotecan (CPT-11). Am J Ther 4: 203-210, 1997.
4. Rothenberg ML and Blanke CD: Topoisomerase I inhibitors in the treatment of colorectal cancer. Semin Oncol 26: 632-639, 1999.
5. Kuhn JG: Pharmacology of irinotecan. Oncology 12 (Suppl. 6): 39-42, 1998.
6. Agrawal S: Importance of nucleotide sequence and chemical modifications of antisense oligonucleotides. Biochim Biophys Acta 1489: 53-68, 1999.
7. Gewirtz AM, Sokol DL and Ratajczak MZ: Nucleic acid therapeutics: state of the art and future prospects. Blood 92: 712-773, 1998.
8. Zangemeister-Witte U, Schenker T, Luedke GH and Stahel RA: Synergistic cytotoxicity of Bcl-2 antisense oligodeoxynucleotide and etoposide, doxorubicin and cisplatin in small-cell lung cancer cell lines. Br J Cancer 78: 1035-1042, 1998.
9. Wang H, Zeng X, Oliver P, Le LP, Chen J, Chen L, Zhou W, Agrawal S and Zhang R: MDM2 oncogene as a target for cancer therapy: an antisense approach. Int J Oncol 15: 653-660, 1999.
10. Tortora G, Caputo R, Damiano V, Bianco R, Pepe S, Bianco AR, Jiang Z, Agrawal S and Ciardiello F: Synergistic inhibition of human cancer cell growth by cytotoxic drugs and mixed backbone antisense oligonucleotide targeting protein kinase A. Proc Natl Acad Sci USA 94: 12586-12591, 1997.
11. Tortora G, Caputo R, Pomatico G, Pepe S, Bianco AR, Agrawal S, Mendelsohn J and Ciardiello F: Cooperative inhibitory effect of novel mixed backbone oligonucleotide targeting protein kinase A in combination with docetaxel and anti-epidermal growth factor-receptor antibody on human breast

12. Wang H, Cai Q, Zeng X, Yu D, Agrawal S and Zhang R: Antitumor activity and pharmacokinetics of a mixed-backbone antisense oligonucleotide targeted to the RIα subunit of protein kinase A after oral administration. Proc Natl Acad Sci USA 96: 13989-13994, 1999.
13. Roh H, Hirose CB, Boswell CB, Pippin JA and Drebin JA: Synergistic antitumor effects of HER2/neu antisense oligodeoxynucleotides and conventional chemotherapeutic agents. Surgery 126: 413-421, 1999.
14. Kornmann M, Danenberg KD, Arber N, Beger HG, Danenberg PV and Korc M: Inhibition of cyclin D1 expression in human pancreatic cancer cells is associated with increased chemosensitivity and decreased expression of multiple chemoresistance genes. Cancer Res 59: 3505-3511, 1999.
15. Ferguson PJ, Collins O, Dean NM, De Moor J, Li CS, Vincent MD and Koropatnick J: Antisense down-regulation of thymidylate synthase to suppress growth and enhance cytotoxicity of 5-FUdR, 5-FU and Tomudex in HeLa cells. Br J Pharmacol 127: 1777-1786, 1999.
16. Agrawal S and Kandimalla ER: Antisense therapeutics. Is it as simple as complementary base recognition? Mol Med Today 6: 72-81, 2000.
17. Chen L, Agrawal S, Zhou W, Zhang R and Chen J: Synergistic activation of p53 by inhibition of mdm2 expression and DNA damage. Proc Natl Acad Sci USA 95: 195-200, 1998.
18. Cersosimo RJ: Irinotecan: a new antineoplastic agent for the management of colorectal cancer. Ann Pharmacother 32: 1324-1333, 1998.
19. Jansen WJ, Hulscher TM, van Ark-Otte J, Giaccone G, Pinedo HM and Boven E: CPT-11 sensitivity in relation to the expression of P170-glycoprotein and multidrug resistance-associated protein. Br J Cancer 77: 359-365, 1998.
20. McDonald AC and Brown R: Induction of p53-dependent and p-53-independent cellular responses by topoisomerase I inhibitors. Br J Cancer 78: 745-751, 1998.
21. Zhang R, Lu Z, Zhao H, Zhang X, Diasio RB, Habus I, Jiang Z, Iyer RP, Yu D and Agrawal S: *In vivo* stability, disposition and metabolism of a 'hybrid' oligonucleotide phosphorothioate in rats. Biochem Pharmacol 50: 545-556, 1995.

314.17. C 38.23%, H 4.49%, Cl 22.57%, N 4.46%, O 10.18%, P 9.86%, S 10.21%. Prepn: Blair *et al., J. Agr. Food Chem.* **11**, 237 (1963). Synthesis of the optical isomers: Seiber, Tolkmith, *Tetrahedron* **25**, 381 (1969). Use as a herbicide: Leasure, US **3074790** (1963 to Dow); as a plant growth regulator: Holmsen, *Weed Sci.* **17**, 187 (1969). Neurotoxicity in chickens: B. M. Francis *et al., J. Environ. Sci. Health* **B15**, 313 (1980). Toxicity study: E. W. Schafer, *Toxicol. Appl. Pharmacol.* **21**, 315 (1972).

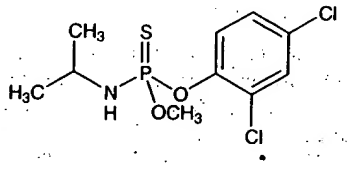

Solid, mp 51.4°. Vapor pressure at 150°: 2 mm. Slightly sol in water (5 ppm); freely sol in acetone, benzene, carbon tetrachloride. LD_{50} orally in rats: 270-360 mg/kg (Schafer).

Note: DMPA® is dimethylolpropionic acid, *q.v.*

USE: Herbicide; plant growth regulator.

3427. DMPO. [3317-61-1] 3,4-Dihydro-2,2-dimethyl-2*H*-pyrrole 1-oxide; 5,5-dimethyl-1-pyrroline 1-oxide. $C_6H_{11}NO$; mol wt 113.16. C 63.68%, H 9.80%, N 12.38%, O 14.14%. Nitrone spin trap. Prepn: R. Bonnett *et al., J. Chem. Soc.* **1959**, 2094; D. L. Haire *et al., J. Org. Chem.* **51**, 4298 (1986); and purification: E. G. Janzen *et al., Chem.-Biol. Interactions* **70**, 167 (1989). uv absorption: L. S. Kaminsky, M. Lamchen, *J. Chem. Soc.* **1968**, 1085. Use as spin trap in biological systems: A. I. Cederbaum, G. Cohen, *Arch. Biochem. Biophys.* **204**, 397 (1980); A. S. W. Li *et al., Biochem. Biophys. Res. Commun.* **146**, 1191 (1987); for neutrophil activation studies: B. E. Britigan, D. R. Hamill, *Arch. Biochem. Biophys.* **275**, 72 (1989); *eidem, Free Rad. Biol. Med.* **8**, 459 (1990); in reperfusion injury: C. M. Arroyo *et al., FEBS Letters* **221**, 101 (1987); A. Tosaki, P. Braquet, *Am. Heart J.* **120**, 819 (1990). Use in HPLC quantitation of oxygen free radicals *in vivo:* P. S. Rao *et al., Chromatographia* **30**, 19 (1990).

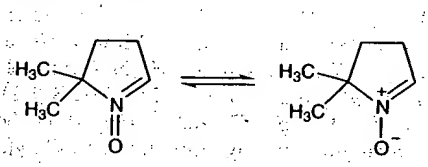

Nitrone as white crystalline solid. Very hygroscopic. Turns yellow with time even at −20°C sealed under vacuum and protected from light. uv max in cyclohexane: 246 nm (ε 9000); ethanol: 234 nm (ε 7700); water: 226 nm (ε 8600); *N*-hydrochloric acid: 226 nm (ε 7000); ether: 246 nm.

USE: Spin trap agent for biological systems.

3428. Dobesilate Calcium. [20123-80-2] 2,5-Dihydroxybenzenesulfonic acid calcium salt; calcium dobesilate; hydroquinone calcium sulfonate; Dexium; Doxium. $C_{12}H_{10}CaO_{10}S_2$; mol wt 418.41. C 34.45%, H 2.41%, Ca 9.58%, O 38.24%, S 15.33%. Prepn: **ES 335945** (1967 to Labs. Esteve), *C.A.* **69**, 106253z (1968); **FR M6163**; A. Esteve-Subirana, US **3509207** (1968, 1970 both to Labs. OM). Clinical trials: Berson, *Praxis* **59**, 1305 (1970); **61**, 52 (1972). Metabolism: A. Benakis *et al., Therapie* **29**, 211 (1974).

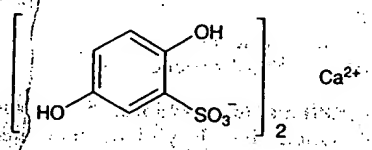

White, powdery crystals from water, mp >300° (dec). Color deepens to pink upon exposure to air. Very soluble in water and alcohol. Practically insol in ether, benzene, chloroform. LD_{50} in mice: 700 mg/kg (Esteve-Subirana).

THERAP CAT: Vasotropic.

3429. Dobutamine. [34368-04-2] 4-[2-[[3-(4-Hydroxyphenyl)-1-methylpropyl]amino]ethyl]-1,2-benzenediol; (±)-4-[2-[[3-(*p*-hydroxyphenyl)-1-methylpropyl]amino]ethyl]-pyrocatechol; 3,4-dihydroxy-*N*-[3-(4-hydroxyphenyl)-1-methylpropyl]-β-phenylethylamine; Compound 81929. $C_{18}H_{23}NO_3$; mol wt 301.38. C 71.73%, H 7.69%, N 4.65%, O 15.93%. β_1-Adrenergic agonist; derivative of dopamine, *q.v.* Prepn: Tuttle, Mills, **DE 2317710** corresp to US **3987200** (1973, 1976 to Lilly). Pharmacology: R. Weber, R. R. Tuttle in *Pharmacological and Biochemical Properties of Drug Substances* **vol. 1**, M. E. Goldberg, Ed. (Am. Pharm. Assoc., Washington, DC, 1977) pp 109-124; E. H. Sonnenblick *et al., N. Engl. J. Med.* **300**, 17 (1979). Comprehensive description: R. H. Bishara, H. B. Long, *Anal. Profiles Drug Subs.* **8**, 139-158 (1979).

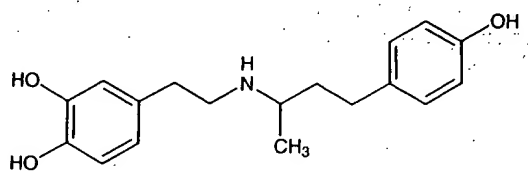

Hydrochloride. [49745-95-1] Inotrex (obsolete); Dobutrex. $C_{18}H_{23}NO_3$.HCl; mol wt 337.85. Crystals, mp 184-186°. uv max (methanol): 281, 223 nm (ε 4768, 14400). pKa 9.45. Rapidly oxidized at pH 11-13. LD_{50} i.v. in mice: ~73 mg/kg (Weber, Tuttle).

THERAP CAT: Cardiotonic.

3430. Docarpamine. [74639-40-0] 4-[2-[[(2*S*)-2-(Acetylamino)-4-(methylthio)-1-oxobutyl]amino]ethyl]-1,2-phenylene diethyl ester; (−)-(*S*)-2-acetamido-*N*-(3,4-dihydroxyphenethyl)-4-(methylthio)butyramide bis(ethylcarbonate) (ester); *N*-(*N*-acetyl-L-methionyl)-*O*,*O*-bis(ethoxycarbonyl)dopamine; *N*-(*N*-acetyl-L-methionyl)-3,4-diethoxycarboxyphenethylamine; TA-870; Tanadopa. $C_{21}H_{30}N_2O_8S$; mol wt 470.54. C 53.60%, H 6.43%, N 5.95%, O 27.20%, S 6.81%. Dopamine prodrug. Prepn: T. Kiguchi *et al.*, **EP 7441**; *eidem*, US **4228183** (both 1980 to Tanabe Seiyaku). Pharmacology: I. Yamaguchi *et al., J. Cardiovasc. Pharmacol.* **13**, 879 (1989). Mechanism of action: S. Nishiyama *et al., ibid.* **14**, 175 (1989). Pharmacokinetics: M. Yoshikawa *et al., Drug Metab. Dispos.* **16**, 754 (1988). Metabolism in humans: *eidem, ibid.* **18**, 212 (1990). HPLC determn in biological fluids: *eidem, Biomed. Chromatog.* **4**, 181 (1990). *Review:* S. Nishiyama *et al., Cardiovasc. Drug Rev.* **10**, 101-116 (1992).

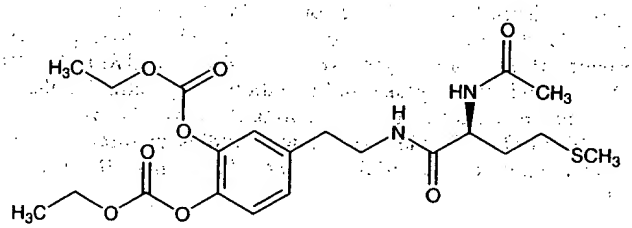

Crystals form ethyl acetate/*n*-hexane, mp 85-90°. $[\alpha]_D^{20}$ −15.6° (c = 2 in methanol). Also reported as crystalline powder, mp 105-108° (Nishiyama, 1992). Slightly sol in water, readily sol in ethanol. LD_{50} in male, female rats (mg/kg): 1000-1400, ~1000 s.c.; in rats, dogs (mg/kg): >2000 orally (Nishiyama, 1992).

THERAP CAT: Cardiotonic.

3431. Docetaxel. [114977-28-5] (αR,βS)-β-[[(1,1-Dimethylethoxy)carbonyl]amino]-α-hydroxybenzenepropanoic acid (2a*R*,4*S*,4a*S*,6*R*,9*S*,11*S*,12*S*,12a*R*,12b*S*)-12b-(acetyloxy)-12-(benzoyloxy)-2a,3,4,4a,5,6,9,10,11,12,12a,12b-dodecahydro-4,6,11-trihydroxy-4a,8,13,13-tetramethyl-5-oxo-7,11-methano-1*H*-cyclodeca[3,4]benz[1,2-b]oxet-9-yl ester; *N*-debenzoyl-*N*-(*tert*-butoxycarbonyl)-10-deacetyltaxol; NSC-628503; RP-56976; Taxotere. $C_{43}H_{53}NO_{14}$; mol wt 807.88. C 63.93%, H 6.61%, N 1.73%, O 27.73%. Semisynthetic derivative of pacli-

taxel, *q.v.*, prepd using a natural precursor, ***10-deacetylbaccatin III***, extracted from the needles of the European yew tree, *Taxus baccata* L., *Taxaceae*. Antimitotic agent that promotes the assembly of microtubules and inhibits their depolymerization to free tubulin. Prepn: M. Colin *et al.*, **EP 253738**; *eidem*, **US 4814470** (1988, 1989 both to Rhône-Poulenc Sante); L. Mangatal *et al.*, *Tetrahedron* **45,** 4177 (1989). Synthesis of the side chain: J.-N. Denis *et al.*, *J. Org. Chem.* **56,** 6939 (1991). Structure-activity study: F. Guéritte-Voegelein *et al.*, *J. Med. Chem.* **34,** 992 (1991). Cytotoxic activity and mechanism of action: I. Ringel, S. B. Horwitz, *J. Natl. Cancer Inst.* **83,** 288 (1991). *In vivo* antitumor activity: M.-C. Bissery *et al.*, *Cancer Res.* **51,** 4845 (1991). HPLC determn: J. C. Vergniol *et al.*, *J. Chromatog.* **582,** 273 (1992). Clinical pharmacokinetics and toxicology: J.-M. Extra *et al.*, *Cancer Res.* **53,** 1037 (1993). Clinical evaluation: H. Burris *et al.*, *J. Clin. Oncol.* **11,** 950 (1993). Symposium on clinical experience: *Semin. Oncol.* **27,** Suppl. 3, 1-29 (2000).

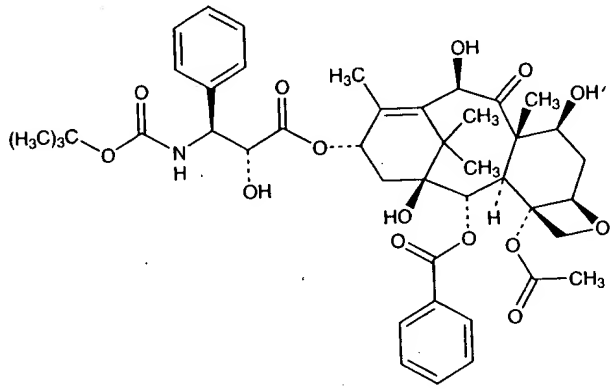

mp 232°. $[\alpha]_D$ −36° (c = 0.74 in ethanol). uv max: 230, 275, 283 nm (ε 14800, 1730, 1670).

THERAP CAT: Antineoplastic.

3432. Docosahexaenoic Acid. [6217-54-5] (4Z,7Z,10Z,13Z,16Z,19Z)-4,7,10,13,16,19-Docosahexaenoic acid; cervonic acid; doconexent; DHA. $C_{22}H_{32}O_2$; mol wt 328.49. C 80.44%, H 9.82%, O 9.74%. Omega-3 fatty acid found in marine fish oils and in many phospholipids. Major structural component of excitable membranes of the retina and brain; synthesized in the liver from α-linolenic acid, *q.v.* Isoln from oil of *Sardina ocellata* J. and structure: J. M. Whitcutt, *Biochem. J.* **67,** 60 (1957). Improved isoln from cod liver oil: S. W. Wright *et al.*, *J. Org. Chem.* **52,** 4399 (1987). Effect on brain and behavioral development: P. E. Wainwright, *Neurosci. Biobehav. Rev.* **16,** 193 (1992). Review of uptake and metabolism by retinal cells: N. G. Bazan, E. B. Rodriguez de Turco, *J. Ocul. Pharmacol.* **10,** 591-603 (1994). Review of clinical studies in infant formula supplementation: M. Makrides *et al.*, *Lipids* **31,** 115-119 (1996).

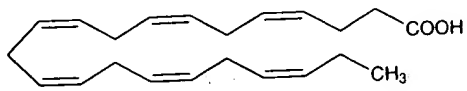

Clear, faintly yellow oil, mp −44.7 to −44.5°. n_D^{26} 1.5017.

USE: Nutritional supplement.

3433. *n*-Docosanol. [661-19-8] 1-Docosanol; behenic alcohol; behenyl alcohol; docosyl alcohol; Abreva; Lidakol. $C_{22}H_{46}O$; mol wt 326.60. C 80.90%, H 14.20%, O 4.90%. $H_3C(CH_2)_{21}OH$. Naturally occurring alcohol; active principal of Pygeum africanum extract, *q.v.*, that has been used to treat benign prostatic hypertrophy (BPH). Prepn: R. Willstätter, E. W. Mayer, *Ber.* **41,** 1475 (1908); P. A. Levene, F. A. Taylor, *J. Biol. Chem.* **59,** 905 (1924). Surface thermodynamic properties: S. Pathak, S. S. Katti, *J. Chem. Eng. Data* **14,** 359 (1969). GC-MS determn in Pygeum africanum extract: N. Pierini *et al.*, *Boll. Chim. Farm.* **121,** 27 (1982). Antiviral activity: D. H Katz *et al.*, *Ann. N.Y. Acad. Sci.* **724,** 472 (1994). Study of mechanism of action in BPH: J. Müntzing *et al.*, *Invest. Urol.* **17,** 176 (1979); vs herpes simplex virus: L. E. Pope *et al.*, *Antivir. Res.* **40,** 85 (1998). Clinical evaluation in recurrent herpes labialis: L. Habbema *et al.*, *Acta Derm. Venerol.* **76,** 479 (1996).

mp 70.5-71.5°. bp_{22mm} 180°. d^{75} 0.8063 g/ml; d^{85} 0.7986 g/ml; d^{95} 0.7911 g/ml. Surface tension (dyne/cm): 21.82 (75°); 21.17 (85°); 20.53 (95°). n^{75} 1.4360.

THERAP CAT: Antiviral (topical).

3434. Docusate Calcium. [128-49-4] Sulfobutanedioic acid 1,4-bis(2-ethylhexyl)ester calcium salt; bis[2-ethylhexyl]-calcium sulfosuccinate; calcium dioctyl sulfosuccinate; dioctyl calcium sulfosuccinate; Surfak. $C_{40}H_{74}CaO_{14}S_2$; mol wt 883.23. C 54.40%, H 8.45%, Ca 4.54%, O 25.36%, S 7.26%. Prepd from dioctyl sodium sulfosuccinate dissolved in isopropanol and from calcium chloride dissolved in methanol: Klotz, **US 3035973** (1962 to Lloyd Brothers).

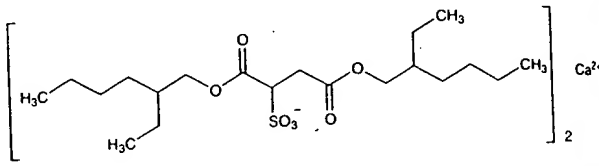

White precipitate. Sol in mineral and vegetable oils, liq polyethylene glycol. Practically insol in glycerol. Claimed to have greater surface-active wetting properties than the sodium salt.

Ingredient of ***Doxidan*** which also contains phenolphthalein.

THERAP CAT: Stool softener.

3435. Docusate Sodium. [577-11-7] Sulfobutanedioic acid 1,4-bis(2-ethylhexyl) ester sodium salt; sulfosuccinic acid 1,4-bis(2-ethylhexyl) ester *S*-sodium salt; bis(2-ethylhexyl)sodium sulfosuccinate; dioctyl sodium sulfosuccinate; sodium dioctyl sulfosuccinate; DSS; Aerosol OT; Colace; Comfolax; Coprola; Dioctylal; Dioctyl; Diotilan; Disonate; Doxinate; Doxol; Dulcivac; Jamylène; Molatoc; Molcer; Nevax; Regutol; Soliwax; Velmol; Waxsol; Yal. $C_{20}H_{37}NaO_7S$; mol wt 444.56. C 54.04%, H 8.39%, Na 5.17%, O 25.19%, S 7.21%. Prepn: Jaeger, **US 2028091**; **US 2176423** (1936, 1939, both to Am. Cyanamid). Structure and wetting power: Caryl, *Ind. Eng. Chem.* **33,** 731 (1941). Comprehensive description: S. Ahuja, J. Cohen, *Anal. Profiles Drug Subs.* **2,** 199-219 (1973); **12,** 713-720 (1983). For structure see Docusate calcium.

Available as wax-like solid, usually in rolls of tissue-thin material; also as 50-75% solns in various solvents. Soly in water (g/l): 15 (25°), 23 (40°), 30 (50°), 55 (70°). Sol in CCl_4, petr ether, naphtha, xylene, dibutyl phthalate, liq petrolatum, acetone, alcohol, vegetable oils. Very sol in water + alcohol, water + water-miscible organic solvents. Stable in acid and neutral solns; hydrolyzes in alkaline solns.

Note: Ingredient of the laxative ***Peri-Colace*** which also contains casanthranol.

Docusate potassium. [7491-09-0] Rectalad. $C_{20}H_{37}KO_7S$; mol wt 460.67.

USE: Sodium salt as pharmaceutic aid (surfactant); as wetting agent in industrial, pharmaceutical, cosmetic and food applications; dispersing and solubilizing agent in foods; adjuvant in tablet formation.

THERAP CAT: Stool softener.

THERAP CAT (VET): Stool softener.

3436. Dodecahedrane. [4493-23-6] Hexadecahydro-2,1,6,3,4-[2,3]butanediyl[1,4]diylidenedipentaleno[2,1,6-*cde*:2′,1′,6′-*gha*]pentalene; pentagonal dodecahedrane. $C_{20}H_{20}$; mol wt 260.37. C 92.26%, H 7.74%. Classical uniform convex polyhedrane. Theoretical studies: O. Ermer, *Angew. Chem. Int. Ed.* **16,** 411 (1977); R. L. Disch, J. M. Schulman, *J. Am. Chem. Soc.* **103,** 3297 (1981). Review of synthetic studies: P. E.

P

7052. Paclitaxel. [33069-62-4] [2a*R*-[2aα,4β,4aβ,6β,9α-(α*R**,β*S**),11α,12α,12aα,12bα]]-β-(Benzoylamino)-α-hydroxybenzenepropanoic acid 6,12b-bis(acetyloxy)-12-(benzoyloxy)-2a,3,4,4a,5,6,9,10,11,12,12a,12b-dodecahydro-4,11-dihydroxy-4a,8,13,13-tetramethyl-5-oxo-7,11-methano-1*H*-cyclodeca-[3,4]benz[1,2-*b*]oxet-9-yl ester; 5β,20-epoxy-1,2α,4,7β,10β,-13α-hexahydroxytax-11-en-9-one 4,10-diacetate 2-benzoate 13-ester with (2*R*,3*S*)-*N*-benzoyl-3-phenylisoserine; taxol A; NSC-125973; Anzatax; Paxene; Taxol. $C_{47}H_{51}NO_{14}$; mol wt 853.90. C 66.11%, H 6.02%, N 1.64%, O 26.23%. Antileukemic and antitumor agent first isolated, as the *l*-form, from the bark of the Pacific yew tree, *Taxus brevifolia, Taxaceae;* promotes the assembly of microtubules and inhibits the tubulin disassembly process. Isoln and structure: M. C. Wani *et al., J. Am. Chem. Soc.* **93,** 2325 (1971). *In vitro* promotion of microtubule assembly: P. B. Schiff *et al., Nature* **277,** 665 (1979). Isoln from *Taxus baccala* L. and *in vitro* inhibition of depolymerization of microtubules into tubulin: G. Chauviere *et al., C.R. Acad. Sci. Paris Ser. II* **293,** 501 (1981). Total synthesis of *taxusin*, which contains the entire ring skeleton: R. A. Holton *et al., J. Am. Chem. Soc.* **110,** 6558 (1988). Total stereosynthesis: R. A. Holton *et al., ibid.* **116,** 1597, 1599 (1994); K. C. Nicolaou *et al., Nature* **367,** 630 (1994). Synthesis and anticancer activity of derivs: D. G. I. Kingston *et al., Studies in Organic Chemistry* **vol. 26,** entitled "New Trends in Natural Products Chemistry 1986", Atta-ur-Rahman, P. W. Le Quesne, Eds. (Elsevier, Amsterdam, 1986) pp 219-235. Production by *Taxomyces andreanae*, an endophytic fungus associated with *T. brevifolia*: A. Stierle *et al., Science* **260,** 214 (1993). Use in study of structure and function of microtubules: S. B. Horwitz *et al., Cold Spring Harbor Symp. Quant. Biol.* **46,** 219 (1982). Clinical evaluation in Kaposi's sarcoma: M. W. Saville *et al., Lancet* **346,** 26 (1995). Review of mechanism of action: J. J. Manfredi, S. B. Horwitz, *Pharmacol. Ther.* **25,** 83-125 (1984); S. B. Horwitz *et al., Ann. N.Y. Acad. Sci.* **466,** 733-744 (1986); S. B. Horwitz, *Trends Pharmacol. Sci.* **13,** 134-136 (1992). Symposium on clinical toxicology, pharmacology and efficacy: *Sem. Oncol.* **20,** Suppl. 3, 1-60 (1993). Review in ovarian cancer: C. D. Runowicz *et al., Cancer* **71,** 1591-1596 (1993). Book: *Taxol®: Science and Applications,* M. Suffness, Ed. (CRC Press, Boca Raton, 1995) 426 pp.

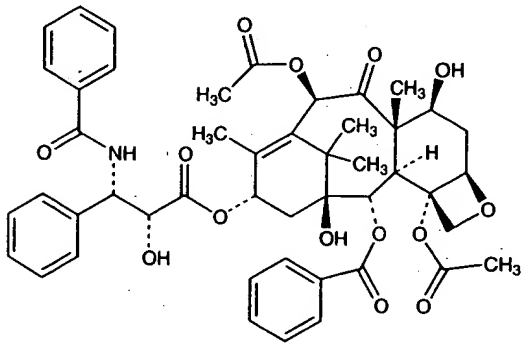

Needles from aq methanol, mp 213-216° (dec). $[\alpha]_D^{20}$ −49° (methanol). uv max (methanol): 227, 273 nm (ε 29800, 1700).
USE: Tool in study of structure and function of microtubules.
THERAP CAT: Antineoplastic.

7053. Paclobutrazol. [76738-62-0] (α*R*,β*R*)-*rel*-β-[(4-Chlorophenyl)methyl]-α-(1,1-dimethylethyl)-1*H*-1,2,4-triazole-1-ethanol; 1-*tert*-butyl-2-(*p*-chlorobenzyl)-2-(1,2,4-triazol-1-yl)ethanol; (2*RS*,3*RS*)-1-(4-chlorophenyl)-4,4-dimethyl-2-(1*H*-1,2,4-triazol-1-yl)pentan-3-ol; ICI-PP-333; PP-333; Bonzi; Cultar; Parlay; Trimmit. $C_{15}H_{20}ClN_3O$; mol wt 293.80. C 61.32%, H 6.86%, Cl 12.07%, N 14.30%, O 5.45%. Plant growth **4243405** (1978, 1981 both to ICI). Physical properties and biological activity: B. G. Lever *et al., Proc. Brit. Crop Prot. Conf. - Weeds* **1982,** 3. Resolution and activity of isomers: B Sugavanam, *Pestic. Sci.* **15,** 296 (1984). GC determn in plant tissue: E. A. Stahly, D. A. Buchanan, *HortScience* **21,** 53 (1986). Comparison with daminozide, *q.v.*, of effect on apple trees: G. R. Stinchcombe *et al., J. Hort. Sci.* **59,** 323 (1984).

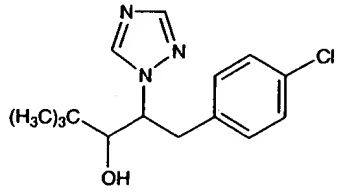

White crystalline solid, mp 165-166°. d 1.22. Vapor pressure at 20°: 1×10^{-6} Pa. Soly: water 35 mg/l, methanol 15%, propylene glycol 5%, acetone 11%, cyclohexanone 18%, methylene dichloride 10%, hexane 1%, xylene 6%.
USE: Plant growth regulator.

7054. Pactamycin. [23668-11-3] 2-Hydroxy-6-methylbenzoic acid [1*S*-[1α,2β,3α,3(*R**),4α,5β]]-[5-[(3-acetylphenyl)amino]-4-amino-3-[[(dimethylamino)carbonyl]amino]-1,2-dihydroxy-3-(1-hydroxyethyl)-2-methylcyclopentyl]methyl ester; NSC-52947; U-15800. $C_{28}H_{38}N_4O_8$; mol wt 558.62. C 60.20%, H 6.86%, N 10.03%, O 22.91%. Antitumor antibiotic produced by *Streptomyces pactum* var *pactum.* Discovery and biological properties: Bhuyan *et al., Antimicrob. Ag. Chemother.* **1961,** 184. Isoln and characterization: Argoudelis *et al., ibid.* 191. Manuf: **GB 980346** (1965 to Upjohn), *C.A.* **62,** 11115f (1965). Structure: Wiley *et al., J. Org. Chem.* **35,** 1420 (1970). Revised structure: D. J. Duchamp, *Am. Crystallogr. Assn.* (Winter Mtg., Albuquerque, 1972) p 23. Mechanism of action: T. A. Beerman *et al., Adv. Enzyme Regul.* **14,** 207 (1976). ^{13}C-NMR study: D. D. Weller *et al., J. Antibiot.* **30,** 997 (1978). Biosynthesis: D. D. Weller, K. L. Rinehart, *J. Am. Chem. Soc.* **100,** 6757 (1978). *Review:* Goldberg in *Antibiotics* **vol. 3,** J. W. Corcoran, F. E. Hahn, Eds. (Springer-Verlag, New York, 1975) pp 498-515.

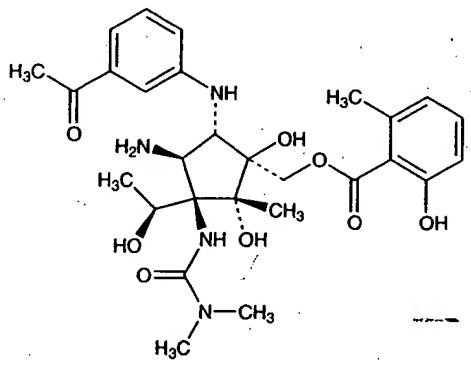

$[\alpha]_D^{25}$ +79° (ethanol) changing to +23° on standing. [α] changes in acetone on standing from +25° to +76° in 24° hours. Amphoteric. Sol in ethanol, chloroform, methylene chloride, benzene, ether, in solns <pH 5 and >9.5. Insol in Skellysolve B, cyclohexane; insol at isoelectric pt, pH 8.3. Unstable in solution. LD_{50} in mice (mg/kg): 10.7 orally; 15.6 i.v.; in rats (mg/kg): 1.4 i.v. (Bhuyan).

7055. Palitantin. [15265-28-8] (2*R*,3*S*,5*R*,6*R*)-*rel*-3-(1*E*,3*E*)-1,3-Heptadienyl-5,6-dihydroxy-2-(hydroxymethyl)cyclohexanone. $C_{14}H_{22}O_4$; mol wt 254.32. C 66.12%, H 8.72%, O 25.16%. Metabolic product of *Penicillium palitans* Westling. Isoln: J. H. Birkinshaw, H. Raistrick, *Biochem. J.* **30,** 801 (1936). Derivs and degradation products: J. H. Birkinshaw, *ibid.* **51,** 271 (1952). Structure: K. Bowden *et al., J. Chem.*

EXHIBIT D

CANCER TREATMENT REVIEWS 2003; 29: 407-415
doi:10.1016/S0305-7372(03)00097-5

ANTI-TUMOUR TREATMENT

CANCER TREATMENT REVIEWS

Mode of action of docetaxel – a basis for combination with novel anticancer agents

Roy S. Herbst[1] and Fadlo R. Khuri[2]

[1]Department of Thoracic/Head and Neck Medical Oncology and Cancer Biology, The University of Texas, Houston, TX, USA; [2]Clinical and Translational Research, Emory University, Atlanta, GA, USA

Different tumors have different aberrations in signaling and growth stimulation pathways that drive cancer growth. An understanding of these processes is key to the development of new anticancer agents and to identifying optimal treatment strategies and patient populations suitable for specific therapies. It is becoming clear that certain chemotherapeutic drugs such as docetaxel are not simply inhibitors of mitosis and may interact with these tumorigenic mechanisms at a number of levels. This review describes docetaxel's mechanism of action, and provides a basis for understanding how its antitumor activity can integrate with that of different novel agents. Against this background, key docetaxel–novel agent combinations that are currently under clinical investigation are reviewed. How these strategies can be targeted towards specific patient populations (e.g., HER-2 overexpressing metastatic breast cancer patients) to provide optimal therapy is highlighted.

Key words: Combination chemotherapy; docetaxel; mechanism; novel agents.

INTRODUCTION

It is becoming clear that certain chemotherapeutic agents such as docetaxel have multiple effects within a tumor and interact with a variety of processes involved in cancer cell growth and metastasis. Different tumors have distinct aberrations in the signaling and growth stimulation pathways that drive these processes. Gaining an understanding of the complexities of docetaxel's mechanism of action, combined with an understanding of the molecular and genetic changes within a particular tumor, may aid the future identification of the most appropriate patients for treatment. Such an approach would allow cancer care to step beyond current treatment paradigms, and into an environment where targeted and individualized combinations provide optimal benefits.

Docetaxel is a second-generation taxane derived from the needles of the European yew tree. Early *in vitro* studies revealed that docetaxel has a wide spectrum of antitumor activity (1) and a number of unique preclinical characteristics compared to other chemotherapeutic agents, including the taxane paclitaxel. For instance, in several murine and human tumor cell lines, docetaxel exhibited 1.3- to 12-fold greater cytotoxicity relative to paclitaxel (2,3). A similar pattern emerges from its broad spectrum of activity *in vivo* with murine tumor models and human tumor xenografts (1). Furthermore, unlike paclitaxel, docetaxel exhibits linear pharmacokinetics and, due to differences in drug efflux, is retained intracellularly for a longer period (4,5).

This preclinical promise has translated into clinical practice. Docetaxel is highly effective as monotherapy and combination therapy across a variety of tumor types, including breast, lung, and ovarian, as well as head and neck, gastric, and prostate carcinomas (6–12).

Correspondence to: Professor Fadlo R. Khuri, MD, Associate Director, Clinical and Translational Research, Winship Cancer Center, Emory University, 1365 Clifton Road, Suite B4100 Atlanta, GA 30322, USA; E-mail: rherbst@mail.mdanderson.orgfkhuri@emory.edu

This review describes docetaxel's mechanism of action and explains the rationale for its combination with a variety of novel anticancer agents. Particular docetaxel–novel agent treatment combinations under clinical investigation are discussed in conjunction with the targeting of these strategies towards specific patient populations to provide optimal therapy.

DOCETAXEL – A DRUG WITH MULTIPLE TARGETS

An antimicrotubule agent

The central role of microtubules in cell division and other relevant cellular functions makes them a focus for anticancer drug development (13). The primary mechanism of action for the taxanes (docetaxel and paclitaxel) is to promote microtubulin assembly and stabilize the polymers against depolymerization, thereby inhibiting microtubule dynamics (2). This mechanism of action employed by taxanes is distinct from that of other antimicrotubule agents, which prevent microtubule assembly (13).

Although docetaxel and paclitaxel share a mutual microtubule binding site (for which docetaxel has a higher affinity (14)), there is evidence that they have distinct effects on microtubule dynamics (15). This may underlie the greater potency of docetaxel as a tubulin assembly promoter and microtubule stabilizer compared to that of paclitaxel (16). Furthermore, preliminary data suggest that low levels of expression of specific microtubule-associated proteins (e.g., the class II β-tubulin isotype) may correlate with higher docetaxel response rates – a potential predictive marker for docetaxel activity (17). The consequences of blocking microtubule dynamics are complex: a number of vital cellular functions in which microtubules play a critical role are compromised. Impairment of mitotic progression leading to cell cycle arrest is considered to be a principal component of docetaxel's mechanism of action. This blocks progression of a cell through its natural division cycle and, consequently, inhibits cell proliferation.

Docetaxel influences apoptosis pathways

Disruption of microtubules not only affects progression through the cell cycle, but may also alter signaling pathways involved in processes such as apoptosis (18). Apoptosis, also known as 'programmed cell death', is a physiologic process involving the activation of certain signaling pathways and genetic programs. Defects in this process are believed to contribute to a number of human diseases and decreased or inhibited apoptosis is a feature of many malignancies (19). Several studies have demonstrated that docetaxel and other microtubule-targeting agents promote apoptosis in cancer cells (20).

Several signal transduction pathways may be involved in docetaxel's effects on apoptosis (18). The *Bcl-2* gene family in particular appears to play a critical role in the regulation of apoptosis. Inhibition of Bcl-2 induces apoptosis, whereas overexpression of Bcl-2 prevents or delays apoptosis (enhancing cell survival) and may be a factor relating to chemotherapeutic drug resistance (21). Consequently, downregulation of Bcl-2 expression has been investigated as a strategy for reversal of resistance (22). Antimicrotubule agents are believed to cause inactivation of Bcl-2 function through phosphorylation (23). Docetaxel is 10- to 100-fold more potent than paclitaxel in phosphorylating Bcl-2 and this may account for the differential pro-apoptotic activity of docetaxel compared with paclitaxel (23–25). An association of docetaxel-induced apoptosis with increases in tumor blood vessel diameter may have the beneficial secondary effect of improving delivery of other therapeutic agents (26).

Docetaxel inhibits angiogenesis

Angiogenesis is the process by which tumors develop new capillary blood vessels (27). The process is vital for tumor progression and is intrinsically connected with metastases (28). Furthermore, new capillaries formed in tumors may be less viable than those in normal tissues and, consequently, present a barrier for the delivery of chemotherapeutic agents to target cells (29). Several positive endogenous modulators of angiogenesis have been identified, including vascular endothelial growth factor (VEGF) and transforming growth factor α (TGF-α), as well as a number of negative modulators (27). Inhibition of angiogenesis is a potential strategy in antitumor drug development, with a number of agents currently undergoing clinical investigation (30). Such a strategy may have advantages in relation to toxicity and drug resistance.

Docetaxel has been shown to inhibit angiogenesis both *in vitro* and *in vivo* (31). The antiangiogenic effect of docetaxel is four times stronger than that of paclitaxel (32). VEGF has been shown to shield tumor cells from the antiangiogenic effects of docetaxel and VEGF antibodies can overcome the protective effect both *in vitro* and *in vivo*. In the

clinic, VEGF overexpression is associated with larger tumor size, increased metastasis, and poor prognosis in metastatic breast cancer (MBC) patients (33,34). Enhancement of the antiangiogenic properties of docetaxel through inhibition of endogenous angiogenic growth factors such as VEGF is a strategy that merits further investigation.

Docetaxel and gene expression

The taxanes have been shown to be inducers of numerous genes involved in a variety of cellular processes (35). Differences in gene expression may underlie distinctions in the clinical profiles of docetaxel and paclitaxel such as the higher incidence of immediate hypersensitivity reactions or neurotoxicity associated with paclitaxel (5). Differences in gene expression may also influence the pharmacokinetic characteristics of the taxanes. For instance, unlike docetaxel, paclitaxel activates the steroid and xenobiotic receptor (SXR) and consequently induces a number of hepatic enzymes and the broad-specificity efflux pump P-glycoprotein (36).

Cellular signaling pathways

The effect docetaxel has on apoptosis, angiogenesis, and gene expression cannot be considered in isolation as these are complex processes involving numerous components. Docetaxel's ability to induce signaling aberrations is likely to trigger numerous messages within tumor cells.

The EGFR pathway

An example of a signaling pathway that feeds into processes affected by docetaxel, namely apoptosis and angiogenesis, is the epidermal growth factor receptor (EGFR) signaling pathway. Members of the EGFR family (e.g., the human epidermal growth factor receptors HER-1 and HER-2) and their signaling pathways influence cell cycle regulation, angiogenesis, and apoptosis (37,38). Signals are transmitted from the cell surface to the cell nucleus via a variety of downstream effector proteins such as Ras and MAP kinase as shown in Figure 1.

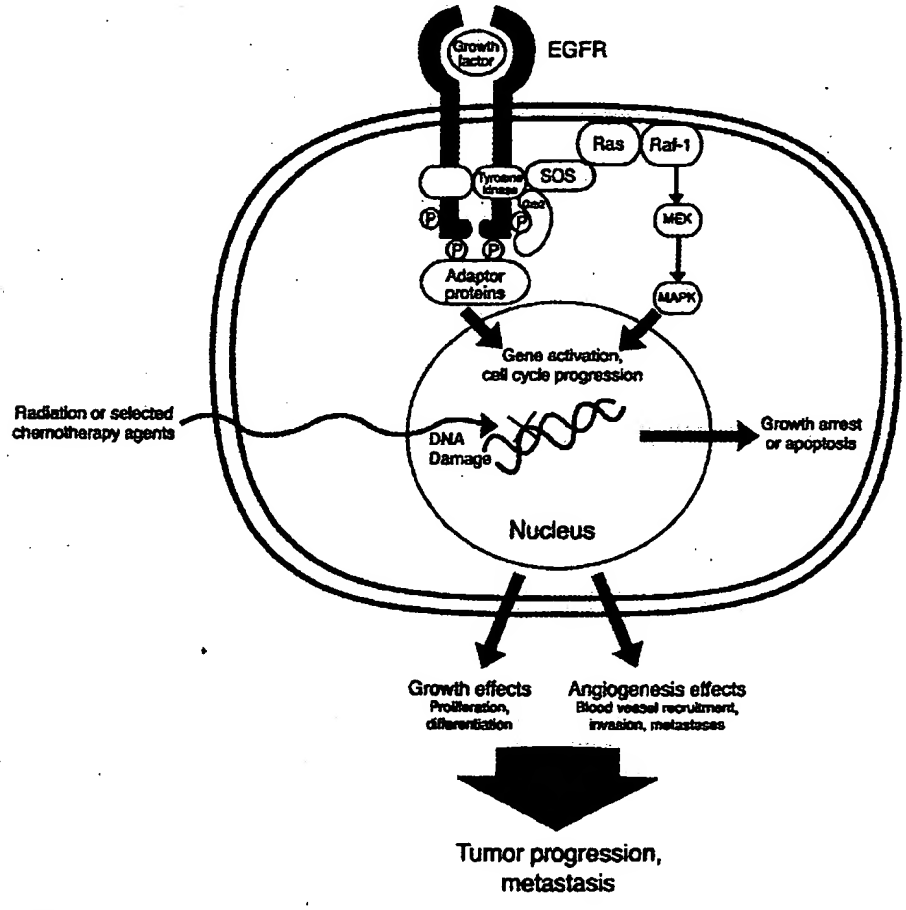

Figure 1 EGFR signaling pathway – signals are transmitted from the cell surface to the nucleus via effector proteins such as Ras and MAP kinase.

HER-1 is overexpressed in a wide range of tumors (39), especially squamous cell carcinoma of the head and neck (SCCHN), where it is associated with poor prognosis (40,41). HER-2 is also overexpressed in many tumor types – in particular, breast cancer (30% of tumors) (42). HER-2 overexpression imparts a metastatic advantage to the cell and is associated with impaired survival in the patient (42,43). There is considerable potential for targeted therapy in patients with HER-1 or HER-2 overexpressing tumors.

The Ras pathway

The Ras proteins interact with receptors such as EGFR (as shown in Figure 1), cytokines, and hormones to play a critical role in intracellular signaling. Ras proteins activate several downstream effector pathways that mediate cell proliferation, gene transcription, and apoptosis. Tumor cells may harbour Ras mutations or continuously activate the Ras protein to ensure downstream effector pathways remain stimulated (44). Overexpression of Ras has been associated with more aggressive types of breast cancer, loss of p53 function and HER-2 overexpression (45,46).

For the Ras protein to function it must be anchored to the inner surface of the cell membrane. The first step in the anchoring process is the addition of a farnesyl group to Ras – a reaction catalyzed by farnesyl transferase (FTPase) enzymes (47) (Figure 2). This is a critical step in the processing of Ras and inhibition of farnesylation alone may be sufficient to block cell signaling and cancer cell growth. In this regard farnesyl transferase inhibitors (FTIs) are likely to be useful agents in the targeted treatment of tumors expressing wildtype Ras protein (48).

NOVEL ANTICANCER AGENTS – POTENTIAL FOR SYNERGY WITH DOCETAXEL?

Docetaxel treatment is clearly associated with a number of cellular changes, and may have multiple effects within a tumor. An understanding of the cellular processes influenced by anticancer agents, and the aberrations specific tumors possess, are essential for effective individualized treatment to move into the clinic. By matching certain tumor defects or markers with the most suitable anticancer agent based on mechanism of action, tumor responses may be maximized. The increasing aware-

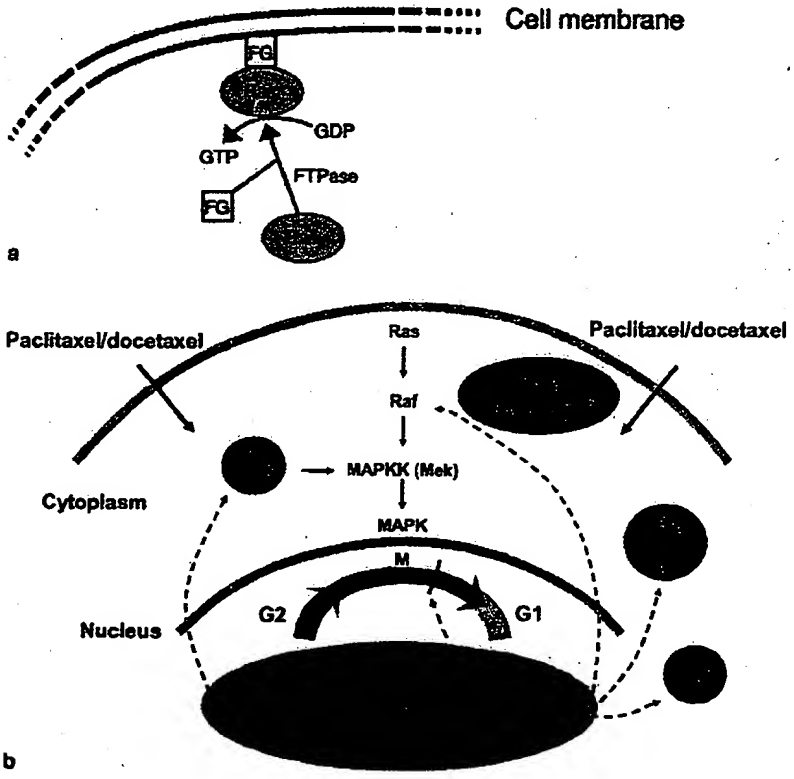

Figure 2 (a) The first step in Ras modification – the addition of a farnesyl group (FG) – is catalyzed by FTPase and enables the protein to localize to the inner surface of the plasma membrane. (b) Mechanisms of resistance to docetaxel may be Ras mediated, even if Ras is wildtype in tumors. Enhanced G2M arrest by farnesyl transferase inhibitors appears to sensitize cancer cells to taxanes, and restore potentially the taxane's ability to phosphorylate Bcl-2, thereby enhancing the agent's proapoptotic activity.

ness of such processes has heralded the development of a range of novel anticancer agents. In particular, therapies targeted against genes or molecules involved in the growth stimulation pathways that drive cancer growth hold promise (e.g., HER-2 positive MBC patients and treatment with trastuzumab).The following section outlines some of the docetaxel-novel agent combination strategies currently being investigated (see Table 1 for summary).

Docetaxel + trastuzumab (Herceptin)

Trastuzumab is a monoclonal antibody directed against the HER-2 receptor. It is active both as a single agent in HER-2 MBC and when combined with chemotherapy (49). Unfortunately, cardiotoxicity limits combination of trastuzumab with some chemotherapeutic agents (e.g., doxorubicin) (50). Docetaxel has not been associated with cardiotoxicity and may, therefore, be a particularly suitable candidate for trastuzumab combination therapy (51).

In vitro studies reveal considerable potential for such a combination strategy – there is a synergistic antitumor effect when trastuzumab is combined with docetaxel, but only an additive effect when it is combined with paclitaxel and some other chemotherapeutic agents (52). An ongoing Phase II study in MBC patients overexpressing HER-2 is evaluating the efficacy and safety of 3-weekly docetaxel (75 mg/m^2) in combination with trastuzumab (4 mg/kg Week1 then 2 mg/kg/week) (51,53, 54). Among 16 evaluable patients, one complete response (CR) and six partial responses (PR) have been confirmed (overall response rate, ORR = 44%). Furthermore, three minor responses (between 25 and 50% reduction in tumor size) were documented and stable disease (SD) was observed in five patients. As predicted, no significant cardiotoxicity has been observed.

Several pilot studies have considered weekly docetaxel (35 mg/m^2/week) plus trastuzumab in HER-2 positive MBC patients (51,54). Uber and colleagues (55) have reported two CRs (11%) and 10 PRs (53%) in 19 evaluable patients (overall response rate, ORR 63%). Cardiotoxicity was limited to a transient asymptomatic decline in ejection fraction observed in one patient. These results are comparable to those observed in the other pilot studies. Esteva and colleagues (56) reported an ORR of 63% (19 PR, 3 MR, 4 SD; $n = 30$), and Meden *et al.* (57) obtained an ORR of 50% (6 PR, 5 SD; $n = 12$). These preliminary data suggest that weekly docetaxel plus trastuzumab has the potential to be a well-tolerated and effective regimen in HER-2 overexpressing MBC.

Table 1 Clinical studies of docetaxel-novel agent combinations

Combination	Patients (evaluable)	Response	Reference
Docetaxel + trastuzumab	MBC ($n = 30$)	19 PR, 3 MR, 4 SD; ORR 63%	Esteva *et al.* (56)
	MBC ($n = 16$)	1 CR, 6 PR, 3 MR, 5 SD; ORR 44%	Kuzur *et al.* (53)
	MBC ($n = 12$)	6 PR, 5 SD; ORR 50%	Meden *et al.* (57)
	MBC ($n = 19$)	2 CR, 10 PR; ORR 63%	Uber *et al.* (55)
Docetaxel + carboplatin + trastuzumab	ABC/MBC ($n = 14$)	3 CR, 7 PR; ORR 71%	Slamon *et al.* (60); Nabholtz *et al.* (58)
Docetaxel + cisplatin + trastuzumab	ABC/MBC ($n = 34$)	3 CR, 23 PR; ORR 76%	Pienkowski *et al.* (59); Nabholtz *et al.* (58)
Docetaxel + cetuximab	NSCLC	Data not yet available	www.imclone.com
Docetaxel + FTI (R115777)	Solid tumor	1 CR, 4PR, 6SD	Piccart et al. (68)
Docetaxel + capecitabine vs capecitabine	MBC ($n = 511$)	ORR 41.6% vs 29.7%	O'Shaughnessy *et al.* (70); Leonard *et al.* (71)
Docetaxel + doxorubucin + capecitabine	ABC/MBC ($n = 18$)	9 PR + CR, 7 SD; ORR 50%	Pagani *et al.* (72)
Docetaxel + augmerosen	Advanced solid tumors	Data not yet available	Hayes *et al.* (75)
	Progressive AIPC ($n = 6$)	4 SD	Morris *et al.* (76)

ABC: advanced breast cancer; AIPC: androgen-independent prostate cancer; MBC: metastatic breast cancer; NSCLC: non-small cell lung cancer; CR: complete response; PR: partial response; MR: minor response (25% to 50% ↓ tumor size); SD: stable disease.

The three-drug combination of docetaxel plus platinum salts plus trastuzumab also shows a high degree of synergy in computer models of *in vitro* data (51,52). Two Phase II studies assessed the safety and efficacy of docetaxel plus platinum salts (cisplatin or carboplatin) plus trastuzumab in advanced breast cancer (ABC) patients overexpressing HER-2 (58–60). Interim results show responses in 26/34 patients receiving the cisplatin regimen (3 CR, 23 PR: ORR 76%) and 10/14 patients receiving the carboplatin regimen (3 CR, 7 PR: ORR 71%). Cardiotoxicity was minimal – one patient in each study developed congestive heart failure (one of whom had a prior cardiac history).

Docetaxel + cetuximab (IMC-C225/Erbitux)

Cetuximab is a monoclonal antibody directed against HER-1 (61). It is one of several agents in development that inhibit HER-1 using this approach. Agents that inhibit the activity of HER-1 using alternative mechanisms have also been developed. For instance, ZD1839 (Iressa) and OSI-774 (Tarceva) each inhibit phosphorylation in the intracellular region of the receptor (62,63).

Clinical responses to cetuximab in combination with chemotherapy or radiation have been observed in several tumor types (e.g., SCCHN, colorectal and NSCLC) (64). Clinical studies of docetaxel plus cetuximab in NSCLC patients are currently underway. Preliminary data from a Phase II study of patients with chemotherapy refractory/resistant advanced NSCLC indicate that docetaxel plus cetuximab is well tolerated and active (65). Pharmacokinetic data from the same study show no direct interaction between docetaxel and cetuximab (65).

Docetaxel and farnesyl transferase inhibitors (FTIs)

Farnesyl transferase inhibitors (FTIs) are novel anticancer agents designed to inhibit tumor growth by interfering with Ras processing. A number of FTIs are undergoing clinical development including Sch-66336, R115777 and L-744832 (44). FTIs have been shown to be synergistic with taxanes in preclinical studies (66) and several Phase I studies of FTIs in combination with the taxanes have been conducted (67,68).

A Phase I dose finding study has investigated a combination of docetaxel with the FTI R115777 in patients with solid tumors. One CR (breast), 4 PR (2 breast, 1 NSCLC, 1 unknown primary tumor) and 6 SD were reported in preliminary results for 24 patients (68). Pharmacokinetic data indicate R115777 has no influence on docetaxel clearance. Accrual is ongoing for two dosing regimens; docetaxel 85 mg/m^2 with R115777 200 mg bid every 14 days (breast) and docetaxel 60 mg/m^2 with R115777 300 mg bid every 14 days (mainly NSCLC). The preliminary data indicate docetaxel–FTI combinations are feasible and that further studies are warranted.

Docetaxel + capecitabine (Xeloda)

Capecitabine is an oral chemotherapy drug that is activated through a three-step enzymatic pathway. It is converted preferentially in tumors from an inactive prodrug to 5-fluorouridine (5-FU – a uracil analog) by exploiting the high activity of the enzyme thymidine phosphorylase (TP) in tumor tissue compared with normal healthy tissue. This novel conversion allows targeted delivery of 5-FU to cancer cells and minimizes unwanted effects on normal tissue.

A combination of capecitabine with docetaxel shows better antitumor efficacy *in vivo* compared to monotherapy. The most potent and synergistic activity occurs when docetaxel is given on Day 8 (69). Possible mechanisms underlying this synergy include upregulation of thymidine phosphorylase by docetaxel. Conversely, capecitabine may enhance the efficacy of docetaxel through other mechanisms, possibly involving the Bcl-2 protein family (69).

A large Phase III trial has been conducted comparing the docetaxel–capecitabine combination therapy with docetaxel monotherapy in MBC patients (70,71). Efficacy data showed that time to disease progression was significantly superior with the combination (median 6.1 months) compared to monotherapy (median 4.2 months; $p = 0.0001$). Overall survival was also superior with the combination (14.5 months) compared to monotherapy (11.5 months; $p = 0.01$), and one-year survival rates were 56.8% and 46.9%, respectively. Tumor response rate was 42% in the combination therapy group compared with 30% in the monotherapy group ($p = 0.006$). The adverse events associated with the docetaxel–capecapecitabine combination were predictable and manageable with appropriate intervention. Preliminary data also suggest that a triple combination regimen of docetaxel, doxorubicin, and capecitabine may also be safe and effective in ABC patients (72).

Docetaxel + augmerosen (G3139/Genasense)

The use of antisense oligonucleotides to modify gene expression is another strategy being employed to

target molecules implicated in tumorigenesis (73). Augmerosen is an antisense oligonucleotide that targets Bcl-2 RNA, thereby causing down-regulation of Bcl-2 protein translation. Augmerosen monotherapy and combination therapy have produced promising results in clinical trials of patients with Bcl-2 overexpressing tumors (22,74). This agent has also been shown to enhance the antitumor effects of docetaxel at subtherapeutic doses in murine models (75).

A Phase I trial determined the maximum tolerated dose and optimal schedule of docetaxel plus augmerosen combination therapy in patients with advanced solid tumors (75). In the first part of the study, patients received a continuous infusion of augmerosen for 21 days plus weekly docetaxel. In the second part of the study, patients received augmerosen as a continuous infusion for Days 1–5, then as a continuous infusion for the 48 h prior to weekly docetaxel administration (for a total of 3 weeks). The study is ongoing, but preliminary results show promise in this mixed patient group, and no dose-limiting toxicity has been observed. A study in progressive androgen-independent prostate cancer patients also suggests that the combination of docetaxel plus augmerosen is well tolerated (76).

CONCLUSIONS

By understanding the aberrations specific tumors possess and the cellular processes influenced by anticancer agents, it may be possible to provide effective individualized treatment for cancer patients in the future. Docetaxel is an anticancer agent with multiple effector targets, including apoptotic, angiogenic, and gene expression processes. Along with the primary antimicrotubule effect, these mechanisms provides a basis for combining docetaxel with a variety of novel anticancer agents across a range of tumor types. Promising clinical results have been obtained for docetaxel in combination with trastuzumab, cetuximab, FTIs, capecitabine, and augmerosen. Other novel agents may have similar potential. For instance, several strategies for inhibiting VEGF receptor signaling are now in development and clinical studies with anti-VEGF antibodies as single agents and in combination with taxanes are underway (48,77). Preclinical data suggest that the combination of docetaxel plus an anti-VEGF antibody deserves further investigation.

Docetaxel–novel agent combinations demonstrate how targeted therapies used in a multimodality approach could reform the treatment of cancer. Research advances suggest we may one day see targeted individualized combinations providing optimal treatment in the clinic. In such an environment, docetaxel has the potential to play a pivotal role.

REFERENCES

1. Bissery MC. Preclinical pharmacology of docetaxel. *Eur J Cancer* 1995; 31A(Suppl 4): S1–6.
2. Ringel I, Horwitz SB. Studies with RP 56976 (Taxotere): a semisynthetic analogue of taxol. *J Natl Cancer Inst* 1991; 83: 288–291.
3. Riou JF, Naudin A, Lavelle F. Effects of Taxotere on murine and human tumor cell lines. *Biochem Biophys Res Commun* 1992; 187: 164–170.
4. Bissery MC, Nohynek G, Sanderink GJ, Lavelle F. Docetaxel (Taxotere®): a review of preclinical and clinical experience. Part I: Preclinical experience. *Anticancer Drugs* 1995; 6: 339–368.
5. Michaud LB, Valero V, Hortobagyi G. Risks and benefits of taxanes in breast and ovarian cancer. *Drug Saf* 2000; 23: 401–428.
6. Crown J, O'Leary M. The taxanes: an update. *Lancet* 2000; 355: 1176–1178.
7. Figgitt DP, Wiseman LR. Docetaxel: an update of its use in advanced breast cancer. *Drugs* 2000; 59: 621–651.
8. Kaye SB and the Scottish Gynaecological Cancer Trials Group. The integration of docetaxel into first-line chemotherapy for ovarian cancer. *Int J Gynecol Cancer* 2001; 11(Suppl 1): 31–33.
9. Petrylak DP. Docetaxel (Taxotere) in hormone-refractory prostate cancer. *Semin Oncol* 2000; 27(Suppl 3): 24–29.
10. Posner MR. Docetaxel in squamous cell cancer of the head and neck. *Anticancer Drugs* 2001; 12(Suppl 1): 21–24.
11. Ridwelski K, Gebauer T, Fahlke J, *et al.* Combination chemotherapy with docetaxel and cisplatin for locally advanced and metastatic gastric cancer. *Ann Oncol* 2001; 12: 47–51.
12. Shepherd FA, Fossella FV, Lynch T, Armand JP, Rigas JR, Kris MG. Docetaxel (Taxotere) shows survival and quality-of-life benefits in the second-line treatment of non-small cell lung cancer: a review of two phase III trials. *Semin Oncol* 2001; 28(Suppl 2): 4–9.
13. Rowinsky EK, Donehower RC. Antimicrotubule agents. In: Chabner BA, Longo DL (eds.), *Cancer chemotherapy and biotherapy*. 2nd ed. Lippincott-Raven: Philadelphia, 1996; 263–296.
14. Diaz JF, Valpuesta JM, Chacon P, Diakun G, Andreu JM. Changes in microtubule protofilament number induced by Taxol binding to an easily accessible site. Internal microtubule dynamics. *J Biol Chem* 1998; 273: 33803–33810.
15. Andreu JM, Diaz JF, Gil R, *et al.* Solution structure of Taxotere-induced microtubules to 3-nm resolution. The change in protofilament number is linked to the binding of the taxol side chain. *J Biol Chem* 1994; 269: 31785–31792.
16. Guéritte-Voegelein F, Guénard D, Lavelle F, Le Goff MT, Mangatal L, Potier P. Relationships between the structure of taxol analogues and their antimitotic activity. *J Med Chem* 1991; 34: 992–998.
17. Bernard C, Fellous A, Di Leo A, *et al.* Evaluation of microtubule associated parameters (MTAPs) as predictive markers for advanced breast cancer (ABC) patients treated with docetaxel. *Eur J Cancer* 2001; 37(Suppl. 6): 182.
18. Wang LG, Liu XM, Kreis W, Budman DR. The effect of antimicrotubule agents on signal transduction pathways of

apoptosis: a review. *Cancer Chemother Pharmacol* 1999; 44: 355–361.
19. Renehan AG, Booth C, Potten CS. What is apoptosis, and why is it important?. *BMJ* 2001; 322: 1536–1538.
20. Schimming R, Mason KA, Hunter N, Weil M, Kishi K, Milas L. Lack of correlation between mitotic arrest or apoptosis and antitumor effect of docetaxel. *Cancer Chemother Pharmacol* 1999; 43: 165–172.
21. Pratesi G, Perego P, Zunino F. Role of Bcl-2 and its post-transcriptional modification in response to antitumor therapy. *Biochem Pharmacol* 2001; 61: 381–386.
22. Jansen B, Wacheck V, Heere-Ress E, *et al.* Chemosensitisation of malignant melanoma by Bcl-2 antisense therapy. *Lancet* 2000; 356: 1728–1733.
23. Haldar S, Basu A, Croce CM. Bcl-2 is the guardian of microtubule integrity. *Cancer Res* 1997; 57: 229–233.
24. Haldar S, Jena N, Croce CM. Inactivation of Bcl-2 by phosphorylation. *Proc Natl Acad Sci USA* 1995; 92: 4507–4511.
25. Haldar S, Chintapalli J, Croce CM. Taxol induced Bcl-2 phosphorylation and death in prostate cancer cells. *Cancer Res* 1996; 56: 1253–1255.
26. Griffon-Etienne G, Boucher Y, Brekken C, Suit HD, Jain RK. Taxane-induced apoptosis decompresses blood vessels and lowers interstitial fluid pressure in solid tumors: clinical implications. *Cancer Res* 1999; 59: 3776–3782.
27. Liekens S, De Clercq E, Neyts J. Angiogenesis: regulators and clinical applications. *Biochem Pharmacol* 2001; 61: 253–270.
28. Kirsch M, Schackert G, Black PM. Angiogenesis, metastasis, and endogenous inhibition. *J Neurooncol* 2000; 50: 173–180.
29. Netti PA, Hamberg LM, Babich JW, *et al.* Enhancement of fluid filtration across tumor vessels: implication for delivery of macromolecules. *Proc Natl Acad Sci USA* 1999; 96: 3137–3142.
30. Rosen L. Antiangiogenic strategies and agents in clinical trials. *Oncologist* 2000; 5(Suppl 1): 20–27.
31. Sweeney CJ, Miller KD, Sissons SE, *et al.* The antiangiogenic property of docetaxel is synergistic with a recombinant humanized monoclonal antibody against vascular endothelial growth factor or 2-methoxyestradiol but antagonized by endothelial growth factors. *Cancer Res* 2001; 61: 3369–3372.
32. Vacca A, Ribatti D, Iurlaro M, *et al.* Docetaxel versus paclitaxel for antiangiogenesis. *J Hematother Stem Cell Res* 2002; 11(1): 103–118.
33. Saaristo A, Karpanen T, Alitalo K. Mechanisms of angiogenesis and their use in the inhibition of tumor growth and metastasis. *Oncogene* 2000; 19: 6122–6129.
34. Linderholm BK, Lindh B, Beckman L, *et al.* The prognostic value of vascular endothelial growth factor (VEGF) and basic fibroblast growth factor (bFGF) and associations to first metastasis site in 1307 patients with primary breast cancer. *Proc Am Soc Clin Oncol* 2001; 20: 13.
35. Moos PJ, Fitzpatrick FA. Taxane-mediated gene induction is independent of microtubule stabilization: induction of transcription regulators and enzymes that modulate inflammation and apoptosis. *Proc Natl Acad Sci USA* 1998; 95: 3896–3901.
36. Synold TW, Dussault I, Forman BM. The orphan nuclear receptor SXR coordinately regulates drug metabolism and efflux. *Nat Med* 2001; 7: 584–590.
37. Woodburn JR. The epidermal growth factor receptor and its inhibition in cancer therapy. *Pharmacol Ther* 1999; 82: 241–250.
38. Nagy P, Jenei A, Damjanovich S, Jovin TM, Szöllősi J. Complexity of signal transduction mediated by ErbB2: clues to the potential of receptor-targeted cancer therapy. *Pathol Oncol Res* 1999; 5: 255–271.
39. Wikstrand CJ, Bigner DD. Prognostic applications of the epidermal growth factor receptor and its ligand, transforming growth factor-α. *J Natl Cancer Inst* 1998; 90: 799–801.
40. Grandis JR, Melhem MF, Gooding WE, *et al.* Levels of TGF-α and EGFR protein in head and neck squamous cell carcinoma and patient survival. *J Natl Cancer Inst* 1998; 90: 824–832.
41. Nicholson RI, Gee JM, Harper ME. EGFR and cancer prognosis. *Eur J Cancer* 2001; 37(Suppl 4): 9–15.
42. Slamon DJ, Clark GM, Wong SG, Levin WJ, Ullrich A, McGuire WL. Human breast cancer: correlation of relapse and survival with amplification of the HER-2/neu oncogene. *Science* 1987; 235: 177–182.
43. Tiwari RK, Borgen PI, Wong GY, Cordon-Cardo C, Osborne MP. HER-2/neu amplification and overexpression in primary human breast cancer is associated with early metastasis. *Anticancer Res* 1992; 12: 419–425.
44. Johnston SR, Kelland LR. Farnesyl transferase inhibitors – a novel therapy for breast cancer. *Endocr Relat Cancer* 2001; 8: 227–235.
45. Smith CA, Pollice AA, Gu LP, *et al.* Correlations among p53, HER2/neu and ras overexpression and aneuploidy by multiparameter flow cytometry in human breast cancer; evidence for a common phenotypic evolutionary pattern in infiltrating ductal carcinomas. *Clin Cancer Res* 2000; 6: 112–126.
46. Theillet C, Lidereau R, Escot C. Frequent loss of H-ras allele correlates with aggressive human primary breast carcinomas. *Cancer Res* 1986; 46: 4776–4781.
47. Kato K, Cox AD, Hisaka MM, Graham SM, Buss JE, Der CJ. Isoprenoid addition to ras protein is the critical modification for its membrane association and transforming activity. *Proc Natl Acad Sci USA* 1992; 89: 6403–6407.
48. Johnson DH, DeVore R, Kabbinavar F, Herbst R, Holmgren E, Novotny W. Carboplatin (C) + paclitaxel (T) + RhuMab-VEGF (AVF) may prolong survival in advanced non-squamous lung cancer. *Proc Am Soc Clin Oncol* 2001; 20: 1256.
49. Baselga J. Clinical trials of Herceptin® (trastuzumab). *Eur J Cancer* 2001; 37(Suppl. 1): 18–24.
50. Sparano JA. Cardiac toxicity of trastuzumab (Herceptin): implications for the design of adjuvant trials. *Semin Oncol* 2001; 28(Suppl. 3): 20–27.
51. Pegram MD. Docetaxel and herceptin: foundation for future strategies. *Oncologist* 2001; 6(Suppl 3): 22–25.
52. Slamon D, Pegram M. Rationale for trastuzumab (Herceptin) in adjuvant breast cancer trials. *Semin Oncol* 2001; 28(Suppl 3): 13–19.
53. Kuzur ME, Albain KS, Huntington MO, *et al.* A phase II trial of docetaxel and Herceptin in metastatic breast cancer patients overexpressing HER-2. *Proc Am Soc Clin Oncol* 2000; 19: 512.
54. Burris 3rd HA. Docetaxel (Taxotere) plus trastuzumab (Herceptin) in breast cancer. *Semin Oncol* 2001; 28(Suppl 3): 38–44.
55. Uber KA, Nicholson BP, Thor AD, *et al.* A phase II trial of weekly docetaxel (D) and herceptin (H) as first- or second-line treatment in HER2 overexpressing metastatic breast cancer. *Proc Am Soc Clin Oncol* 2001; 20: 1949.
56. Esteva FJ, Valero V, Booser D, *et al.* Phase II study of weekly docetaxel and trastuzumab for patients with HER-2 overexpressing metastatic breast cancer. *J Clin Oncol* 2002; 20: 1800–1808.
57. Meden H, Beneke A, Hesse T, Novophashenny I, Wischnewsky M. Weekly intravenous recombinant humanized anti-P185HER2 monoclonal antibody (Herceptin) plus docetaxel in patients with metastatic breast cancer: a pilot study. *Anticancer Res* 2001; 21: 1301–1305.
58. Nabholtz JM, Pienkowski T, Northfelt D, *et al.* Results of two open label multicentre phase II pilot studies with Herceptin

in combination with docetaxel and platinum salts (cis or carboplatin) (TCH) as therapy for advanced breast cancer (ABC) in women with tumours overexpressing the HER2-neu proto-oncogene. *Eur J Cancer* 2001; 37(Suppl 6): 190.

59. Pienkowski T, Fumuleau P, Eiermann W, *et al.* Taxotere, cisplatin and Herceptin (TCH) in first-line HER-2 positive metastatic breast cancer (MBC) patients: a phase II pilot study by the Breast Cancer International Research Group (BCIRG 101). *Proc Am Soc Clin Oncol* 2001; 20: 2030.
60. Slamon DJ, Patel R, Northfelt D, *et al.* Phase II pilot study of Herceptin combined with Taxotere and carboplatin (TCH) in metastatic breast cancer (MBC) patients overexpressing the HER-2-neu proto-oncogene: a pilot study of the UCLA Network. *Proc Am Soc Clin Oncol* 2001; 20: 193.
61. Herbst RS, Langer CJ. Epidermal growth factor receptors as a target for cancer treatment: the emerging role of IMC-C225 in the treatment of lung and head and neck cancers. *Semin Oncol* 2002; 29(1 Suppl 4): 27–36.
62. Ciardiello F. Epidermal growth factor receptor tyrosine kinase inhibitors as anticancer agents. *Drugs* 2000; 60(Suppl 1): 25–32.
63. Raymond E, Faivre S, Armand JP. Epidermal growth factor receptor tyrosine kinase as a target for anticancer therapy. *Drugs* 2000; 60(Suppl 1): 15–23.
64. Baselga J. The EGFR as a target for anticancer therapy – focus on cetuximab. *Eur J Cancer* 2001; 37(Suppl 4): 16–22.
65. Kim ES, Mauer AM, Fossella FV, *et al.* A phase II study of Erbitux (IMC-C225), an epidermal growth factor receptor (EGFR) blocking antibody, in combination with docetaxel in chemotherapy refractory/resistant patients with advanced non-small cell lung cancer (NSCLC). *Proc Am Soc Clin Oncol* 2002; 21: 1168.
66. Moasser MM, Sepp-Lorenzino L, Kohl NE, *et al.* Farnesyl transferase inhibitors cause enhanced mitotic sensitivity to taxol and epothilones. *Proc Natl Acad Sci USA* 1998; 95: 1369–1374.
67. Khuri FR, Glisson BS, Meyers ML, *et al.* Phase I study of farnesyl transferase inhibitor (FTI) SCH66336 with paclitaxel in solid tumours: dose finding, pharmacokinetics, efficacy/safety. *Proc Am Soc Clin Oncol* 2000; 19: 799.
68. Piccart MJ, Branle F, de Valeriola M, *et al.* A phase I, clinical and pharmacokinetic (PK) trial of the Farnesyl Transferase Inhibitor (FTI) R115777 + Docetaxel: a promising combination in patients (PTS) with solid tumours. *Proc Am Soc Clin Oncol* 2001; 20: 318.
69. Fujimoto-Ouchi K, Tanaka Y, Tominaga T. Schedule dependency of antitumor activity in combination therapy with capecitabine/5′-deoxy-5-fluorouridine and docetaxel in breast cancer models. *Clin Cancer Res* 2001; 7: 1079–1086.
70. O'Shaughnessy J, Miles D, Vukelja S, Moiseyenko V, Ayoub J-P, Cervantes G, Fumoleau P, Jones S, Lui W-Y, Mauriac L, Twelves C, Van Hazel G, Verma S, Leonard R. Superior survival with capecitabine plus docetaxel combination therapy in anthracycline-pretreated patients with advanced breast cancer: Phase III trial results. *J Clin Oncol* 2002; 20(12): 2812–2823.
71. Leonard R, Cervantes G, Lui W-Y, *et al.* Survival update of SO14999 – a large phase III trial of capecitabine/docetaxel combination therapy vs docetaxel monotherapy in patients with locally advanced (LABC) or metastatic breast cancer (MBC). *Eur J Cancer* 2001; 37(Suppl 6): 151.
72. Pagani O, Sessa C, Longhi S, *et al.* Dose-finding study of docetaxel (T) and doxorubicin (A) day 1 and 8 plus capecitabine (X) day 1 to 14 (TAX) as first line treatment in advanced breast cancer (ABC). *Eur J Cancer* 2001; 37(Suppl 6): 194.
73. Khuri FR, Kurie JM. Antisense approaches enter the clinic. *Clin Cancer Res (Ed)* 2000; 6(5): 1607–1610.
74. Waters JS, Webb A, Cunningham D, *et al.* Phase I clinical and pharmacokinetic study of Bcl-2 antisense oligonucleotide therapy in patients with non-Hodgkin's lymphoma. *J Clin Oncol* 2000; 18: 1812–1823.
75. Hayes DF, Chen, HX, Marshall JL, Lippman D, Figuera M, Fingert H. G3139 (oligonucleotide antisense against bcl-2) and docetaxel in patients with Bcl-2-positive malignancies. In: *American Society of Clinical Oncology, 37th Annual Meeting; 12–15 May 2001; San Francisco, CA, USA.* Symposium: beyond chemotherapy – emerging targeted therapies for the treatment of cancer.
76. Morris MJ, Tong WP, Cordon-cardo C, *et al.* BCL-2 antisense (G3139) plus docetaxel for treatment of progressive androgen-independent prostate cancer. *Eur J Cancer* 2001; 37(Suppl 6): 218.
77. McMahon G. VEGF receptor signaling in tumor angiogenesis. *Oncologist* 2000; 5(Suppl 1): 3–10.

EXHIBIT E

Journal of Experimental Therapeutics and Oncology 3: 27–35, 2003

Targeted prodrug treatment of HER-2-positive breast tumor cells using trastuzumab and paclitaxel linked by A-Z-CINN™ Linker

Carl W. Gilbert [1], Eleanor B. McGowan [1], Gerald B. Seery [2], Kirby S. Black [2], and Mark D. Pegram [3]

[1] AuraZyme Pharmaceuticals, Inc., and [2] CryoLife, Inc., Kennesaw, GA, and [3] UCLA School of Medicine and Jonsson Comprehensive Cancer Center, Los Angeles, CA.

Correspondence to Carl W. Gilbert, PhD., Director, Manufacturing, AuraZyme Pharmaceuticals, Inc., 1655 Roberts Boulevard, Kennesaw, GA 30144. Tel.: +1-678-290-4405. Fax: +1-770-590-3790. E-mail: gilbert.carl@aurazyme.com.

(Received August 5, 2002; revised September 27, 2002; accepted October 1, 2002)

Targeting drugs for delivery and release has the potential to increase the efficacy of treatment. A bifunctional linker, A-Z-CINN™ Linker was used to create a targeted prodrug, A-Z-CINN 310. A-Z-CINN Linker links to a potent chemotherapeutic agent, paclitaxel, via an energy-reversible ester bond and also binds a targeting agent, the monoclonal antibody trastuzumab (Herceptin®). This study demonstrates the effectiveness of a single-treatment use of A-Z-CINN 310 in decreasing tumor volume and tumor cell density of human HER-2-positive BT-474 mammary tumor cells implanted in scid mice, compared to treatment with simultaneously administered trastuzumab and paclitaxel and with saline control. After treatment with A-Z-CINN 310, some mice received light exposure at 6 h for 5 min adjacent to the tumor to cause light-accelerated release of paclitaxel. Changes in tumor volume were measured for 28 days following treatment; changes in histology were measured at 31 days. Animals treated with A-Z-CINN 310, then light, showed dose-dependent decreases in tumor volume and tumor cell density which were more rapid and extensive than those seen with A-Z-CINN 310 without light or a 10-fold higher concentration of co-administered trastuzumab plus paclitaxel. This suggests that targeted delivery of paclitaxel using A-Z-CINN 310 kills tumor cells by localized release of paclitaxel at the tumor site, which can be accelerated by light treatment. These results indicate that a targeted prodrug therapy containing trastuzumab as the targeting agent and A-Z-CINN-paclitaxel as the prodrug results in a conjugate that is more effective in killing tumor cells than equivalent concentrations of co-administered trastuzumab and paclitaxel. Targeting of a drug can reduce the dose needed for effective therapy and can increase local bioavailability. This makes targeted therapy using an A-Z-CINN prodrug delivery system feasible for treating both primary and metastatic tumors.

Keywords: Cancer, paclitaxel, prodrug, targeting, trastuzumab

INTRODUCTION

Chemotherapy drugs are invaluable weapons in the effort to kill cancer cells but also have cytotoxic effects on normal cells. Systemic chemotherapy requires multiple treatments and has limited effectiveness. Several approved drugs in current use have side chains that can be used to form prodrugs. These include taxanes (paclitaxel and docetaxel), which are mitotic spindle inhibitors (1,2), anthracyclines (doxorubicin and epirubicin), which are DNA intercalation agents (3), and camptothecins (camptothecin and irinotecan), which are topoisomerase I inhibitors (4,5). These drugs are cytotoxic for dividing cells in vitro at nanomolar concentrations but have narrow therapeutic windows for treatment because of toxicity and solubility issues. Preparing cytotoxic drugs as prodrugs may reduce their toxicity, increase their solubility and circulation time, and increase their effectiveness (6). Prodrugs formed by reaction of drug side chains with A-Z-CINN Linker can be converted back into native, active drugs upon additional chemical or enzymatic reactions or exposure to light energy.

Monoclonal antibodies (MAbs) directed against target molecules can provide highly specific binding and localization (7). The potential of MAbs to target tumor cell antigens and kill tumors has been exploited, and several MAbs are in clinical use. However, treatment with MAbs alone is not as successful as desired. Combination therapy, using MAbs and specific chemotherapy drugs to attack two or more different targets in tumor cells, is often more effective. For example, for HER-2-positive breast tumors (about 30% of breast tumors), trastuzumab plus paclitaxel is the current recommended treatment procedure, giving a 44% response rate. Neither treatment alone (trastuzumab 17% and paclitaxel 14%) is as successful (8).

Conjugates that combine MAbs as targeting molecules with therapeutic molecules (drugs and toxins) in a prodrug form provide a means to increase the specificity of cell killing. Use of MAbs that bind to tumor cell antigens with high selectivity reduces the impact of treatment on nontumor cells; therapeutic molecules can then be released to exert their effects in the local environment of the tumor cell.

Trastuzumab, a humanized antibody to HER-2, inhibits the growth of breast tumor cells that overexpress HER-2/neu. When combined with paclitaxel, it provides clinical benefit in patients with HER-2-positive breast cancer (8). To test whether the activity of trastuzumab could be further enhanced, we created an immunoconjugate using trastuzumab, A-Z-CINN, and paclitaxel. A-Z-CINN and paclitaxel are linked in an energy-reversible bond. Whether a targeted prodrug, trastuzumab–A-Z-CINN–paclitaxel (A-Z-CINN 310), could bind to tumor cells, release drug on the tumor cells by hydrolysis of prodrug ester, and kill tumor cells more effectively than equivalent amounts of concomitantly co-administered trastuzumab plus paclitaxel was tested. Release of paclitaxel from A-Z-CINN 310 is by hydrolysis, which can be accelerated by light treatment. The feasibility of A-Z-CINN-targeted therapy for killing tumor cells in a single treatment is described.

MATERIALS AND METHODS

Chemicals

Trastuzumab: Trastuzumab (Herceptin®, lot L9037A) was from Genentech, So. San Francisco, CA.

Paclitaxel: Paclitaxel (P0092, lot 200–12–26) was obtained from LKT Labs (Minneapolis, MN).

A-Z-CINN: A-Z-CINN is a bifunctional linker prepared in our laboratory. It binds targeting agent and forms esters with alcohols such as paclitaxel.

A-Z-CINN–paclitaxel prodrug: A-Z-CINN–paclitaxel was prepared by coupling tBOC–A-Z-CINN acid to paclitaxel in dichloromethane using carbodiimide and then removing tBOC by acid hydrolysis.

A-Z-CINN 310: A-Z-CINN 310 was prepared using trastuzumab and A-Z-CINN–paclitaxel. The conjugate was handled under red light or subdued light. After 0.2 μm filtration, A-Z-CINN 310 was stored in amber vials in 0.05 M sodium phosphate–0.15 M NaCl, pH 6.5, at 4°C.

Measurement of paclitaxel released from tBOC–A-Z-CINN–paclitaxel: Paclitaxel was released from tBOC–A-Z-CINN–paclitaxel in dichloromethane using 10 mW/cm^2 of white light, delivered through a 5 mm fiber-optic cable for 5 min. The material was chromatographed using C-18 reversed phase high performance liquid chromatography (RP-HPLC) (6). HPLC procedures used a gradient of 66% methanol/34% water (containing 0.02% phosphoric acid) to 100% methanol in 30 min to resolve paclitaxel, a photoproduct, and precursor tBOC–A-Z-CINN–paclitaxel molecules.

Mice

Scid mice (5-week-old females) were obtained from the Frederick Cancer Research and Development Center, Frederick, MD. They were quarantined for 2 weeks before use. Mice were housed in plastic micro-isolator cages with sterile hardwood bedding. They received standard laboratory diet and filtered tap water *ad libitum*. Air temperature in the animal rooms was 74 ± 2°F; humidity was approximately 50 ± 10%. Except as noted, light/dark cycles were automatically controlled at 12 h each.

BT-474 Cells

BT-474 human mammary carcinoma cells (HER-2-positive) were obtained from American

Type Culture Collection (Rockville, MD). The cells were grown in RPMI-1640 media supplemented with 10% fetal bovine serum and 2 mM L-glutamine.

Animal Study

The animal study and histological evaluation were carried out at Southern Research Institute (SRI), Birmingham, AL, under the direction of Dr. William Waud.

Preparation of mice bearing BT-474 tumor cells: One day before tumor cell implantation (day − 1), mice were implanted with slow-release estradiol pellets (0.72 mg, 60-day release). On day 0, mice were implanted with BT-474 cells. Three millilitres of pelleted BT-474 cells was mixed with 11 ml of Matrigel® (BioCoat, Ft. Washington, PA); 0.2 ml (1×10^7 cells) was implanted subcutaneously on the flank. Mice were randomized to three groups of four mice and three groups of six mice, and labeled with ear marks. Animals were treated on day 9 postimplant (tumor size ~200 mm^3; see below).

Treatment of mice: Mice were handled under red light. Articles were delivered by tail vein as 0.2 ml bolus injections. Control mice received phosphate-buffered saline (PBS). Treatment groups received concurrent co-administration of trastuzumab and paclitaxel (unlinked therapy), or A-Z-CINN 310 (A-Z-CINN-targeted therapy) at three concentrations. The compositions of treatment groups are summarized in Table 1. Six hours after injection, three groups of mice were treated with light as follows. Mice were anesthetized with a Ketamine/Rompun mixture, and a 16-gauge needle was used to create an incision in the skin near the tumor. A fiber-optic probe was inserted through the incision and brought to the edge of the tumor. Light was delivered from a Cuda Products Corp. Model M2-150-300 light source (~0.5 mW/cm^2, 75% output from a halogen bulb) for 5 min. The probe was washed with Bac-down/water and then with 70% ethanol before use. All mice were maintained under red light for 72 h and then returned to a normal dark/light cycle.

Histology: At the conclusion of the experiment, 14 mice from groups 1–6 were euthanized with CO_2. Their tumors were excised from the flank and preserved in neutral-buffered formalin. The tumors were embedded in paraffin, sectioned, and stained with hematoxylin and eosin (H&E).

Measurements: Mice were observed daily for survival. Tumors were measured by caliper in two dimensions twice weekly. Recorded measurements were converted to tumor mass using the formula $V=(a \times b^2)/2$, where "a" is the longer dimension and "b" the shorter dimension, and assuming 1 mm^3 = 1 mg. Mouse weights were measured twice weekly. Measurements were made for 4 weeks post-treatment. For the analysis of area of tumor cells in histological preparations, low-power micrographs were printed. In some sections, the weight of the entire tumor section and the weight of all areas containing cells were determined, and a ratio was calculated. Muscle tissue, if present, was excluded from the calculations.

Statistical analyses: Data were analyzed using the Student *t* test from Sigma Plot 2000 to determine if the mean values from two different data sets are significantly different. A value of $P > 0.05$ indicates that the two data groups are not significantly different. Standard deviations (SDs) for tumor weights were calculated from the raw data using Sigma Plot 2000.

RESULTS

Release of Paclitaxel from tBOC-A-Z-CINN-Paclitaxel

Figure 1 shows that paclitaxel can be released from tBOC-A-Z-CINN-paclitaxel by exposure to light and hydrolysis of the energy-reversible bond. tBOC-A-Z-CINN-paclitaxel was exposed to white light for 5 min, as described in *Materials and methods*, and the products were resolved by C-18 RP-HPLC. Five minutes of light exposure releases all of the paclitaxel. When A-Z-CINN–paclitaxel is linked to trastuzumab to generate A-Z-CINN 310, the paclitaxel remains linked to the MAb under the storage conditions chosen. Light release of paclitaxel from A-Z-CINN 310 yields 0.023 mg paclitaxel/mg trastuzumab.

Table 1: Treatment articles and conditions[a]

Group (*n*)	Condition	Article	Concentration	Light[b]
1 (4)	Control	PBS	NA	0
2 (4)	Unlinked therapy (concurrent co-administration)	Unlinked T plus P	1 mg of T, 0.023 mg of P	0
3 (4)	Targeted therapy, A-Z-CINN 310–0.1	A-Z-CINN 310–0.1	0.1 mg of T linked via A-Z-CINN to 0.0023 mg of P	0
4 (6)	Targeted therapy, light-accelerated release, A-Z-CINN 310–0.1	A-Z-CINN 310–0.1	0.1 mg of T linked via A-Z-CINN to 0.0023 mg of P	5 min
5 (6)	Targeted therapy, light-accelerated release, A-Z-CINN 310–0.5	A-Z-CINN 310–0.5	0.5 mg of T linked via A-Z-CINN to 0.012 mg of P	5 min
6 (6)	Targeted therapy, light-accelerated release, A-Z-CINN 310–1.0	A-Z-CINN 310–1.0	1 mg of T linked via A-Z-CINN to 0.023 mg of P	5 min

[a]PBS, phosphate-buffered saline; T, trastuzumab; P, paclitaxel; NA, not applicable.
[b]Light was delivered 6 h after injection of article, for 5 min at the edge of the tumor.

Changes in Tumor Volume

Mice were treated with the articles listed in Table 1. Six hours after treatment, three groups of mice were further treated with 5 min of light delivered to the tumor to cause accelerated release of paclitaxel. Tumor volumes were measured twice weekly for 4 weeks after treatment. The results are shown in Figures 2–5 and Table 2.

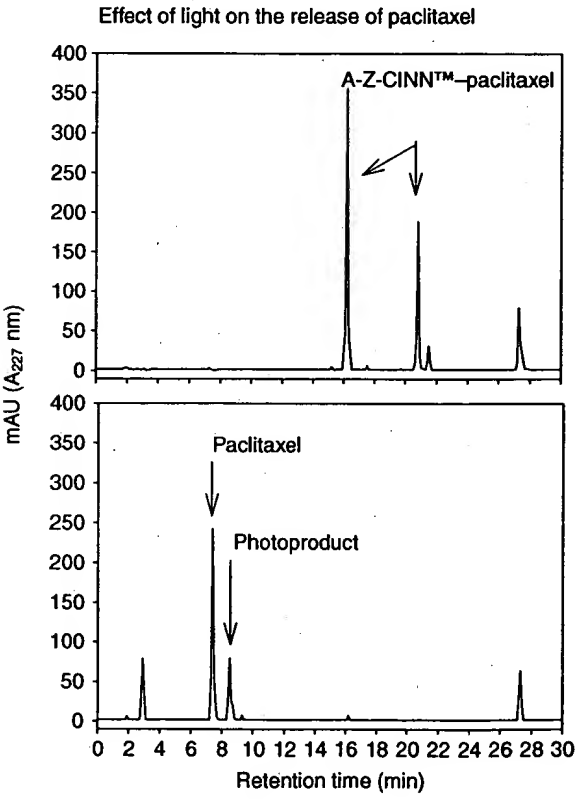

Figure 1. High-pressure liquid chromatograph (HPLC) analysis of release of paclitaxel from tBOC–A-Z-CINN–paclitaxel by light treatment. HPLC was performed as described in *Materials and methods*; absorbance was measured at 227 nm. tBOC–A-Z-CINN–paclitaxel consists of two esters, with elution times at 16.2 and 20.8 min. Exposure to light results in the release of paclitaxel (elution time 7.4 min) and the formation of A-Z-CINN photoproduct (elution time 8.5 min).

Figure 2 shows the dose–response curve for mice treated with three concentrations of A-Z-CINN 310 over a 10-fold range, followed by treatment with light 6 h later. The tumor volume of animals receiving control (saline) increased ~20% and then leveled off. Animals receiving A-Z-CINN 310, then light, showed similar results with all concentrations used, with a rapid decrease in tumor volume by 7 days, followed by little further change. Changes in tumor volume below ~65 mm^3 were not statistically significant because of observer variation. Thus, at the highest concentration tested, tumor volumes decreased and became immeasurable. Figure 3 shows a comparison between light-accelerated release of paclitaxel from A-Z-CINN 310-1.0 and treatment with co-administered unlinked paclitaxel and trastuzumab, at the same concentrations. The volume change obtained with A-Z-CINN 310-targeted therapy, then light, is rapid, while with unlinked therapy (trastuzumab plus paclitaxel), tumor volume first increases and then decreases slowly. Figure 4 compares treatment with the lowest concentration of A-Z-CINN 310 (A-Z-CINN 310-0.1), with and without subsequent light exposure. While there is a more rapid decrease in tumor volume with light treatment than without, the same endpoint is reached, suggesting that both mechanisms of paclitaxel release (hydrolytic or light-accelerated) following targeting

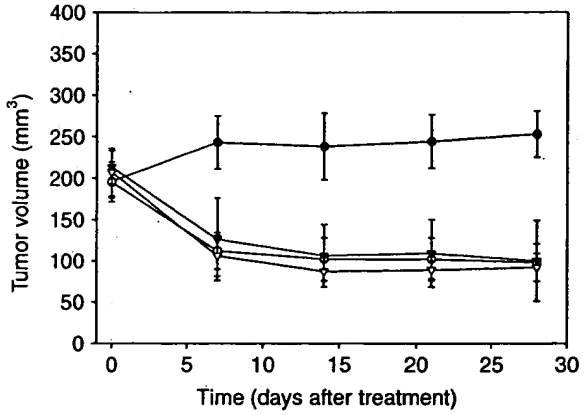

Figure 2. Effects on tumor volume of A-Z-CINN 310-targeted therapy with light-accelerated release of paclitaxel. Mice were treated with control (saline) or three concentrations of A-Z-CINN 310, followed by light exposure, as described in *Materials and methods*. Tumor volume was measured at the times shown. See Table 1 for concentrations of A-Z-CINN 310 samples. •, saline control; ▽, A-Z-CINN 310-1.0; ○, A-Z-CINN 310-0.5; ▼, A-Z-CINN 310-0.1.

are effective. Figure 5 shows a comparison between hydrolytic release from A-Z-CINN 310 and concurrent co-administration of trastuzumab plus paclitaxel. The concentration of paclitaxel and trastuzumab in the group receiving A-Z-CINN 310-0.1 is 10-fold lower than that in the group receiving unlinked trastuzumab and paclitaxel therapy, yet the same endpoint is achieved.

Table 2 summarizes the statistical analyses of comparisons of changes in tumor volume in groups as a result of various treatments. Statistically significant differences are seen between controls (saline) and all targeted therapy using A-Z-CINN 310 followed by light acceleration (Figure 2), between unlinked therapy using paclitaxel and trastuzumab at the same concentration as A-Z-CINN 310 followed by light treatment (Figure 3), and between A-Z-CINN 310-targeted therapy, with and without light treatment, for the first 21 days. There was no significant difference between A-Z-CINN 310-0.1-targeted therapy without light acceleration and a 10-fold higher concentration of unlinked trastuzumab plus paclitaxel.

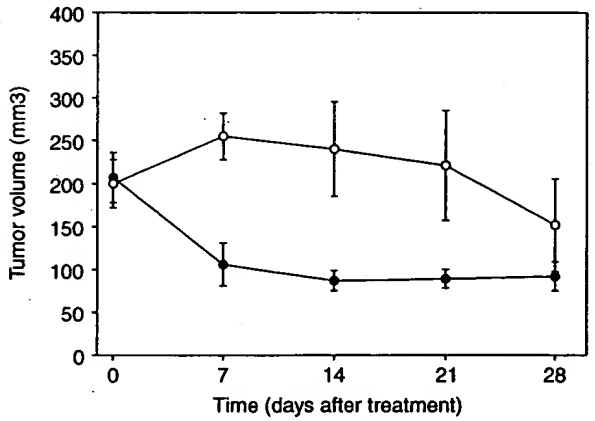

Figure 3. Effects of A-Z-CINN 310-targeted therapy with light-accelerated release of paclitaxel or unlinked therapy (concurrent administration of unlinked trastuzumab plus paclitaxel) on tumor volume. The two treatments contained the same amounts of trastuzumab (1 mg) and paclitaxel (0.023 mg). •, A-Z-CINN 310-1.0 plus light; ○, unlinked trastuzumab plus paclitaxel.

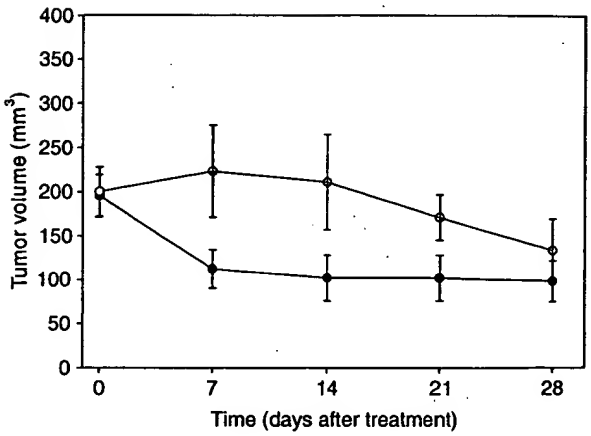

Figure 4. Effects of A-Z-CINN 310-targeted therapy with and without light-accelerated release of paclitaxel on tumor volume. •, A-Z-CINN 310-0.1 plus 5 min of light; ○, A-Z-CINN 310-0.1, no light.

Changes in Histology

Mice from each group were euthanized 31 days after treatment to obtain tumor tissue for histological analysis. Tumors were processed and stained with H&E, as described in *Materials and methods*, and read by a pathologist at SRI. The overall appearance of the cells was consistent with human mammary carcinoma cells. The results are shown in Figures 6 and 7 and Table 3.

Figure 6 shows a comparison of tumor cell density (blue-stained cells) in animals 31 days after treatment with control saline (Figure 6A), co-administered unlinked trastuzumab plus paclitaxel (Figure 6B), and A-Z-CINN 310-0.1 in the dark (Figure 6C). There are significant decreases in tumor cell density in both treatment groups compared with control saline. The trastuzumab and paclitaxel concentrations of A-Z-CINN 310-0.1 are 10-fold lower than

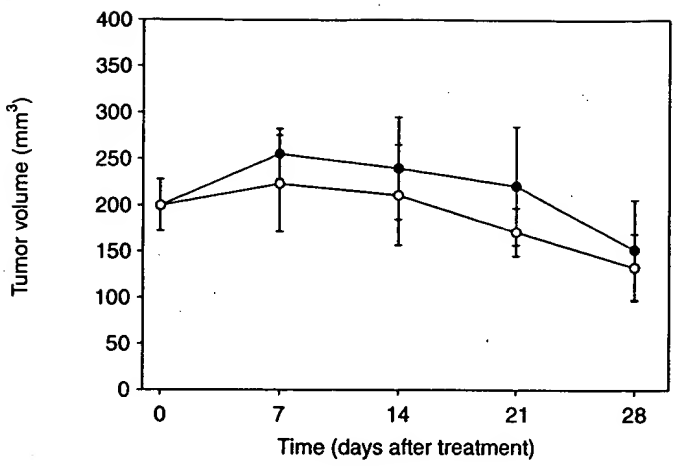

Figure 5. Effects of A-Z-CINN 310-targeted therapy without light or unlinked therapy with simultaneously delivered trastuzumab plus paclitaxel on tumor volume. A-Z-CINN 310-0.1 treatment contained 10-fold lower concentrations of trastuzumab and paclitaxel than unlinked therapy. ○, A-Z-CINN 310-0.1; ●, unlinked therapy (1 mg of trastuzumab and 0.023 mg of paclitaxel).

that in the unlinked therapy. Figure 7A-C shows tumor cell density in animals 31 days after treatment with three concentrations of A-Z-CINN 310, followed by light exposure. Decreases in the tumor cell population in Figure 7 are dose-dependent; all doses are highly effective. Table 3 summarizes the measured changes in tumor cell areas shown in Figures 6 and 7, obtained from low-power photomicrographs of the prepared sections. Of the treatments used, unlinked therapy using co-administered trastuzumab and paclitaxel has the greatest number of residual tumor cells, followed by A-Z-CINN 310-0.1 in the dark. Trastuzumab and paclitaxel concentrations were the same in unlinked therapy with co-administered trastuzumab and paclitaxel (Figure 6B) and with A-Z-CINN 310-1.0 followed by light treatment (Figure 7C), indicating greater efficacy of treatment when the targeting agent and the drug were linked by A-Z-CINN Linker than when they were unlinked. These results parallel those obtained by measurement of tumor cell volume in vivo.

Comparison of Delivered Doses to Human Clinical Dose

The concentrations of trastuzumab and paclitaxel delivered to mice in this study were compared with that used clinically for a treatment-loading dose for a 60 kg patient. The data are summarized in Table 4. The concentration of paclitaxel in A-Z-CINN 310 groups and in unlinked trastuzumab plus paclitaxel groups were 3–32% of the current clinical dose, while the concentration of trastuzumab equaled or exceeded the current clinical dose, depending on the experimental conditions.

Table 2: Statistical analysis of treatment groups using Student t-test (unpaired)[a]

Comparison	*P* value			
	Day 7	Day 14	Day 21	Day 28
Control versus unlinked T + P	0.602	0.931	0.547	0.016
Control versus A-Z-CINN 310-0.1, dark	0.518	0.450	0.023	0.004
Control versus A-Z-CINN 310-0.1, light	0.0002	0.0004	0.0001	0.00004
Control versus A-Z-CINN 310-0.5, light	0.003	0.0007	0.001	0.002
Control versus A-Z-CINN 310-1.0, light	0.00006	0.00002	0.000003	0.000003
A-Z-CINN 310-1.0, light versus unlinked T + P (Figure 3)	0.00002	0.0001	0.0009	0.033
A-Z-CINN 310-0.1, dark versus A-Z-CINN 310-0.1, light (Figure 4)	0.003	0.005	0.011	0.145
A-Z-CINN 310-0.1, dark versus unlinked T + P (Figure 5)	0.311	0.464	0.262	0.915

[a]Comparisons were made between control saline and each treatment, and the treatment pairs are shown in Figures 3–5. A value of $P > 0.05$ indicates that the two data groups are equal. T, trastuzumab; P, paclitaxel.

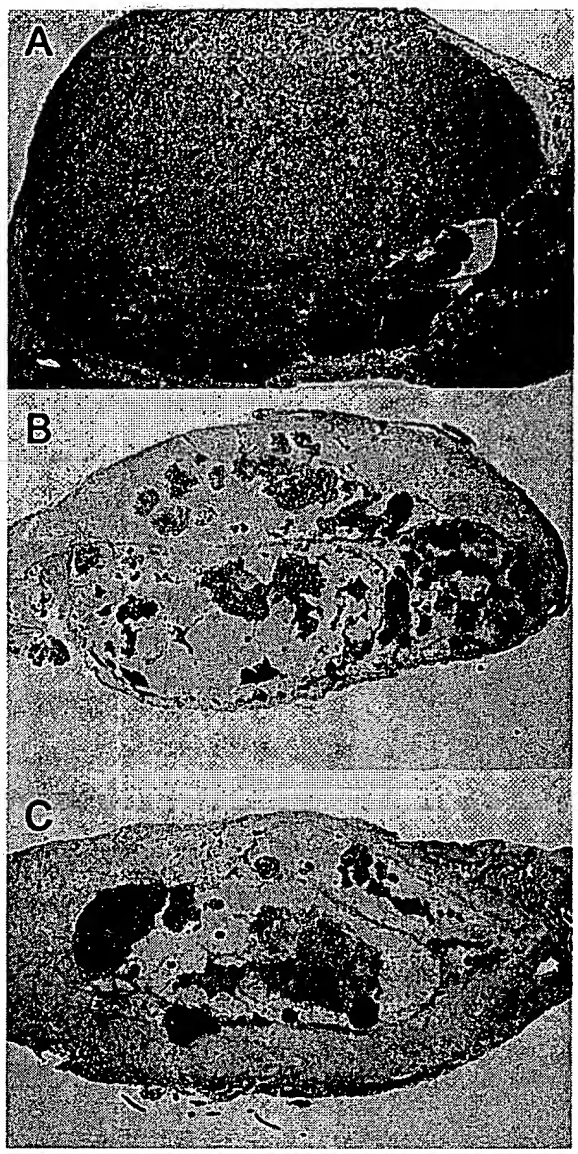

Figure 6. Effects of treatment with control (saline), unlinked therapy using concurrently administered trastuzumab plus paclitaxel, or A-Z-CINN 310-0.1 without subsequent light exposure on histological profile. Trastuzumab and paclitaxel concentrations are 10-fold lower in the treatment with A-Z-CINN 310-0.1. Mice were treated as described in *Materials and methods*. **A**, control saline; **B**, unlinked trastuzumab plus paclitaxel; **C**, A-Z-CINN 310-0.1. Magnification, × 2.

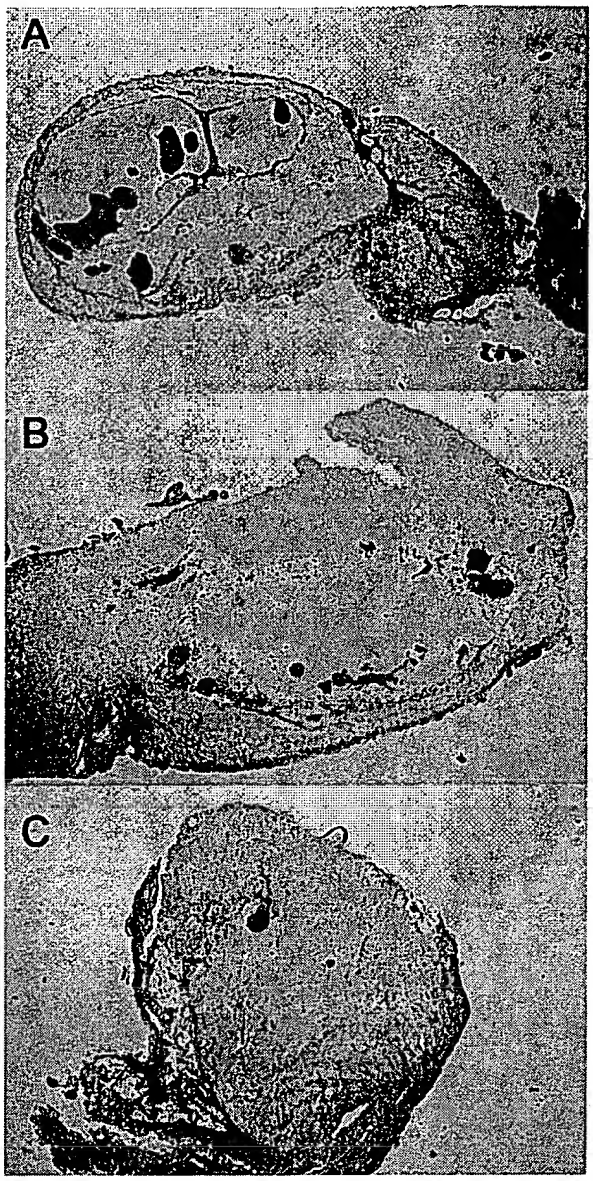

Figure 7. Effects of treatment with three concentrations of A-Z-CINN 310-targeted therapy with light-accelerated release of paclitaxel on histological profile. Mice were treated with A-Z-CINN 310 at the indicated concentrations, followed by light exposure, as described in *Materials and methods*. Samples were processed for histology on day 31 after treatment. Blue-staining material represents tumor cells. **A**, A-Z-CINN 310-0.1; **B**, A-Z-CINN 310-0.5; **C**, A Z-CINN 310-1.0. Magnification, × 2.

DISCUSSION

Systemic cancer chemotherapy delivers drugs that interfere with cellular metabolism or cell division but have no selectivity for tumor cells. These drugs are administered intravenously or orally and affect both tumor cells and normal cells. Effects on tumor cells are often greater, because of their higher rates of metabolism and cell division. The maximum tolerable dose of a chemotherapeutic drug indicates the amount that can be given to a patient before side effects such as marrow suppression outweigh clinical benefits. Preparation of potent chemotherapeutic drugs as prodrugs that

Table 3: Tumor cell areas as percentage of total tissue section area[a]

Treatment	Tumor area (%)
Saline (control)	88.0
1 mg of T + 0.023 mg of P, unlinked	19.2
A-Z-CINN 310-0.1, dark	12.5
A-Z-CINN 310-0.1, light	5.3
A-Z-CINN 310-0.5, light	1.8
A-Z-CINN 310-1.0, light	0.5

[a]Measurements were made as described in Materials and methods. P, paclitaxel; T, trastuzumab.

can be targeted and released at the site of tumors should allow more effective delivery of these drugs, increase the local bioavailability of drug, and thus favor more effective killing, with fewer side effects. MAbs targeted to tumor cell antigens can localize targeted prodrugs on tumor cell surfaces; for example, the MAb trastuzumab binds to the HER-2/neu receptor on BT-474 human mammary tumor cells (9).

We created a targeted prodrug, trastuzumab-A-Z-CINN-paclitaxel (A-Z-CINN 310), and tested it on HER-2-positive human mammary tumor cells implanted in mice. We first demonstrated that the exposure of the prodrug A-Z-CINN-paclitaxel to visible light could release paclitaxel by hydrolyzing the energy-reversible bond in vitro (Figure 1). Cinnamic acid esters undergo rapid hydrolysis on exposure to light, releasing the alcohol group; this has been demonstrated using serine proteases (10). We compared single treatments with A-Z-CINN 310, with or without later light exposure, and equivalent concentrations of unlinked trastuzumab and paclitaxel. The hypothesis was that targeting would increase the effectiveness of tumor killing by paclitaxel in a single treatment, and that paclitaxel bound to A-Z-CINN in an energy-reversible bond could be released at the tumor site slowly by hydrolysis or more rapidly by light treatment. Targeting using A-Z-CINN 310 would increase local bioavailability over that obtained with unlinked paclitaxel. The concentrations tested in these experiments were based on current human clinical dosing regimes for trastuzumab (8).

The results indicate that targeted prodrug delivery using A-Z-CINN 310 is more effective than unlinked trastuzumab plus paclitaxel in reducing tumor cell volume measured serially in situ and in reducing tumor cell density shown by histochemistry. Changes in tumor cell volume after A-Z-CINN 310 treatment followed by light exposure indicate the most rapid decreases of all treatment groups, and the difference between unlinked trastuzumab plus paclitaxel at equivalent doses is statistically significant at all time points (Figures 2 and 3 and Table 2). Changes in tumor cell area shown by histology performed at the end of the experiment parallel the changes in tumor cell volume (Figures 6 and 7 and Table 3). The results suggest that A-Z-CINN 310 has the potential for treating the 30% of breast cancer patients with HER-2-positive disease, who currently have poor prognoses.

A-Z-CINN 310 is a prototype targeted prodrug, which contains three essential molecules: (1) a MAb-targeting agent, trastuzumab, against a known tumor cell surface antigen; (2) A-Z-CINN, a versatile bifunctional linker; and (3) paclitaxel, an effective chemotherapeutic drug with high toxicity and high efficacy. Compared to the loading dose for the current clinical use of trastuzumab and paclitaxel (8), targeted

Table 4: Comparison of trastuzumab (T) and paclitaxel (P) compositions of A-Z-CINN 310 doses and current human clinical dose[a]

Mouse treatment	Mouse dose[b]	Conversion of mouse to human dose[c]	Comparison to clinical loading dose[d]
A-Z-CINN 310–0.1	0.1 mg of T; 0.0023 mg of P	240 mg of T; 5.5 mg of P	100% T; 3.2% P
A-Z-CINN 310–0.5	0.5 mg of T; 0.012 mg of P	1200 mg of T; 27.6 mg of P	500% T; 16% P
A-Z-CINN 310–1	1 mg of T; 0.023 mg of P	2400 mg of T; 55.2 mg of P	1000% T; 32% P
Unlinked T + P	1 mg of T; 0.023 mg of P	2400 mg of T; 55.2 mg of P	1000% T; 32% P

[a]Values for clinical loading dose of T and P were taken from Ref. 8. Treatment doses for 25 g mouse were converted to values for 60 kg human.
[b]Per 25 g mouse.
[c]Per 60 kg human.
[d]240 mg of trastuzumab; 175 mg of paclitaxel.

therapy using A-Z-CINN 310-0.1 contains the same amount of trastuzumab and 3% of the amount of paclitaxel, and unlinked therapy using trastuzumab and paclitaxel contains 10 times the amount of trastuzumab and 32% of paclitaxel (Table 4). When injected into scid mice bearing BT-474 human mammary tumors, the immunoconjugate A-Z-CINN 310 caused tumor regression in all mice, whereas co-delivered unlinked trastuzumab and paclitaxel caused slower tumor regression. Similar endpoints were obtained regardless of whether the paclitaxel was released through hydrolysis or through accelerated release following light activation, although the rate of tumor regression was faster with light-accelerated release. We tested A-Z-CINN 310 with light-accelerated release at three concentrations and achieved aggressive tumor regression at all dosages. All concentration levels exhibited superior results of tumor regression, in marked contrast to the unlinked trastuzumab plus paclitaxel group. However, the tumor regression seen in the unlinked trastuzumab plus paclitaxel group is consistent with published results in a BT-474 model (11). No evidence of tumor regrowth was seen in the 31 days of the experiment, despite the presence of residual viable tumor cells. Although no pathologically complete responses were seen by objective tumor measurements following the single treatment of this study, such responses might be seen following repeated treatments or different dosing levels.

CONCLUSIONS

These results confirm that A-Z-CINN Linker can be used to prepare a targeted prodrug, A-Z-CINN 310 (trastuzumab–A-Z-CINN–paclitaxel), for the delivery of chemotherapy to tumor sites in an animal model. The targeting of A-Z-CINN 310 to tumor cell surfaces allows efficient delivery of paclitaxel to the tumor site, demonstrating more effective treatment than concurrent treatment with unlinked trastuzumab and paclitaxel. A-Z-CINN Linker can enhance the therapeutic benefits of MAbs and existing drugs, and A-Z-CINN 310 can provide therapy that is superior to concomitant co-administration of the free single agents trastuzumab and paclitaxel at equivalent concentrations. A-Z-CINN Linker can be used to link any targeting molecule with any drug, using appropriate chemistry. Therefore, by selecting targeting agents with high tumor specificity, and drugs that kill cells at nanomolar concentrations, optimized targeted prodrugs can be designed to attack and kill primary tumors as well as metastatic tumors. Accelerated release of paclitaxel by light provides a way to have high local concentrations of free drug at the tumor site and may be suitable for the treatment of primary tumors. We hypothesize that sustained release of targeted paclitaxel may be effective at tumor sites where use of light is not feasible, such as metastatic sites.

REFERENCES

1. Rowinsky EK, Donehower RC. The clinical pharmacology and use of antimicrotubule agents in cancer chemotherapeutics. *Pharmacol Ther* 52: 35–84, 1991.
2. Horwitz SB, Lothstein L, Manfredi JJ, Mellado W, Parness J, Roy SN, Schiff PB, Sorbara L, et al. Taxol: mechanisms of action and resistance. *Ann N Y Acad Sci* 466: 733–744, 1986.
3. Yokoyama M, Miyauchi M, Yamada N, Okano T, Sakurai Y, Kataoka K, Inoue S. Characterization and anticancer activity of the micelle-forming polymeric anticancer drug adriamycin-conjugated poly(ethylene glycol)-poly(aspartic acid) block copolymer. *Cancer Res* 50: 1693–1700, 1990.
4. Slichenmyer WJ, Donehower RC. Recent clinical advances with camptothecin analogues. In: Muggia, FM, ed. *Concept, Mechanisms, and New Targets for Chemotherapy*. Vol. 78, Cancer Treatment and Research. Boston: Kluwer Academic Publishers. 29-43, 1995.
5. Edelman MJ, Gradara DR. Promising new agents in the treatment of non-small cell lung cancer. *Cancer Chemother Pharmacol* 37: 385–393, 1996.
6. Greenwald RB, Gilbert CW, Pendri A, Conover CD, Xia J, Martinez T. Drug delivery systems: water soluble taxol 2′-poly(ethylene glycol) ester prodrugs-design and in vivo effectiveness. *J Med Chem* 39: 424–431, 1996.
7. Morrow KJ. Recent advances in recombinant antibody technology. Part 1. *Am Lab* June, 15–19, 2000.
8. Trastuzumab® Product Information Sheet, Genentech, 2000.
9. Park JW, Hong K, Carter P, Asgari H, Guo LY, Keller GA, Wirth C, Shalaby R. Development of anti-p185^{HER2} immunoliposomes for cancer therapy. *Proc Natl Acad Sci USA* 92: 1327–1331, 1995.
10. Porter NA, Bruhnke JD. Photocoagulation of human plasma: acyl serine proteinase photochemistry. *Photochem Photobiol* 51: 37–43, 1990.
11. Baselga J, Norton L, Albanell J, Kim Y-M, Mendelsohn J. Recombinant humanized anti-HER2 antibody (Herceptin®) enhances the antitumor activity of paclitaxel and doxorubicin against HER2/*neu* overexpressing human breast cancer xenografts. *Cancer Res* 58, 2825–2831, 1998.